Organic & Biomolecular Chemistry

REVIEW

CrossMark
← click for updates

Transition-metal catalyzed valorization of lignin: the key to a sustainable carbon-neutral future

Markus D. Kärkäs, Bryan S. Matsuura, Timothy M. Monos, Gabriel Magallanes and Corey R. J. Stephenson*

The development of a sustainable, carbon-neutral biorefinery has emerged as a prominent scientific and engineering goal of the 21st century. As petroleum has become less accessible, biomass-based carbon sources have been investigated for utility in fuel production and commodity chemical manufacturing. One underutilized biomaterial is lignin; however, its highly crosslinked and randomly polymerized composition have rendered this biopolymer recalcitrant to existing chemical processing. More recently, insight into lignin's molecular structure has reinvigorated chemists to develop catalytic methods for lignin depolymerization. This review examines the development of transition-metal catalyzed reactions and the insights shared between the homogeneous and heterogeneous catalytic systems towards the ultimate goal of valorizing lignin to produce value-added products.

1. Introduction

Petroleum is a critically important commodity resource that modern society is reliant on as a carbon feedstock for the production of fuel and fine chemicals. Aside from the environmental and political impact of its extraction and distribution, petroleum is a non-renewable resource with unmatched sus-

tainable alternatives. Currently, biomass is the largest source of renewable energy, supplying 3% of the total consumption of energy in the United States, surpassing hydroelectric and wind power. The United States has the capacity to produce 190 million tons of biomass each year, with the potential to increase production to 1 billion tons by 2050.[1,2] As the only available renewable carbon feedstock, utilization of biomass for this purpose is considered essential to reducing humanity's unsustainable consumption of non-renewable resources. Converting biomass into fuel or fine chemicals on a scale that would rival petroleum refining represents an enormous collec-
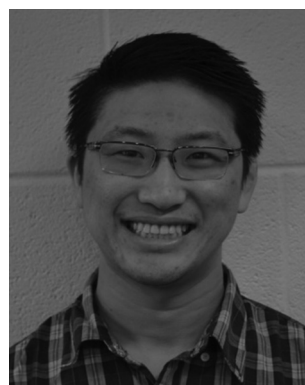
Department of Chemistry, University of Michigan, Ann Arbor, Michigan 48109, USA. E-mail: crjsteph@umich.edu

Markus D. Kärkäs received his M.Sc. degree in Chemistry from Stockholm University in 2008, where he conducted undergraduate research in the laboratory of Prof. Åkermark. In the same year, he began his Ph.D. studies under the guidance of Professor Björn Åkermark and Professor Jan-Erling Bäckvall. In 2013, he obtained his Ph.D. degree after conducting research on the development of artificial water oxidation catalysts. He is currently

Markus D. Kärkäs

working as a postdoctoral fellow at the University of Michigan with Professor Corey Stephenson where he is developing methods for valorization of lignin.

Bryan S. Matsuura received his B.A. from Boston University in 2009 and started his Ph.D. studies in the same year. In 2015 he obtained his Ph.D. at the University of Michigan working under the supervision of Professor Corey Stephenson where he studied the biomimetic synthesis of the resveratrol oligomers and the degradation of biomass derived polymers using visible-light photoredox catalysis. He is currently working as

Bryan S. Matsuura

a postdoctoral fellow in the research group of Professor Dirk Trauner at the Ludwig-Maximilians-Universität München.

This journal is © The Royal Society of Chemistry 2016

Org. Biomol. Chem., 2016, **14**, 1853–1914 | **1853**

tion of challenges from a scientific, engineering, and economic standpoint that will take several years of research and development from all fronts. However, this is a chemistry problem at its core, and the development of novel chemical transformations for processing biomass is central to the realization of this ambitious goal.

Although it is unlikely that biomass will replace the demand for petroleum outright, it possesses great potential as a replacement for crude oil as the carbon feedstock for the production of commodity chemicals, solvents, pharmaceuticals, and agrochemicals. Prior to 2006, biomass conversion largely escaped the attention of synthetic chemists, despite the great scientific and societal significance of this problem.[3–6] Since then, biomass conversion-particularly lignin depolymerization has undergone rapid development from chemists and chemical engineers. The progress in lignin depolymerization chemistry has been reviewed by several groups, documenting the rapid advances in the liquefaction of lignocellulosic biomass,[7,8] oxidative valorization,[9,10] and hydrogenolysis.[11] This review seeks to provide a comprehensive overview of current lignin depolymerization chemistry within the context of synthetic chemistry. The majority of the reactions described herein involve the cleavage of lignin model compounds using homogeneous catalysis, though stoichiometric reactions are discussed where applicable. For further reading we recommend the recently published review by Deuss and Barta.[12]

1.1 Structure and biosynthesis of lignin

Lignocellulosic biomass (dry plant matter) is the most abundant renewable carbon resource on earth. It is mainly composed of the carbohydrate polymers cellulose and hemicellulose and the aromatic polymer lignin. While technologies to process cellulose and hemicellulose are well developed, lignin processing constitutes a considerably more challenging task. Lignin is the second most abundant biopolymer on earth, comprising up to 20–35% of lignocellulosic biomass and greater than 40% of the energy content. Unlike polysaccharides or lipids, lignin is the only biopolymer possessing a high content of aromatic groups and is an ideal candidate as a renewable resource for aromatic commodity chemicals. Lignin's highly branched and irregular structure plays a vital role in providing the plant biomechanical support, aiding in pathogenic defense and water transport. Lignin is composed of three phenylpropanol alcohol precursors–coumaryl alcohol (1), coniferyl alcohol (2) and sinapyl alcohol (3) (Fig. 1)—collectively called monolignols. Although all monolignols are derived biosynthetically from the cinnamate pathway (Scheme 1), the monomer composition is species dependent.[13–16]

After their biosynthesis, the monolignols are transported through the cell membrane to the cell wall, through an unknown mechanism, where co-polymerization occurs. It is generally accepted that polymerization is initiated by undirected oxidative radical polymerization of the cinnamyl alcohol precursors. For example, the oxidation of coumaryl alcohol (1) results in the formation of a highly stabilized phenoxyl radical (16) that is best described by the resonance hybrids A, B, and C (Fig. 2). Radical 16 can couple in a random, radical–radical combinatorial fashion, resulting in the formation of highly reactive quinone methide intermediates (17–19). Subsequent intermolecular nucleophilic substitution with water and other monolignols (causing cross-linking) or intramolecular cyclization reactions yields a structurally diverse array of linkage motifs (20–22) (Fig. 2).[13,14] Consequently, the lignin polymer is random in both monomer sequence, linkage motif, and stereochemical configuration.[17] Of the different linkages, the β-O-4 motif (see Fig. 1) is by far the most abundant, comprising 45–60% of all linkages found in lignin with the dihydrobenzofuran, β–β′ linkage, and the 5–5′ linkages present in significant but less abundant quantities.[18,19]

1.2 Valorization of lignin – a sustainable solution for producing value-added chemicals

In the hypothetical carbon-neutral biorefinery, biomass would be converted into fuel or fine chemicals over several steps in a process analogous to petroleum refining. The first, and perhaps the most critical step, is the mechanochemical separation of raw plant biomass, such as stover or bagasse, into its

Timothy M. Monos received his B.Sc. in Chemistry from the University of Connecticut in 2013 and began his Ph.D. studies in the same year. He is currently a Ph.D. candidate at the University of Michigan under the direction of Professor Corey Stephenson, studying methodology development and applications of photoredox catalysis.

Timothy M. Monos

Gabriel Magallanes received his B.Sc. in Chemistry from Purdue University in 2014. He started his Ph.D. studies at the University of Michigan in 2014 where he is currently working under the supervision of Professor Corey Stephenson. Gabriel is studying the degradation of biomass derived polymers using visible-light photoredox catalysis.
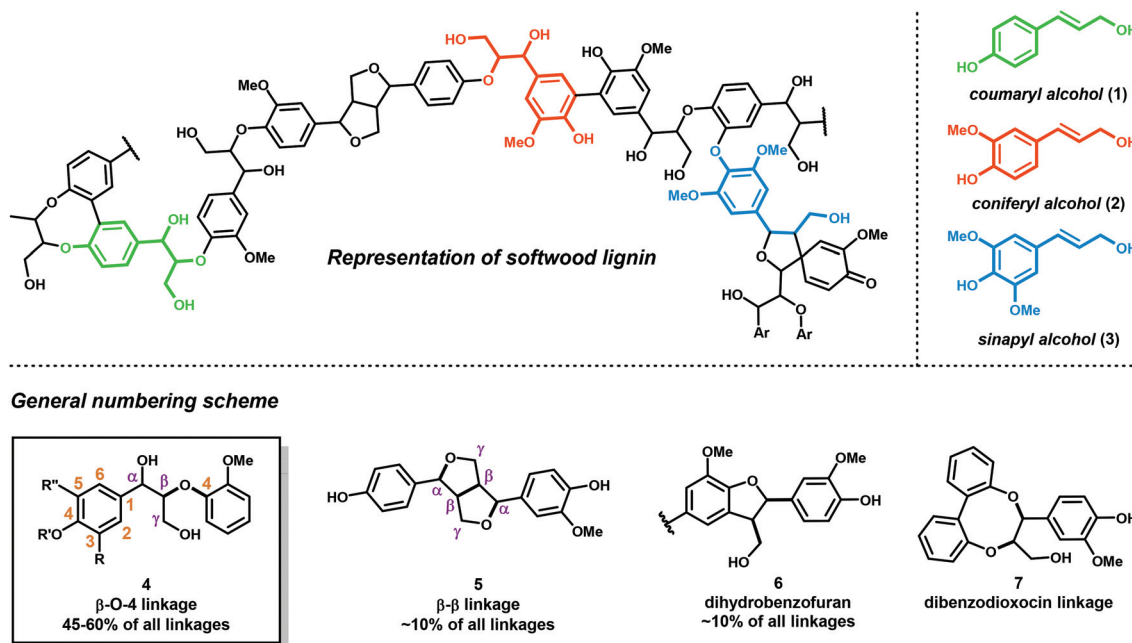
Gabriel Magallanes

1854 | *Org. Biomol. Chem.*, 2016, **14**, 1853–1914

This journal is © The Royal Society of Chemistry 2016

Fig. 1 Structure of lignin and the main linkage motifs present in lignin.

constituent parts in a process called 'pulping', which produces two significant fractions: a cellulosic fraction and lignin (Fig. 3). The former, which consists of cellulose and hemicellulose, comprises about 60–75% of biomass by weight. Current biomass processing research is primarily focused on processing cellulose as the main carbon source because it is amenable to both chemical and enzymatic processing techniques.[20–26] Cellulose and oligosaccharides are typically broken down *via* acidic digestion and can be further processed by fermentation to yield important non-aromatic commodity chemicals, such as ethanol, *n*-butanol and hydroxy methylfurfural. These products can then be refined into saturated hydrocarbons, analogous to olefin–alkane distillates from petroleum refining.[27,28] Although the technologies to convert alkanes and alkenes into aromatic compounds exist,[29] these processes generally require high temperatures and are not energetically feasible to perform on a scale needed for commodity chemical synthesis. In contrast, the high aromatic content of lignin makes it an ideal feedstock for the renewable production of high value aromatics such as phenol, benzene, toluene and xylene (BTX), complementing the products obtained from cellulose or algal bio-oil processing. However, the highly complex and irregular structure of lignin has severely complicated the development of controlled methods for depolymerizing lignin for the production of fine chemicals. In the absence of any chemical processing technology, pyrolysis of pretreated lignin yields syngas (a mixture of CO and H_2) in about 15–20% yield, plus an intractable char that is rich in polyaromatic hydrocarbons.[30] This process, which is inefficient and highly energy intensive could be used to generate synthetic alkanes through the Fischer–Tropsch process,[31] but destroys the aromatic backbone of lignin. The development of more suitable lignin conversion chemistry that preserves the aromatic structure is considered an essential objective in establishing the sustainable, carbon-neutral bio-refinery of the future (Fig. 3).[32]

1.3   Preprocessing and isolation of lignin

Lignin is separated from wood during the wood pulping by three industrial processes: the Kraft process, sulfite process, and the organosolv processes (Fig. 4).[18,33,34] In the Kraft[35] and sulfite processes,[36,37] wood chips, corn stover, or plant bagasse are digested under high heat in either basic or acidic conditions to delignify cellulose and solubilize the lignin by-product in water. Under these harsh conditions, lignin undergoes structural rearrangement, displacement of aryl ethers and
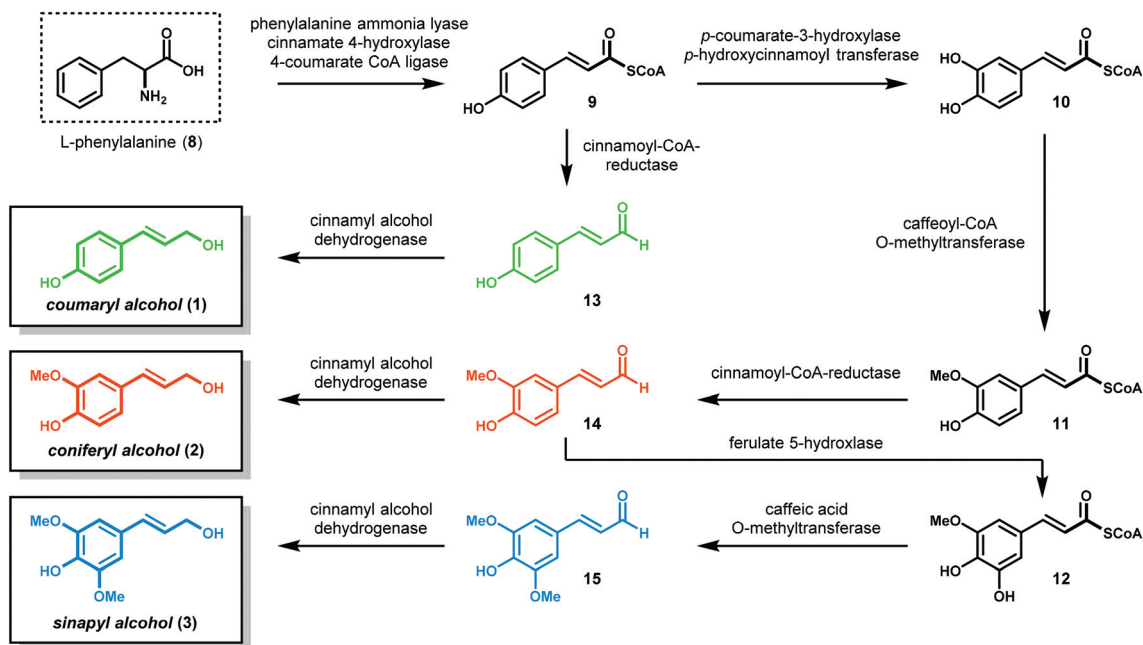
Corey R. J. Stephenson earned his Ph.D. from the University of Pittsburgh under Professor Peter Wipf before pursuing his post-doctoral studies at ETH Zürich with Professor Erick M. Carreira. He began his independent career at Boston University in 2007 and moved to the University of Michigan in 2013. His research interests are broadly focused on biomass degradation, complex molecule synthesis and catalysis.

Corey R. J. Stephenson

This journal is © The Royal Society of Chemistry 2016

Org. Biomol. Chem., 2016, **14**, 1853–1914 | **1855**

Biosynthesis of monolignols

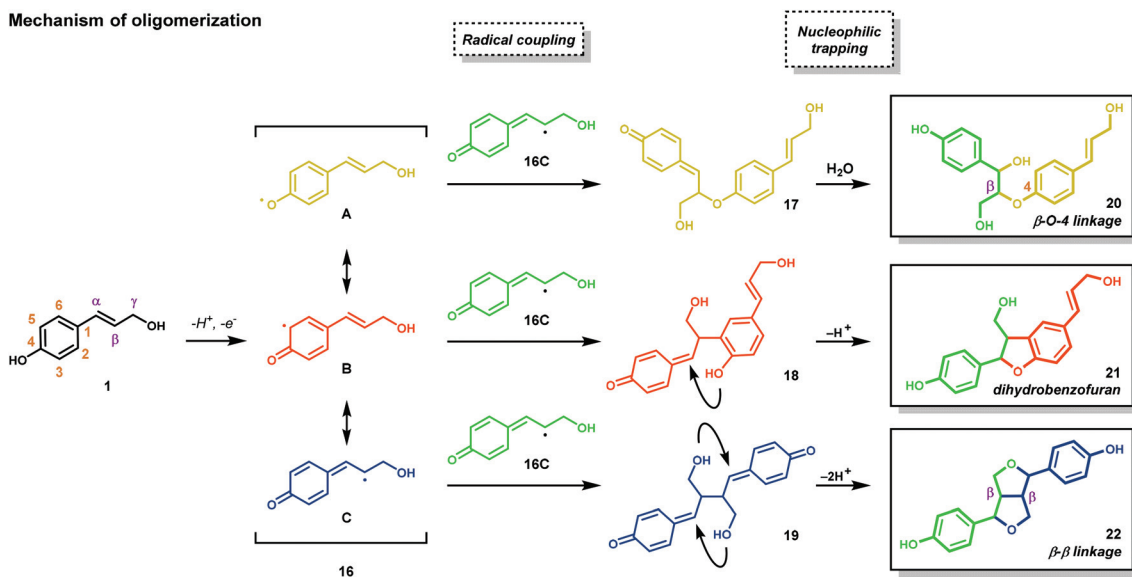**Scheme 1** Biosynthesis of the monolignols present in lignin.

Fig. 2 Mechanism of oligomerization.

benzylic ethers with sulfides and sulfites, while simultaneously promoting other C–O and C–C bond cleavage reactions. The resulting Kraft or sulfite lignin is generally a highly intractable, water-soluble dark brown powder of unknown structure. In addition, these processes incorporate up to 4 wt% of sulfur into the lignin backbone. This adds additional difficulties in designing post-processing reactions since sulfur

is a well-known poison for transition metal catalysts. These pulping processes, which were designed solely to delignify cellulose, render lignin unsuitable for further processing. Nearly 40 million tons of lignin are produced from these pulping processes, whereby 95% of it is burned as a low value fuel. In select cases, people have designed lignin-based newspaper, composite boards and plastic bags, whereby lignin is a com-

1856 | *Org. Biomol. Chem.*, 2016, **14**, 1853–1914

This journal is © The Royal Society of Chemistry 2016
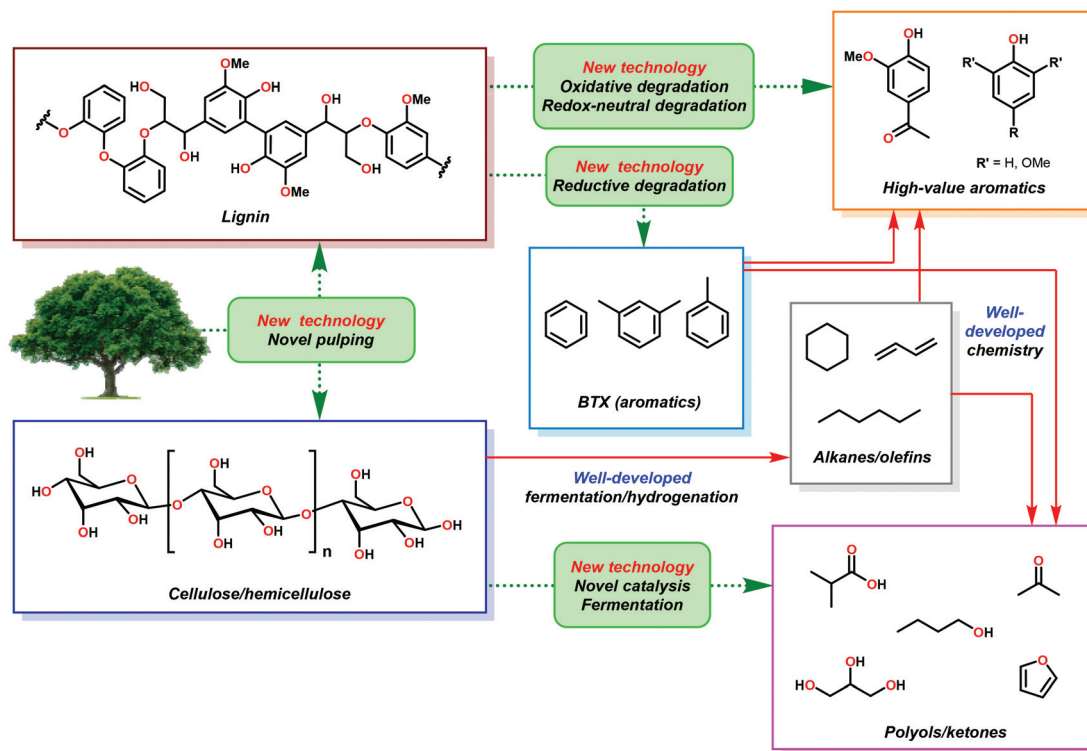
Fig. 3 The hypothetical biorefinery and its fundamental challenges.
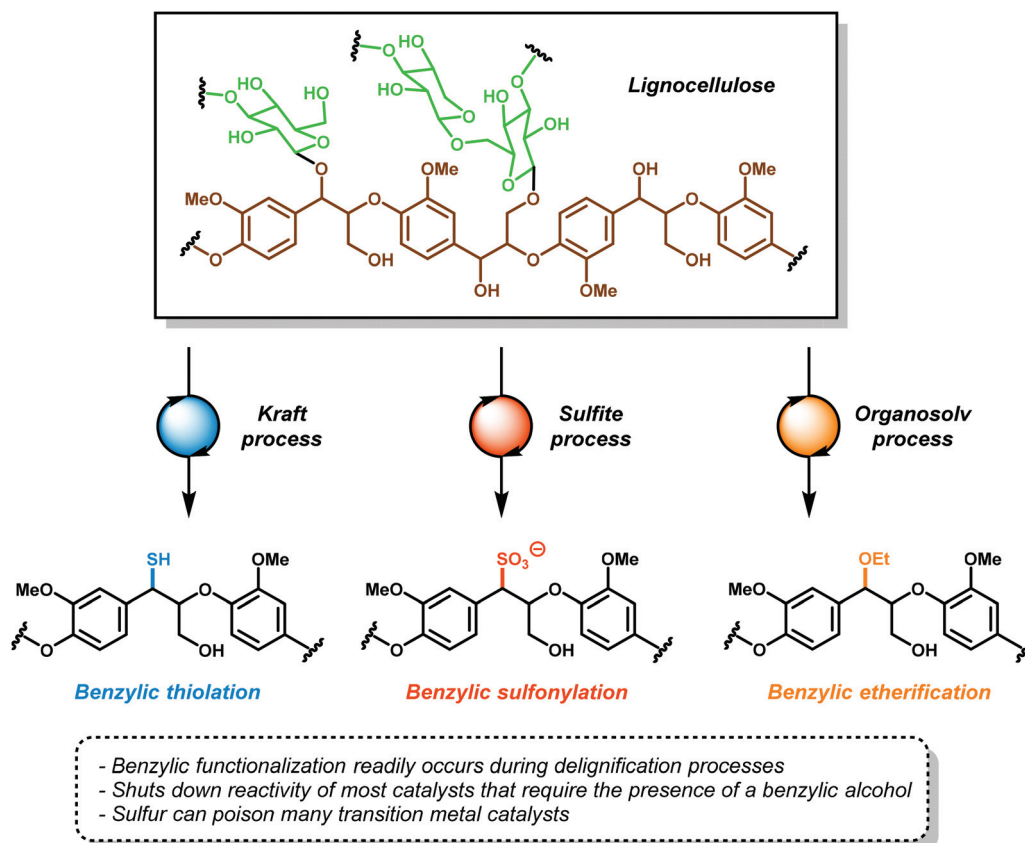
Fig. 4 The lignin pulping processes.

This journal is © The Royal Society of Chemistry 2016

Org. Biomol. Chem., 2016, **14**, 1853–1914 | **1857**

ponent of a polymeric mixture, giving the biosourced consumables.[38] Attempts to valorize this waste stream led to the development of a short-lived chemical process for the synthesis of vanillin from the oxidation of Kraft lignin in 7–10% yield, which was eventually abandoned due to high cost and low efficiency.[9,39]

The organosolv process is a milder delignification process that occurs through the organic extraction of lignin with organic solvents, such as ethanol, dioxane, or acetone.[40,41] Like the Kraft and sulfite processes, organosolv pulping significantly alters the native structure of lignin. All three processes modify the labile β-O-4 linkages, rendering the polymer even more intractable for further degradation. These types of processed lignin are unsuitable for studying the depolymerization of the β-O-4 linkage motif, which is estimated to compose 45–60% of the linkages in native lignin.[18] Utilization of these lignins as a carbon feedstock is hampered by a poor understanding of their structure, which is not only difficult to depolymerize but also likely to produce a large number of inseparable compounds instead of a discrete, easily purified set of products. More advanced pulping technologies such as ball milling[42] or the recently developed γ-valerolactone liquefaction[43] are milder and preserve the overall lignin structure and produce product streams that are more amenable to postprocessing. The development of more advanced preprocessing techniques is an essential challenge to address for the development of a sustainable biorefinery. However, it is unlikely that these techniques will gain any widespread adoption in industry until it is economically viable to do so.

1.4 Strategies towards catalytic depolymerization of lignin

From a topical standpoint, the depolymerization of lignin appears to be a collection of engineering challenges rather than chemical, especially considering the scale by which biomass processing must occur. However, this perception could not be further from the truth—fundamental aspects surrounding lignin's structure, chemoselectivity and general reactivity are poorly understood. The principle challenge of lignin depolymerization arises from its complex chemical structure. This highly branched polymer is not only composed of three different monomers, but the linkage motifs between each monomer are structurally different and non-uniform in sequence. The ideal depolymerization process should thus be able to selectively degrade lignin into discrete, high-value small molecule products. In order to address these issues, a depolymerization catalyst not only has to be able to tolerate the functional groups found in lignin, but also react selectively and resist catalyst deactivation. It is highly probable that the depolymerization of lignin will need to occur over a series of steps to adequately engage the several linkage motifs found in the polymer backbone. The depolymerization strategies that have been exploited thus far can be categorized into three groups: oxidative, reductive, and redox-neutral catalysis and will be further discussed throughout this review.

2. Reductive methods for C−O bond reduction in lignin model systems and lignin

The history of reductive lignin depolymerization began in the late 1930s when scientists experimented with hydrogenating the insoluble biomass isolated from tree sawdust. The central question in these studies was two-fold: how much hydrogen gas could lignin absorb, and what were the products of the hydrogenation? Analysis of the reaction products by distillation and elemental analysis revealed mixtures of alcohols resulting from the hydrogenation and hydrogenolysis of phenol and alkyl phenol derivatives. These early studies greatly contributed towards the understanding of the lignin monomeric constituents, and demonstrated the central chemical challenge for lignin valorization: selective hydrogenolysis over hydrogenation. Formally, hydrogenolysis converts lignin to valuable oxygenated aromatics such as polymethoxylated phenols, benzyl alcohols and phenylpropanols. Alternatively, hydrogenation yields methoxylated carbohydrate derivatives. In most methods, hydrogenation is a result of over-reduction and renders cyclohexyl ether products, which are more easily produced from cellulosic biomass. This section, which covers the development of reductive depolymerization methods, is focused on reports that demonstrated hydrogenolysis selectivity as well as processes that yielded valuable lignin reduction products.

2.1 Early lignin precedent and structure elucidation

Selective hydrogenolysis over hydrogenation was identified by Sauer and Adkins in 1937.[44] At that time, it was known that hydrogenation of alkenes occurred in the presence of Ni, Pd or Pt catalysts with atmospheric pressures of hydrogen gas. Yet, the corresponding ester reduction over platinum group metals required higher reaction temperatures (>200 °C) and hydrogen pressures (>100 atm).[45] This distinct difference in reactivity between alkenes and esters motivated their study of selective hydrogenolysis of unsaturated esters using bimetallic oxide catalysts. Based on reports by Kraft, metallic oxides effectively reduced esters to the corresponding alcohols.[46] Sauer and Adkins then applied this to the reduction of unsaturated esters of butyl oleate and butyl erucate. By screening various bimetallic catalysts, they identified two heterogeneous catalysts—zinc–chromium oxide (ZnCrO) and copper–chromium oxide (CuCrO)—that were capable of selectively reducing unsaturated esters to unsaturated alcohols in good yields (Fig. 5). While selective hydrogenolysis of unsaturated esters to unsaturated alcohols was achieved, Sauer and Adkins noted that this only occurred at a minimum of 300 °C with a 50 mol% metal–oxide loading.[44]

The importance of Sauer and Adkins' findings were realized a year later by Harris, D'Ianni and Adkins when they used a copper–chromium oxide catalyst (Cu–Cr–O) for the reduction of 80 g of hardwood lignin.[47] While selectivity for hydrogenolysis was not observed, the reduction of lignin led to the iso-
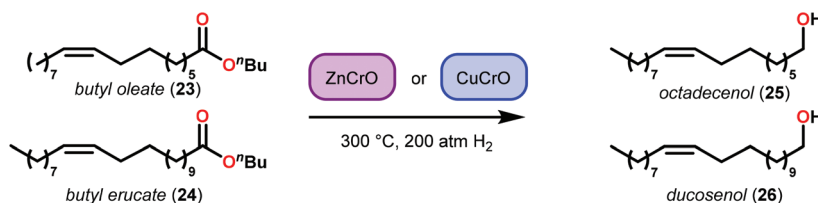
1858 | *Org. Biomol. Chem.*, 2016, **14**, 1853–1914

This journal is © The Royal Society of Chemistry 2016

Sauer and Adkins, 1937

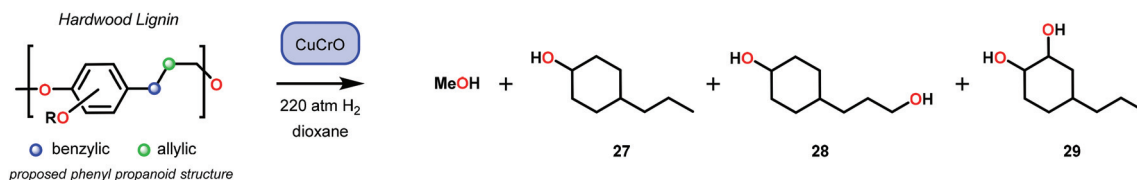**Fig. 5** Sauer and Adkins' selective ester hydrogenolysis in the presence of an alkene.

Adkins and co-workers, 1938

Fig. 6 Isolation of lignin products by Adkins and co-workers, supporting the presence of the phenyl propanoid structure in lignin.
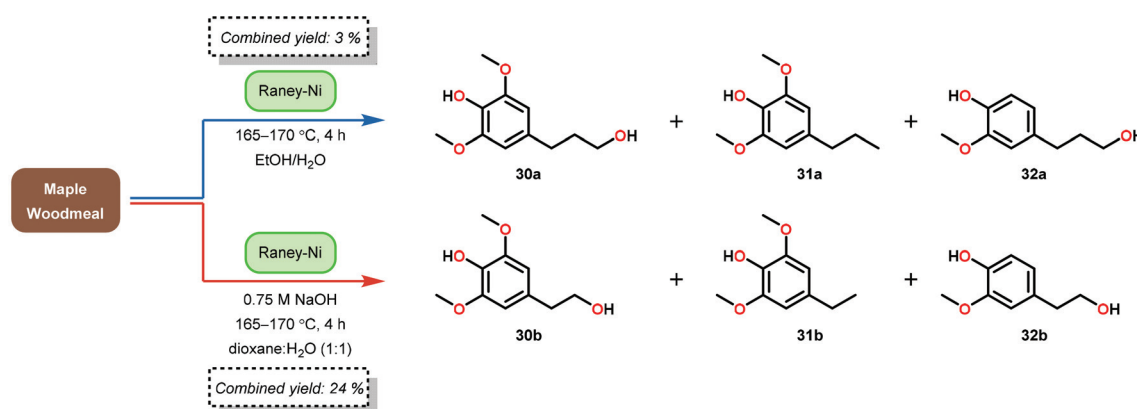
Hibbert and co-workers, 1938

Fig. 7 Reduction of lignin and initial isolation of phenyl propanoids by Hibbert and co-workers.

lation of a few key structure-elucidating products. From the 80 g lignin sample, methanol (22 g), 4-propylcyclohexan-1-ol, (9 g, **27**), 4-(3-hydroxypropyl)cyclohexan-1-ol (20 g, **28**) and 4-propylcyclohexan-1,2-diol (3 g, **29**) were isolated. This report represented the highest recoveries of lignin depolymerization products, at that time and provided support to the hypotheses that lignin was composed of phenyl propanoid units of either C_8 or C_9 length (Fig. 6).

About ten years later, Hibbert and co-workers confirmed the phenyl propanoid monomer structure by isolating 4-(3-hydroxypropyl)-2,6-dimethoxyphenol (**30**), 4-(propyl)-2,6-dimethoxyphenol (**31**) and 4-(3-hydroxypropyl)-2-methoxyphenol (**32**) in a combined yield of 3% from lignin biomass.[48] Hibbert and co-workers applied a reduction procedure using

RANEY®-Ni (previously developed by Adkins[49]), whereby maple woodmeal was reacted at 165–170 °C for 4 hours.[48] The products were subsequently isolated from the unwanted cellulose and hemicellulose biomass by filtration and precipitation, respectively. Furthermore, Hibbert and co-workers reduced the generated products (**30–32**) with Adkins' copper–chromium catalyst to yield the same diol products (**27–29**) that Adkins observed. These studies by Hibbert demonstrated the selective hydrogenolysis of unprocessed lignin, albeit in low yield (Fig. 7).[48]

While the isolation of the actual guaiacyl (**32**) and sinapyl products (**30**) was a major achievement for elucidating the structure of lignin, the isolated yields for this reaction were low (3%). Hibbert further optimized his reduction conditions

by studying the reaction pH. Hibbert found that a mixture of ethanol, water and lignin naturally exhibited a slightly acidic pH of 5.5. Highly acidic conditions proved to be detrimental to the reduction of lignin as acid promoted cross-linking and Ni-catalyst poisoning occurred, while basic conditions promoted Ni reduction and prevented polymerization. Interestingly, these alkaline conditions yielded phenylethanoid monomers in a slightly higher yield of ~24%, suggesting the existence of a β-O-4 lignin linkage and a selectivity basis for hydrogenolysis. Variations in the lignin source (hardwood *vs.* softwood) also afforded different ratios of guaicyl to syringyl monomers.[50]

It is clear from the seminal work of Adkins and Hibbert and their predecessors, that the structure of lignin is highly complex, with source dependent ratios of monomers. Since then, the advancement of nuclear magnetic spectroscopy (NMR) experimentation, including quantitative ^{13}C NMR, ^{1}H NMR, and two-dimensional (2D) NMR, have contributed towards a general understanding of the molecular composition of lignin.[51,52] Ultimately, the body of work describing the chemical structure of lignin has attracted chemists to apply tangentially developed synthetic methodologies to the depolymerization of lignin.

2.2 Hydrodeoxygenation using homogeneous Ni catalysis

Recently, the use of homogeneous transition metal catalysts has been employed for the selective hydrogenolysis of model lignin substrates. The development of this chemistry arose from a fundamental understanding of the mechanism of traditional transition metal-catalyzed cross-coupling chemistry[53–59] (Fig. 8). In this sense, arene C–O bonds are activated by a Pd or Ni catalyst for replacement by a transmetallating hydride. While the ultimate goal of lignin depolymerization has yet to be realized due to catalyst inefficiencies and the complexity of lignin, a variety of metal complexes and hydride sources have been demonstrated for the reductive cleavage of C–O bond frameworks in lignin models.[60–62]

Observation of C–O bond oxidative insertion using Ni was first reported by Wenkert in 1979.[63] Using Ni(PCy$_3$)$_2$Cl$_2$ as a precatalyst, Wenkert and co-workers demonstrated Ni-catalyzed Kumada cross-coupling using phenylmagnesium bromide and a variety of methoxy napthelene and anisole derivatives, demonstrating that methoxy arenes are competent substrates for oxidative additions to Ni. Comparing the reactivity of the methoxy naphthalene to anisole, Wenkert noted a significantly faster reduction of methoxy napthelene substrates opposed to anisole derivatives. This result suggested an initial π-coordination of the Ni^{II} complex to the substrate prior to C–O insertion, in which the polycyclic aromatic structure of the methoxynaphthalenes, compared to the methoxybenzenes, was more amenable for reactivity. Overall, the success of this reaction was an early example of a selective Ni-catalyzed C$_{aryl}$–O bond insertion over the C$_{alkyl}$–O insertion and affect overall deoxygenation.

Inspired by Wenker's report, Dankwardt and co-workers investigated a greater Kumada cross-coupling scope using a
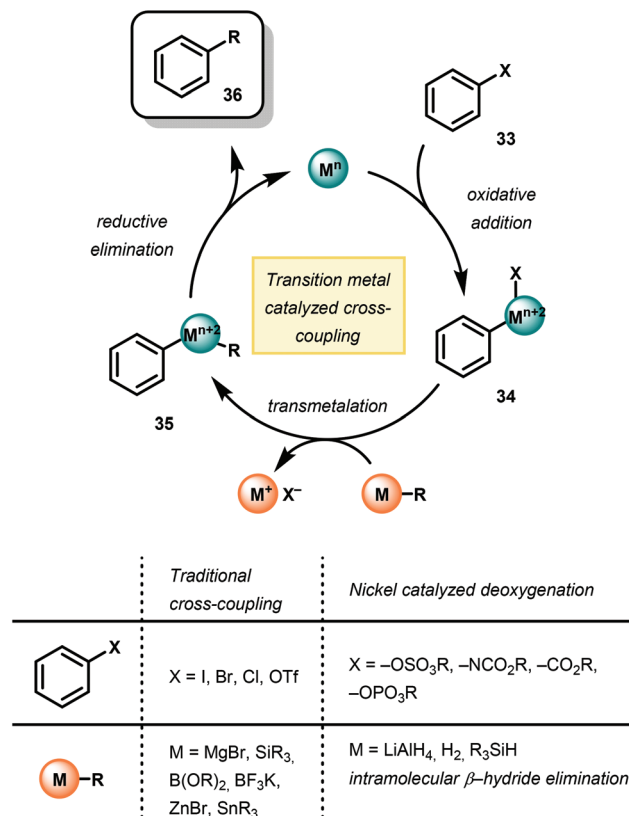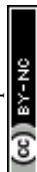

Fig. 8 Comparison of traditional cross-coupling methodology and Ni-catalyzed arene deoxygenation.

	Traditional cross-coupling	Nickel catalyzed deoxygenation
(aryl)–X	X = I, Br, Cl, OTf	X = –OSO$_3$R, –NCO$_2$R, –CO$_2$R, –OPO$_3$R
M–R	M = MgBr, SiR$_3$, B(OR)$_2$, BF$_3$K, ZnBr, SnR$_3$	M = LiAlH$_4$, H$_2$, R$_3$SiH *intramolecular β–hydride elimination*

more electron-rich Ni catalyst.[64] Using a Ni(PCy$_3$)$_2$Cl$_2$ precatalyst, Dankwardt and co-workers successfully demonstrated the Ni-catalyzed cross-coupling on a large variety of methoxyarenes with phenyl magnesium bromide. This Ni–phosphine precatalyst proved more efficient and versatile than Wenkert's catalyst (Ni(PPh$_3$)$_2$Cl$_2$), tolerating a number of nucleophilic functionalities, including hydroxy, phenol, amine, enamine and N-heterocyclic moieties. More relevant to lignin valorization, Dankwardt and co-workers focused on dimethoxy-benzenes and naphthalanes to explore the scope of arene substitution tolerance (Fig. 9). Regardless of the functional group tolerance observed, the poor yields of the Kumada-coupling products with dimethoxynaphthalene and dimethoxybenzene suggested poor compatibility with guaiacyl and syringyl-type substrates.

Since Wenkert's intial report, Ni-mediated C–O bond activation strategies have been reported for a large variety of activated oxyarene bonds including sulfonates, sulfates, mesylates, vinyl esters, carbamates and carbonates for C–C bond synthesis.[65–67] In search of a general hydrogenolysis methodology of oxyarenes, Martin and co-workers screened a number of hydride reagents including silanes, borohydride salts, alkyl zinc and alkyl aluminum reductants. Optimally, they found the combination of Ni(COD)$_2$ with 1,1,3,3-tetramethyl-disiloxane (TMSDO) was an efficient method for reductive demethoxylation of arenes (Fig. 10).[68] Importantly, methoxy
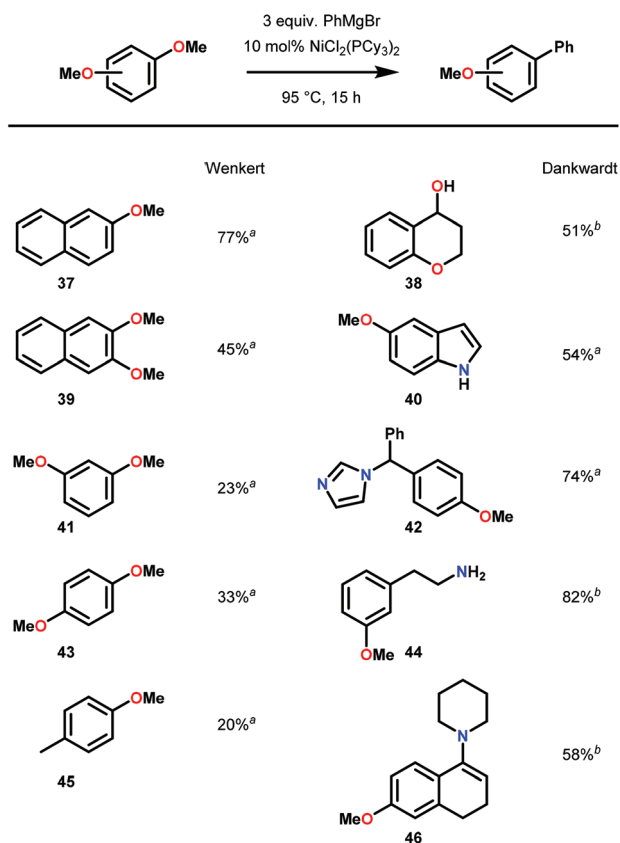
1860 | *Org. Biomol. Chem.*, 2016, **14**, 1853–1914

This journal is © The Royal Society of Chemistry 2016

Fig. 9 Ni-catalyzed Kumada cross-coupling of methoxy arenes. [a] Yields of isolated products. [b] Conversions were determined by GC using tridecane as internal standard.
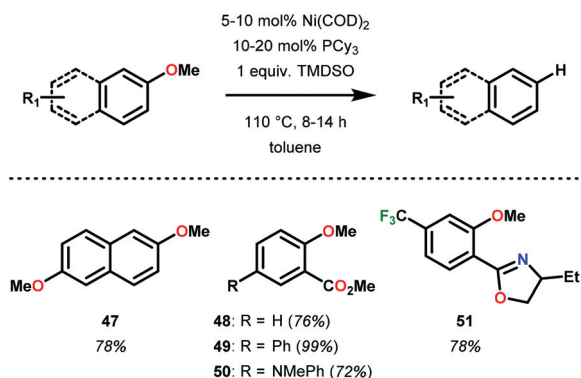

Fig. 10 Ni-catalyzed C–O bond reduction of aryl ethers. TMSDO = 1,1,3,3-tetramethyldisiloxane.

arenes were reduced in highest yield in comparison to other oxygen functionalities, such as OEt, OAc, OPiv, OTs and OMs.

Soon after Martin's report, Hartwig and Sergeev reported the C_{aryl}–O bond cleavage of a variety of alkyl aryl ether substrates (Fig. 11). Hartwig and Sergeev accomplished these challenging reductions *via* a Ni–NHC (N-heterocyclic carbene, SIPr) complex that is uniquely resistant towards irreversible reduc-

tive elimination to a heterogeneous solid, a common issue in homogeneous cross-coupling chemistry. Impressively, the Ni-catalyst formed *in situ* was compatible with a number of hydride sources (including DIBAL-H, LiAl(O^{i}Bu)$_3$H, Et$_3$SiH), however, the system garnered the interest of the catalysis community by engaging H$_2$ as the terminal reductant. In practice, Hartwig demonstrated a general substrate tolerance of Ar–OAr (52), Ar–OMe (53) and ArCH$_2$–OMe (54), showcasing the ability of Ni to reduce both C_{sp^2}–O and C_{sp^3}–O bonds. Notably, this catalyst selectively reduced aryl–aryl ethers in the presence of aryl–alkyl ethers, showing promise for a selective 4-O-5 depolymerization of lignin and lignin model systems (Fig. 11).[69] Despite the high selectivity and mild reaction conditions in comparison to classic lignin hydrogenolysis reactions, this system employs high loadings of potassium *tert*-butoxide as an additive and an expensive NHC ligand (~$66/g Sigma Aldrich[70]).

About two years later, Hartwig and co-workers refined their Ni catalyzed deoxygenation by excluding the carbene ligand (SIPr) after discovering heterogeneous conditions capable of similar C–O reductions.[71] This second generation system solely relied upon NaO^{t}Bu and 1 atm of H$_2$ to achieve the wanted C–O hydrogenolysis. Further pre-catalyst screening uncovered that the use of Ni(CH$_2$TMS)$_2$(TMEDA) (in a ten times lower catalyst loadings than the first generation conditions), could achieve similar C–O bond reduction. Lastly, the first and second generation conditions exhibited orthogonal efficiency in aryl ether reductions of electron-rich and electron-deficient arenes.

Overall, the impressive reactivity of Martin's and Hartwig's Ni-based systems represents orthogonal reactivity amongst reductive methodologies. Martin's approach exemplifies a homogeneous cross-coupling method in which hydride transmetalates and reductively eliminates to yield a deoxygenated arene. The reactivity observed under Hartwig and co-workers' conditions is intriguing and indicates that slight changes in reaction conditions can significantly affect the selectivity. While Hartwig's first generation "Ni carbene" approach mechanistically mimics that of Martin's, the second generation "ligandless Ni" system is heterogeneous and likely mechanistically unrelated, allowing milder reaction temperatures and H$_2$ pressures.

In a subsequent mechanistic study,[72] Agapie and co-workers studied the hydrogenolysis of aryl ethers by Ni. By using a specially designed phosphine-methoxyarene ligand, the authors directly observed the Ni^0 complex 73 as a dark red solid where the Ni center interacts with two carbon centers of the central arene. Additionally, after C–O bond insertion, the Ni^{II} complex (74) readily underwent β-hydride elimination to afford a Ni^{II} aryl hydride species (75) and the corresponding carbonyl compound. Subsequent reductive elimination and decarbonylation afforded an isolable Ni^{II} complex (76). While the stoichiometric studies provided isolable intermediates, Agapie and co-workers further studied the β-hydride elimination in a Ni catalytic reaction. Applying Hartwig's deoxygenation conditions to trideuteromethoxy naphthalene (78) and
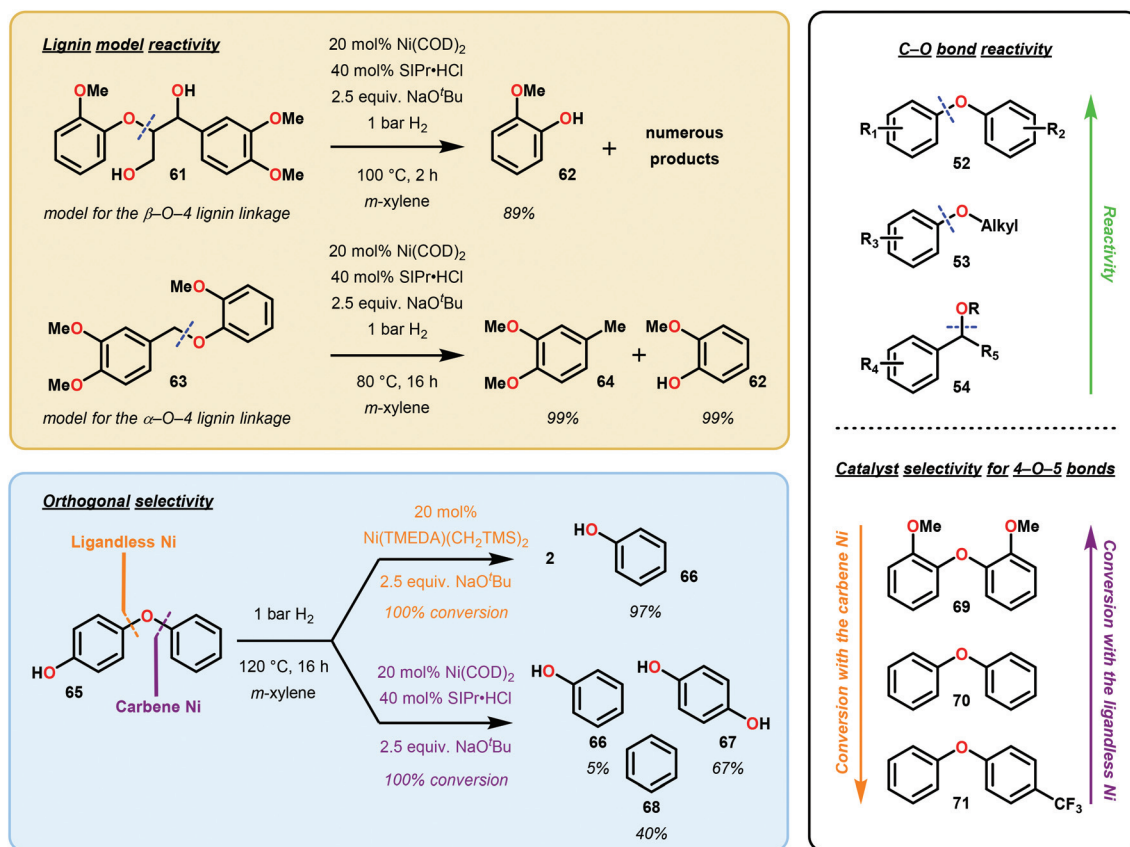
This journal is © The Royal Society of Chemistry 2016

Org. Biomol. Chem., 2016, **14**, 1853–1914 | **1861**

Fig. 11 Ni-catalyzed hydrogenolysis of aryl ethers.

2-((hexyl-1,1-d_2)oxy)naphthalene (**79**), 90% deuterium incorporation from deoxygenation was observed. These studies suggested that β-hydride elimination is a competent pathway and explained why other methods are capable of using mild atmospheres of H$_2$. Furthermore, the obtained results also illustrated that the selectivity for C_{aryl}–O insertion over the weaker C_{alkyl}–O insertion was due to π-coordination of the arene to the Ni center, which promoted insertion of Ni into the C_{aryl}–O bond (Scheme 2).

Prompted by Agapie's work, Martin and co-workers investigated the catalytic mechanism of Ni catalyzed arene deoxygenation, under the pretence that the system did not operate *via* a β-hydride elimination mechanism.[73] Martin found that Agapie's C–O inserted complexes, such as complex **74**, were not reactive towards exogenous silane sources for deoxygenation and were not indicative of an intermolecular reaction between hydride reductants and Ni inserted species. Yet, empirical evidence for a Ni⁰/Ni^II cross-coupling mechanism for Martin's first generation Ni(COD)$_2$ arene deoxygenation using TMSDO was not proven. Lastly, the following experimental observations were gleaned from their initial study:[68] (1) Ni(COD)$_2$ was the only Ni precatalyst capable of deoxygenating methoxy arenes, (2) control experiments performed in the absence of silane indicated that silane was necessary for the reduction to occur, (3) napthalene substrates consistently

afforded higher yields compared to their anisole derivatives, and (4) PCy$_3$ was the critical ligand.

The mechanistic experiments performed by Martin and co-workers suggest that the formation of a Ni^I-SiR$_3$ species is necessary for arene deoxygenation (Fig. 12). Firstly, they found that preparation of a napthyl-Ni–O species was not possible by simple oxidative insertion with the Ni(COD)$_2$ precatalyst (Fig. 12A). Alternative synthesis by means of oxidative insertion into 2-napthylchloride, followed by sodium methoxide transmetalation was indeed feasible (Fig. 12A). However, this complex decomposed at room temperature to yield naphthalene (from H/arene reductive elimination) and the Ni(PCy$_3$)$_2$(CO) complex. In order to successfully synthesize a napthyl-Ni–O complex, [Ni(PCy$_3$)$_2$]$_2$N$_2$ was needed for direct C–O oxidative insertion, to give naphthalene in 54% yield. Lastly, they found that silane reduction outcompeted intramolecular β-hydride elimination, even when using the activated precatalyst [Ni(PCy$_3$)$_2$]$_2$N$_2$. The experiments are highly suggestive that the β-hydride elimination pathway is merely a minimally contributing pathway.[73]

The authors subsequently determined the kinetic dependence of each of the reaction components and found that all three components—substrate, catalyst, and the silane—exhibited a first-order dependence. Analysis of silane consumption by GC indicated an induction period which was further exasper-

1862 | *Org. Biomol. Chem.*, 2016, **14**, 1853–1914

This journal is © The Royal Society of Chemistry 2016
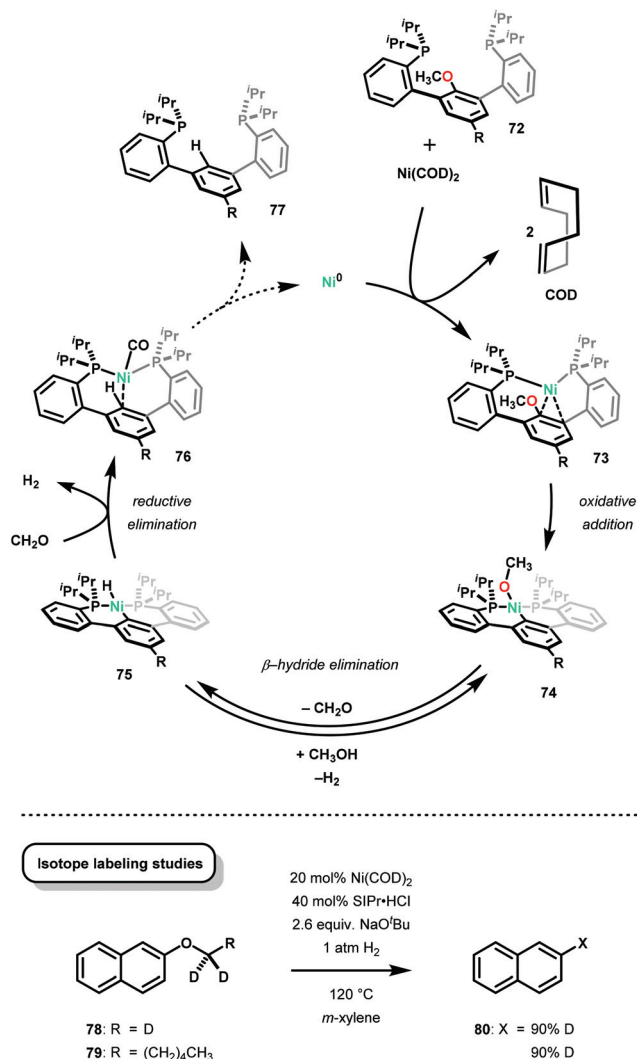
Scheme 2 Ni-mediated hydrogenolysis of C_{aryl}–O bonds.

ated by a kinetic isotope effect when Et_3SiD was used. Rapid consumption of the silane was observed by ^1H NMR in the presence of a stoichiometric amount of Ni, even in the absence of naphthalene production. Support for a Ni^IH–Si insertion product was given by the observation of a ^1H NMR signal at −15.8 ppm, indicative of a Ni–H intermediate, and a characteristic Ni^I EPR spectrum. These results together with computational modeling suggested the formation of a catalytically active Ni^I species as shown in Fig. 12C.[73] Overall, this study concluded that the mechanism in which Ni deoxygenates arenes is greatly dependent upon the exogenous reductant employed. While intramolecular β-hydride elimination from the napthyl-Ni–OCH_3 intermediate is precedented,[74] it is not the dominant process when stoichiometric amounts of hydride (R_3SiH, $LiAlH_4$) or H_2 are used.

2.3 Heterogeneous Ni-catalyzed deoxygenation

A major limitation of homogeneous Ni catalysis is the incompatibility of most Ni precursors with aqueous solvents. To

address this concern, Lercher and co-workers developed a heterogeneous Ni–SiO_2 catalyst capable of hydrogenolysing α-O-4 and β-O-4 linkages in lignin model systems. For the synthesis of the catalyst, Ni was deposited on silica using urea as the hydrolysis reagent, where the particle size of Ni was controlled by the calcination temperature (400–800 °C). Catalyst activity, as measured by turnover frequency (TOF), peaked at 26 h^{-1} when the particle size was 5.9 nm. Using the heterogeneous catalyst and 6 bar of H_2, the reduction of simple lignin model ethers was demonstrated (Fig. 13), with moderate selectivity for hydrogenolysis in the α-O-4 and β-O-4 model systems *versus* over reduction to cyclohexanols. For the hydrogenolysis, a kinetic distinction between the α-O-4, 4-O-5 and β-O-4 systems was observed, consistent with an increasing order of activation energy (E_a).[75] The development of a heterogeneous catalyst that utilizes relatively low hydrogenation pressures of H_2 (6 bar) in aqueous media was a substantial step towards the reductive valorization of lignin. Although the Ni/SiO_2 was shown to reduce simple lignin model systems, more complex systems containing free alcohol moieties, which are known to deactivate transition metal catalysts, were not evaluated.

A variety of heterogeneous catalysts have been prepared and shown to reduce lignin and associated models. Design aspects of these catalysts include: immobilization on a solid phase (typically carbon or silica), doping with another metal, or synthesized as the metal or bimetallic oxide.[76] In certain cases, these catalysts were demonstrated to perform selective hydrogenolysis over hydrogenation.[77–80] The results from these studies highlight the fact that the isolated lignin monomer units greatly vary and a controlled depolymerization has been difficult to accomplish. Despite this fact, bimetallic catalysts and heterogeneous catalysts are the subject of intense research for reductive methods towards the valorization of lignin. The key effects exhibited by bimetallic catalysts in the reduction of lignin feedstocks have been summarized by Dumesic and co-workers.[81]

2.4 Pd and Ni mediated hydrogen transfer methods for reduction of C–O bonds

In this section, details on the work of Rinaldi,[82] Samec[83–85] and Rauchfuss[86] are described as it highlights the C–O bond reduction through a formal redox-neutral hydrogen shuttle from an alcohol, ether or formic acid. Transfer hydrogenation chemistry that utilizes lignin as the hydrogen source is detailed in the redox-neutral section (section 4). Both exogenous and endogenous transfer hydrogenation methods have been directly studied for depolymerizing native lignin feedstocks and exemplify valorization through the isolation of monomeric or dimeric units, suggesting that these methods are the closest to industrialization.

Recent development in catalytic lignin reduction through hydrogen transfer reduction was achieved by Rinaldi and co-workers, who showed the hydrogenation and hydrogenolysis of a number of sinapyl and guaiacyl models using RANEY®-Ni and 2-propanol at moderate temperatures (120 °C). While
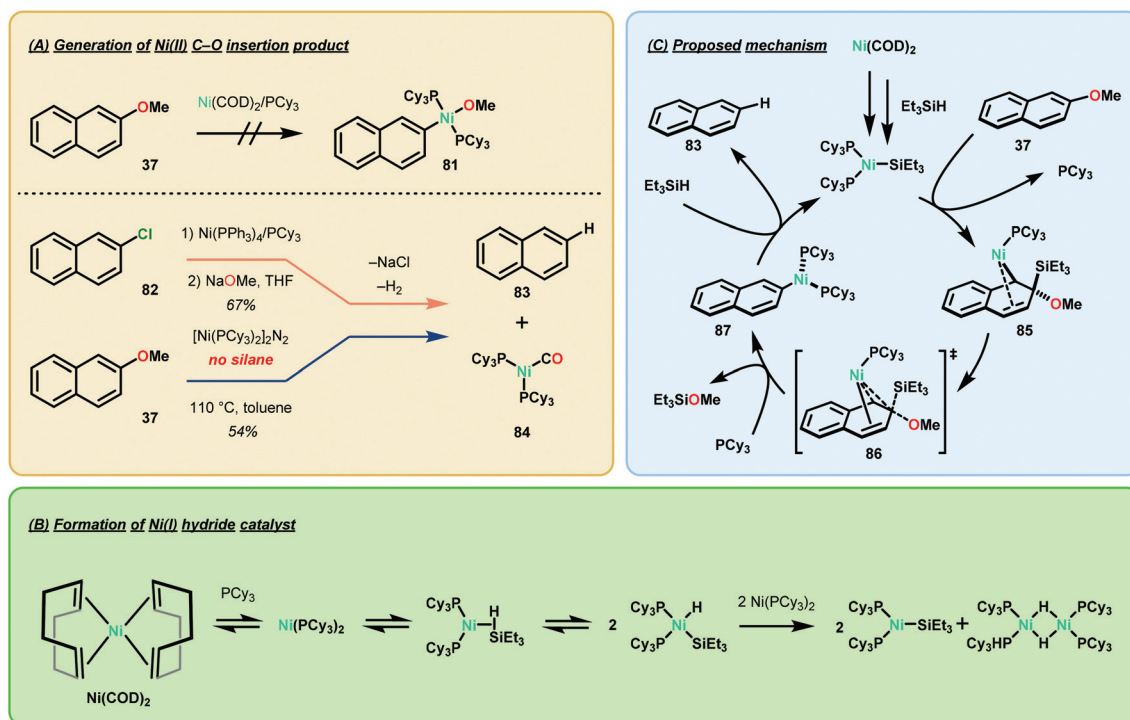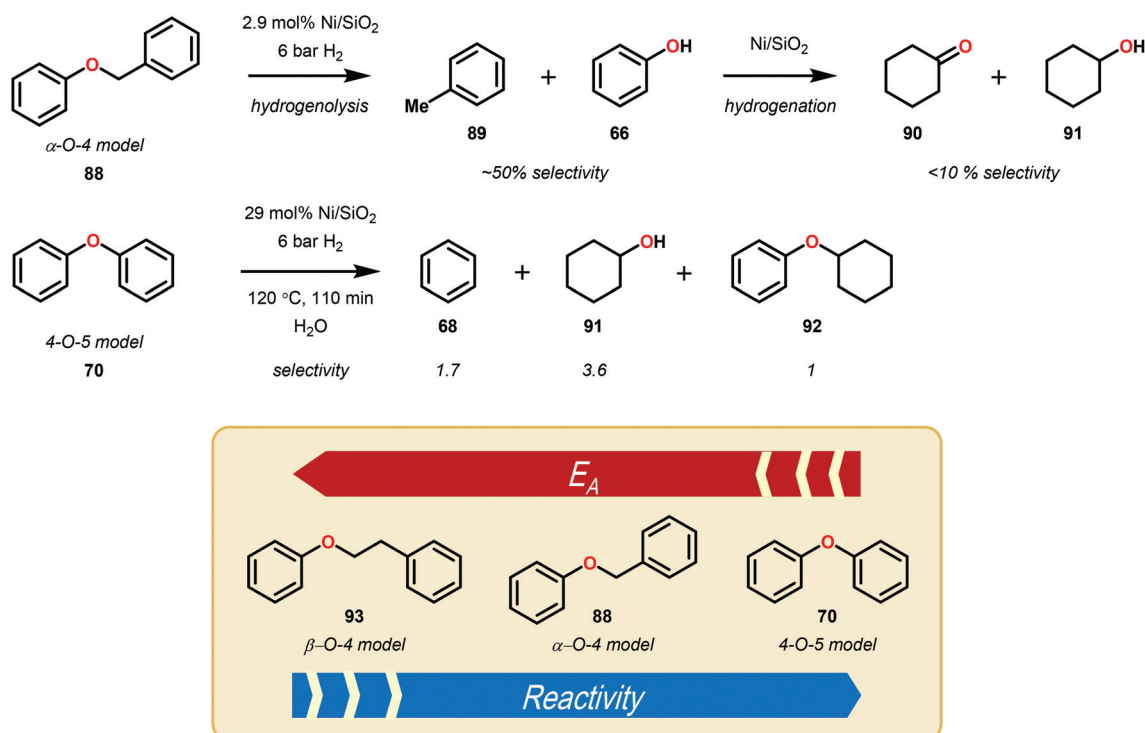
This journal is © The Royal Society of Chemistry 2016

Org. Biomol. Chem., 2016, **14**, 1853–1914 | **1863**

Fig. 12 Mechanistic considerations of Ni-catalyzed reductive C−O bond cleavage.

Fig. 13 Hydrogenolysis of simple lignin model systems utilizing a heterogeneous Ni/SiO₂ catalyst.
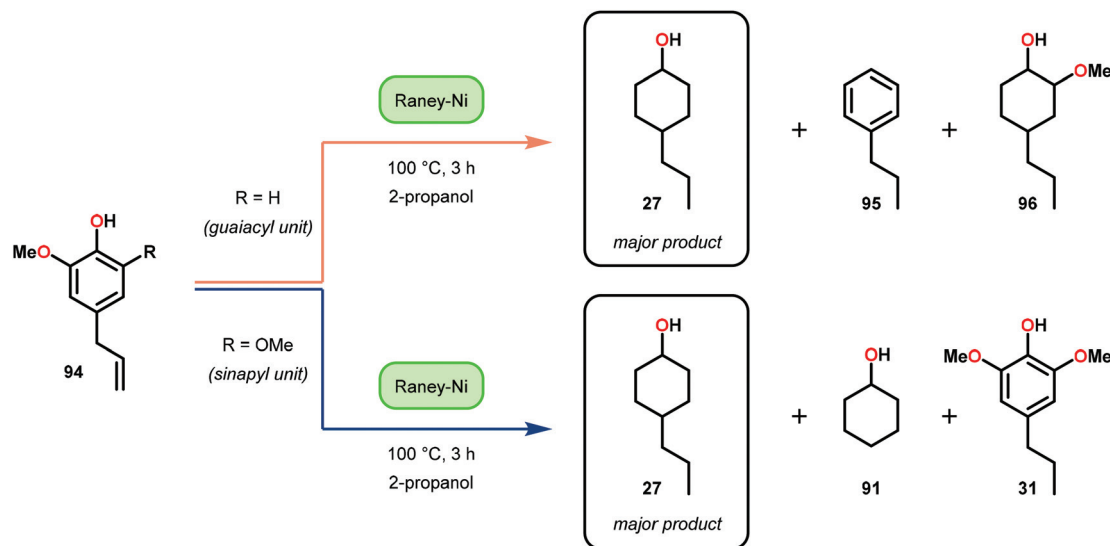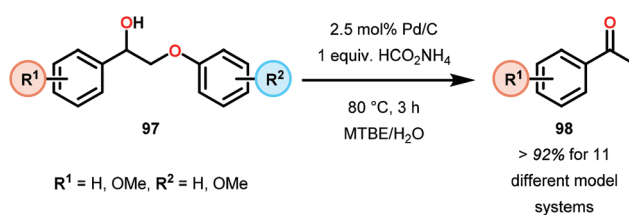
Fig. 14 RANEY®-Ni catalyzed transfer hydrogenation of lignin model substrates.

reduction between 80–150 °C using 2-propanol as the reductant is a notable achievement, each reaction produces an array of partially reduced products (Fig. 14). The selectivity is biased towards hydrogenation over hydrogenolysis; however, hydrogenolysis occurs in both the absence and presence of alkene and arene functionalities. The authors found that the selectivity of arene hydrogenation could be diverted when using bulky *tert*-butyl substituted substrates, albeit these are not recognized functionalities in the monomer constituents of native lignin. More importantly, the RANEY®-Ni catalyzed reduction on a mixture of benzaldehyde, benzofuran, diethyl maleate and guaiacyl acetone was evaluated. Transfer hydrogenation transformed the starting mixture to 2,3-dihydrobenzofuran, diethyl succinate, 4-(2-hydroxypropyl)-2-methoxyphenol and cyclohexane-1,2-diol, and showcased the reductive capability of hydrogen transfer in the presence of a mixture of oxygenated functionalities. Unfortunately, during their investigation they recognized that the presence of primary alcohol moieties inhibited the transfer hydrogenation when using 2-propanol as the hydrogen source. Although primary alcohols were not destructive for the catalyst system, they were shown to inhibit catalyst turnover. Overall, reaction efficiency was measured by starting material consumption, thus proving transfer hydrogenation with alcohols as a possible biomass conversion process for further applications.[82]

Samec and co-workers advanced reductive hydrogen transfer catalysis by demonstrating the reduction of β-O-4 lignin model systems using Pd/C and transfer hydrogenation. These conditions were developed by screening a variety of transition metals and hydrogen donors. A comparison of Pd/C, Rh/C, Ir/C, Re/C, Ni/C, revealed that Pd was unique in reducing β-O-4 model compounds to the corresponding acetophenone and phenol. Addition of a stoichiometric equivalent of amine (ammonia, ethyl amine, allylamine), directed the selectivity of

this reaction towards β-O-4 cleavage and not the disproportionation reaction (to yield **100** and **102**). Lastly, formic acid was found to efficiently facilitate reduction as compared to H_2 or 2-propanol. Using these conditions, the authors demonstrated the reduction of a variety of β-O-4 model systems (**97**) to afford the cleaved products (**98**) in excellent yields (Scheme 3). The extent of the reduction was controlled by time and stoichiometric addition of formic acid (Scheme 4). The authors demonstrated that the β-O-4 cleavage was specific to benzylic alcohols containing at least one β-hydrogen (Fig. 15). These observations, in combination with an observed kinetic isotope effect of the benzylic C–H bond, suggested that the operating mechanism involves dehydrogenation and deprotonation to afford a Pd enolate species as the operative mode of transition metal activation (*cf.* Scheme 45). Further reduction by formic acid subsequently yields the acetophenone and phenol β-O-4 cleavage products. Finally, applying the reduction system on a β-O-4 model polymer resulted in almost quantitative formation of the acetophenone (**109**) or ethylbenzene product (**110**) depending on the reaction conditions (Scheme 5). Encouraged by these results, the authors applied the catalytic system on organosolv lignin from *Pinus sylvestris*. GPC analysis showed a moderate change towards lower molecular weight fragments.[84]

Scheme 3 Heterogeneous Pd-catalyzed cleavage of β-O-4 model systems.

This journal is © The Royal Society of Chemistry 2016

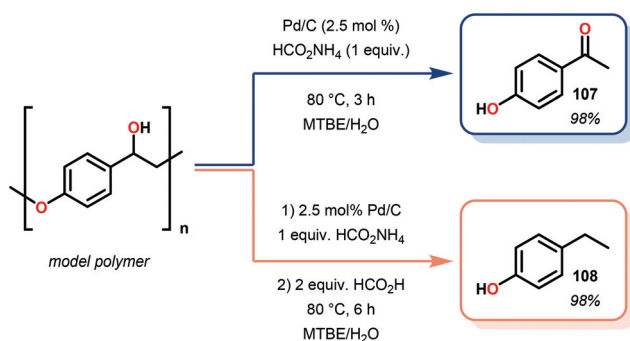*Org. Biomol. Chem.*, 2016, **14**, 1853–1914 | **1865**
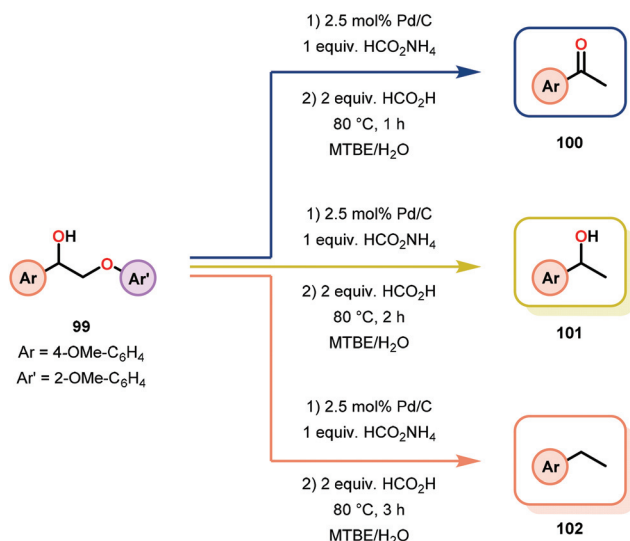
Scheme 4 Pd-catalyzed selective transformation of lignin model systems.
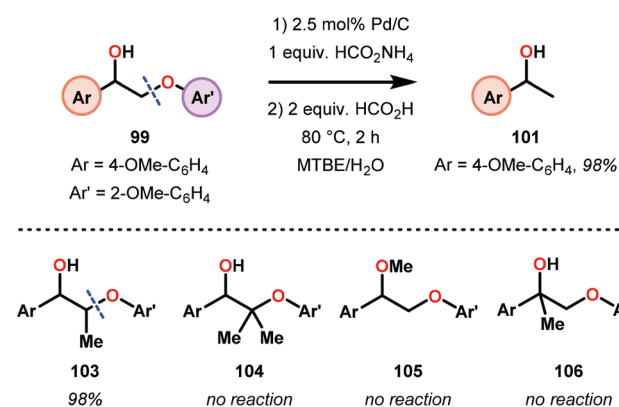
**Fig. 15** Reactivity pattern for heterogeneous Pd-catalyzed cleavage of lignin model systems.

**Scheme 5** Depolymerization of lignin model polymer by Pd/C.

Soon after this publication, Samec and co-workers reported on a key insight regarding traditional organosolv processing. Realizing that formic acid is generated in the organosolv

lignin pulping process,[87] the authors developed a tandem organosolv-hydrogen transfer protocol that depolymerized lignin. Specifically, pine sawdust was processed using ethanosolv conditions with Pd/C (195 °C, 1 h, EtOH/H_2O 1 : 1). From the resulting biomass mixture, cellulose was filtered off, hemicellulose is removed by precipitation and a clear lignin bio-oil was obtained. In a comparison between an organosolv process with and without Pd reduction, it was found that the reduced feedstock had an average molecular weight half of the non-reduced stock, as well as 58% monomeric composition of the reduced material. 2D NMR spectroscopy additionally revealed that the targeted β-O-4 bonds were reduced. Interestingly, the major monomeric component from the pine feedstock was 3-methoxy-4-hydroxyphenyl-2-butene (**109**), isolated in 23% yield. This was proposed to be produced by sequential dehydration–hydrogenation, which ultimately produced arylbutenes **109** (Fig. 16).[85] This study of lignin degradation is unique since the tandem organosolv transfer hydrogenolysis (TOTH) process reduced actual lignin to an isolable monomer and that the presence of an alkene functionality in this monomer indicates that the TOTH process is highly selective for C–O bond reduction over C=C bond reduction.

Similar approaches towards TOTH have been investigated by Rauchfuss and co-workers.[86] Using Pd/C reduction, Rauchfuss and co-workers demonstrated the ability of ethereal solvents to donate hydrogen analagous to Rinaldi and co-
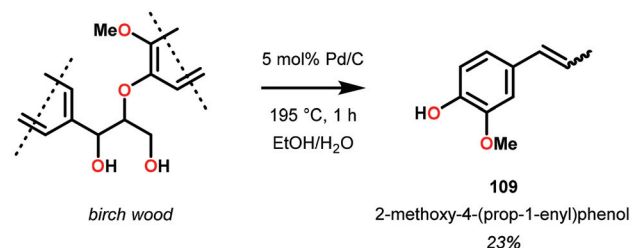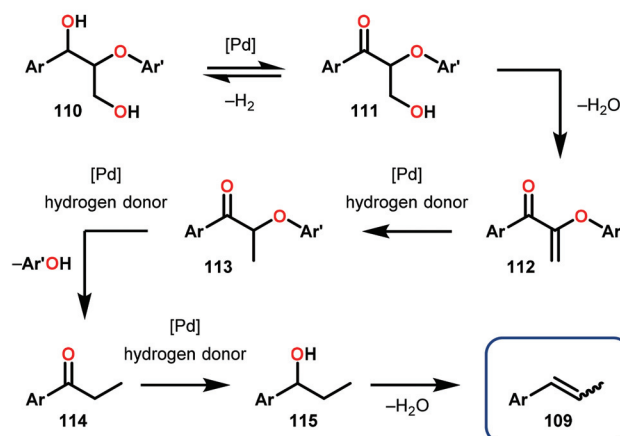
Fig. 16 (Top) Pd/C catalyzed tandem organosolv transfer hydrogenolysis (TOTH) of birch wood and (bottom) proposed mechanism of aryl propene formation.

1866 | *Org. Biomol. Chem.*, 2016, **14**, 1853–1914

This journal is © The Royal Society of Chemistry 2016
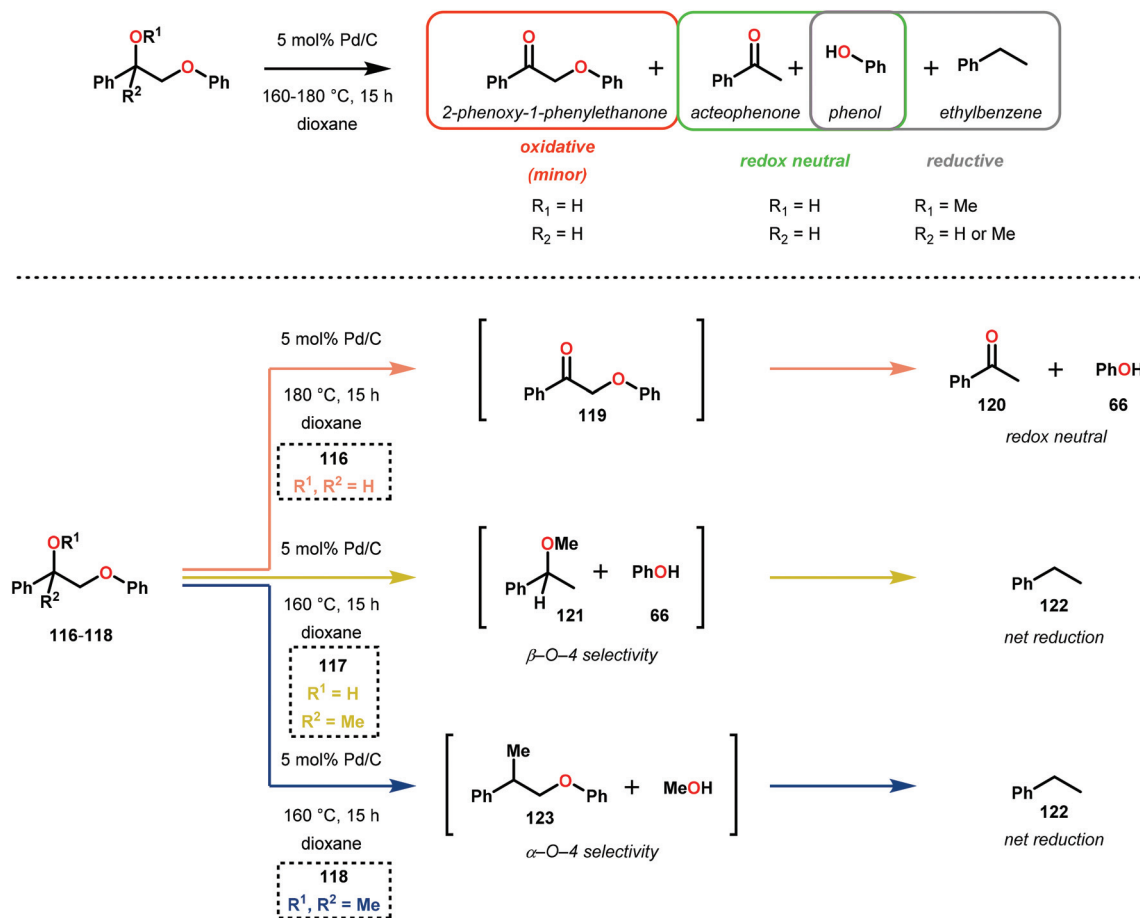
Fig. 17 Pd/C catalyzed C−O bond cleavage using dioxane as hydrogen source.

workers.[82] Yet, Rauchfuss found contradictory mechanistic results to Samec. For lignin motifs containing a primary benzylic alcohol unit, β-O-4 reduction was proposed to occur in one of two ways (Fig. 17). Firstly, the redox-neutral pathway of dehydrogenation and reduction could potentially occur, furnishing acetophenone (**120**) and phenol (**31**). Additionally, the same pathway could be reversed, whereby direct β-O-4 cleavage could occur by a Pd–H species (to produce phenol **31**), followed by oxidation of 1-phenylethanol (**124**) to yield acetophenone (**120**). Unique to this investigation was the observance of the reduction of benzylic ethers. Conversion of these motifs proceeded in a net reductive fashion because the benzylic ether cannot initially be oxidized to the ketone. In this sense, Rauchfuss and co-workers observed selective β-O-4 reduction over α-O-4 reduction in the case of benzylic ethers containing a benzylic hydrogen, and selective α-O-4 reduction merely when the benzylic ether substrate contained an additional alkyl group at the benzylic position. Regardless of this, the lignin model systems were fully reduced to the corresponding phenol and alkyl arene components in these reactions.[86] By showing that the reduction proceeded without the need of external hydrogen donors, the non-innocent role of dioxane in the reduction of lignin model systems containing both

benzylic alcohol and benzylic ether motifs were demonstrated (Scheme 6).

2.5 Other metal-mediated methods for conversion of lignin related systems

While Ni and Pd have mainly been investigated with great promise towards conversion of lignin related systems through a combination of C–O bond activation or direct hydrogenolysis, other homogeneous metal catalysts have been probed for aryl ether C–O bond reduction. One such metal is Ti, which has been demonstrated to stoichiometrically cleave β-O-4 bonds through an enolate arlyoxide complex (**127**) of a model lignin substrate. Smith and co-workers designed this approach, targeting Ti for its oxophilicity and realizing that the vicinal oxygen functionalities of lignin could ligate and promote a Ti-mediated method. Using a TiCp$_2$(BTSMA) complex (**125**; Cp = cyclopentadienyl; BTSMA = bis(trimethylsilyl)acetylene), Smith and co-workers observed the α-aryloxy ketone **126** to ligate and fragment at the β-O-4 bond. The identity of this TiCp$_2$(enolate)(aryloxy) complex (**127**) was confirmed by a separate *de novo* synthesis and structural data was affirmed through X-ray crystal structure determination. Despite these results, the oxophilicity of Ti^{IV} proved too great to allow

This journal is © The Royal Society of Chemistry 2016

Org. Biomol. Chem., 2016, **14**, 1853–1914 | **1867**
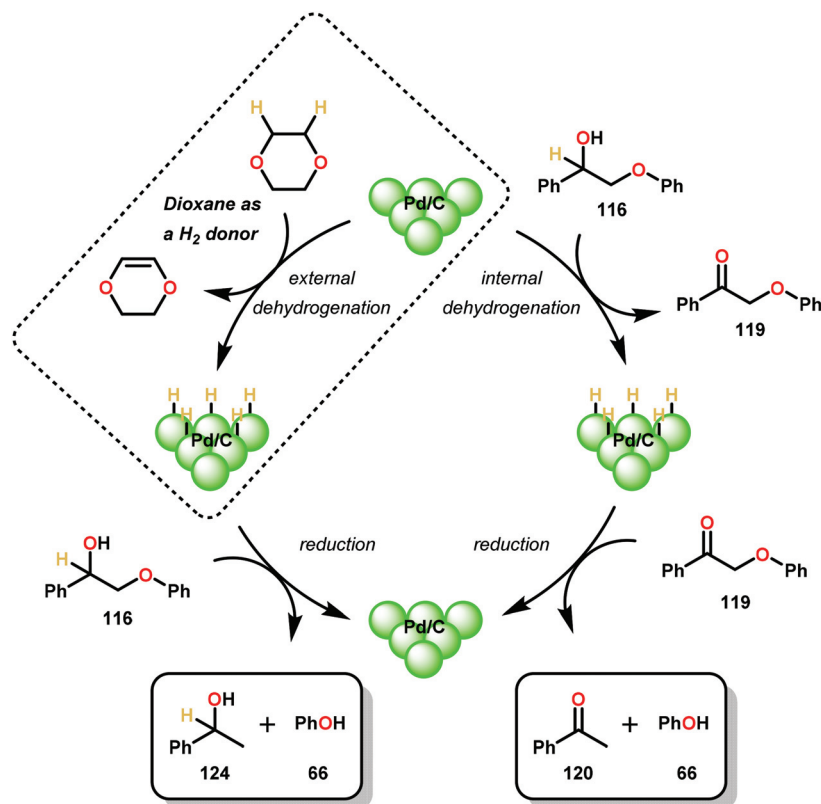
Scheme 6 Plausible mechanisms for Pd/C catalyzed C−O bond cleavage.

for catalytic turnover to be realized. Strong acids such as triflic acid were tested to promote ligand dissociation and generation of a $TiCp_2(OTf)_2$ complex, yet the aryloxy ligand was ultimately unwilling to undergo ligand exchange (Scheme 7).[88] Although this method did not afford a catalytically viable procedure, further development in this area could address the issue of aryloxy disassociation and yield a Ti^{IV} catalyst capable of fragmenting lignin related compounds in a catalytic fashion. This scenario could perhaps be realized by identifying an ancillary ligand framework that can address the reactivity challenges identified in this study.

Another abundant transition metal shown to reduce lignin model systems is Fe. Yao and co-workers recently demonstrated the reduction of diaryl ethers using $Fe(acac)_3$ (acac = acetylacetonate) in combination with either $LiAlH_4$ or H_2 as a terminal reductant. Ligand selection proved crucial in the identification of an effective catalyst for this transformation. Yet, the active catalyst was found to be heterogeneous, as filtration of the reaction mixture ceased reaction progress.[89] Additional support for a heterogeneous operating catalytic entity was determined from a mercury test,[90] which poisoned the catalyst. Regardless, a combination of 20 mol% of $Fe(acac)_3$ with 1 atm of H_2 under basic conditions was sufficient to cleave the diaryl ether bond.[89]

The catalytic methods summarized thus far are all dependent upon inner-sphere coordination and transformation.

A uniquely, outer sphere catalyst was developed by Nozaki and co-workers to avoid potentially insurmountable ligation issues encountered in inner-sphere catalysis. In doing so, Nozaki and co-workers identified a dihydridoiridium complex (**131**) capable of catalyzing arene deoxygenation, proceeding through an outer sphere mechanism. Utilizing the hydroxycyclopentadienyl dihydridoiridium complex **131**, the authors observed this catalyst to facilitate the reduction of phenols and hydroxy napthalenes at high temperatures using low H_2 pressures via metal–ligand cooperative hydrogen transfer (Fig. 18). Excellent yields were obtained for the more reactive naphthenol substrates, such as substrate **136**, and the "conventional" reduced reactivity was observed with the phenol derivatives **132–135**. This catalyst was proposed to operate through an intricate hydrogen-bonding network to effectively activate the aryl C–O bond for hydride reduction to yield benzene and water (Scheme 8).[91] The relatively mild reaction conditions associated with this protocol together with a cooperative metal–ligand catalytic cycle can be of importance for future conversion of lignin to value-added products.

2.6 Reductive cleavage of lignin model systems through photoredox catalysis

Recently, the emergence of photosensitive metal catalysts, and organic dyes, for organic redox transformations has attracted significant attention. One of the fascinating properties of

1868 | *Org. Biomol. Chem.*, 2016, **14**, 1853–1914

This journal is © The Royal Society of Chemistry 2016
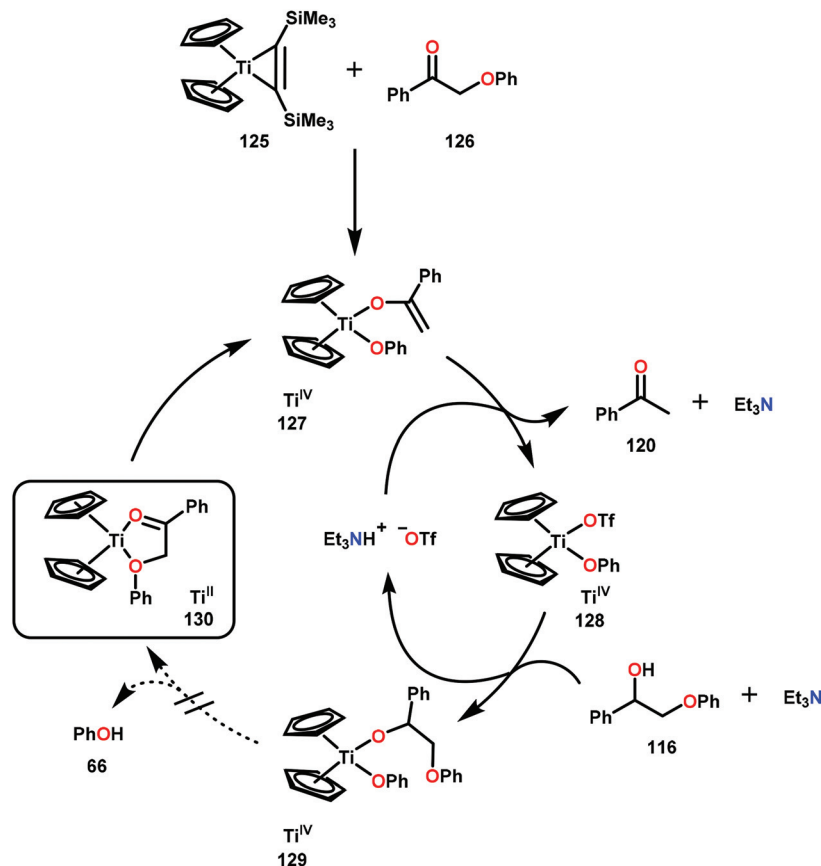
Scheme 7 Titanium catalyzed C−O bond cleavage.
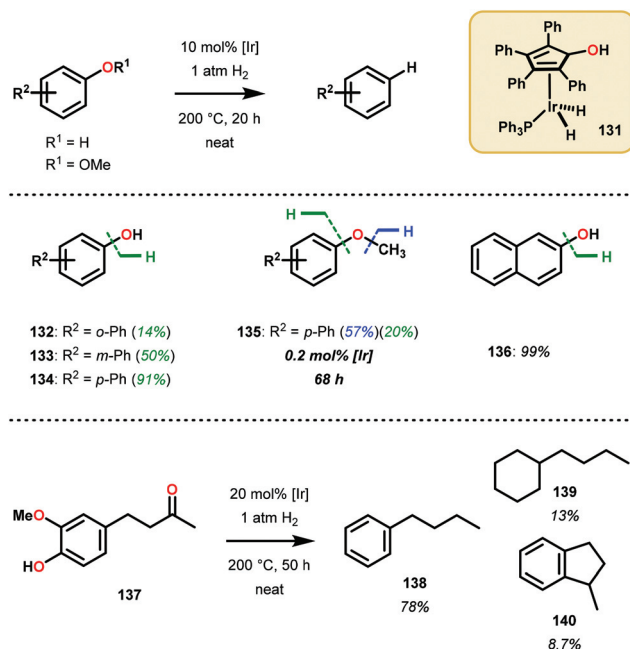
Fig. 18 Ir-catalyzed hydrogenolysis of arenols and aryl methyl ethers.

photoredox catalysis (PRC) is its ability to engage in both oxidation and reduction chemistry from a visible light promoted photoexcited state (PC*, Fig. 19).[92–97] Visible light-mediated PRC presents a number of advantages that makes it an attractive method of catalysis for lignin depolymerization: (1) PRC is operable at room temperature, compatible with aqueous–organic solvent mixtures, and insensitive to oxygen and water in select reactions, (2) PRC utilizes organic substrates for electron transfer, thus negating the need for stoichiometric transition metal additives traditionally used to reduce C–O bonds, and (3) PRC reacts *via* outer-sphere electron transfer; thereby avoiding detrimental ligation issues observed in other catalytic systems (see section 4). In this regard, PRC possesses the unique capacity to approach all three lignin depolymerization strategies (oxidative, reductive and redox-neutral) using a unified reaction design logic.

While the polyether structure of native lignin does not present reactivity opportunity with PRC, Stephenson and co-workers drew inspiration from the works of Hasegawa[98] and Ollivier[99] to develop a β-O-4 reduction. In these reports, simple phenyl keto-epoxides were reduced to afford β-hydroxy ketones. In order to employ this reactivity on model lignin substrates, Stephenson and co-workers identified a selective benzylic oxidation using 4-(acetylamino)-2,2,6,6-tetramethyl-1-

This journal is © The Royal Society of Chemistry 2016

Org. Biomol. Chem., 2016, **14**, 1853–1914 | **1869**
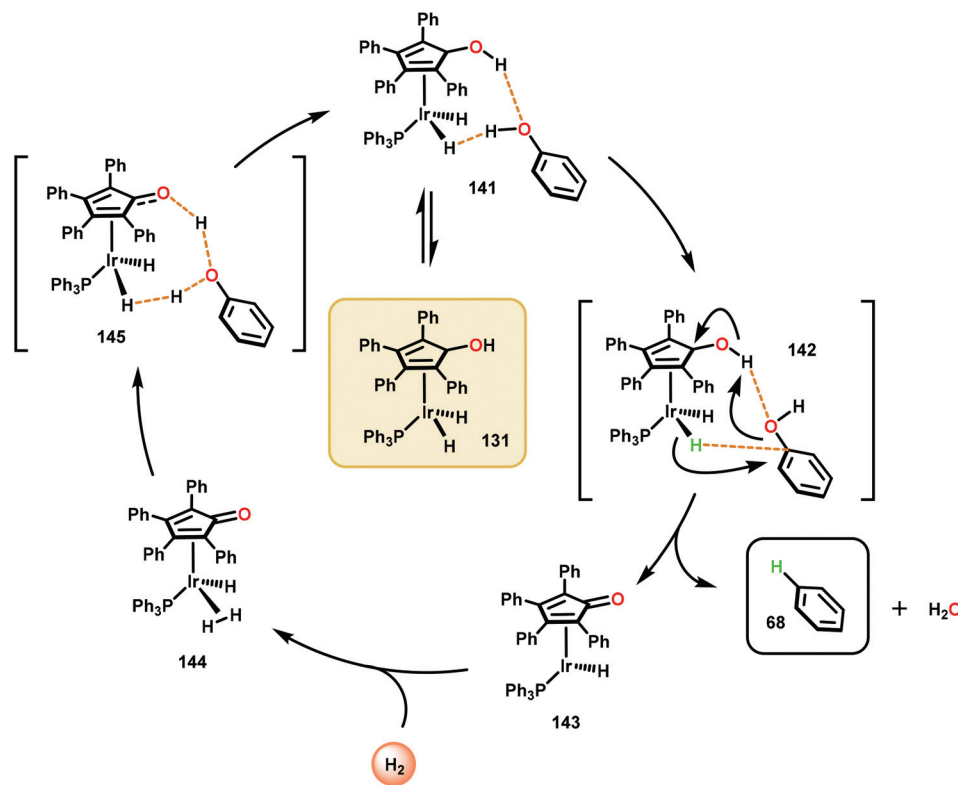
Scheme 8 Proposed mechanism for the metal–ligand cooperative hydrogenolysis of phenol.
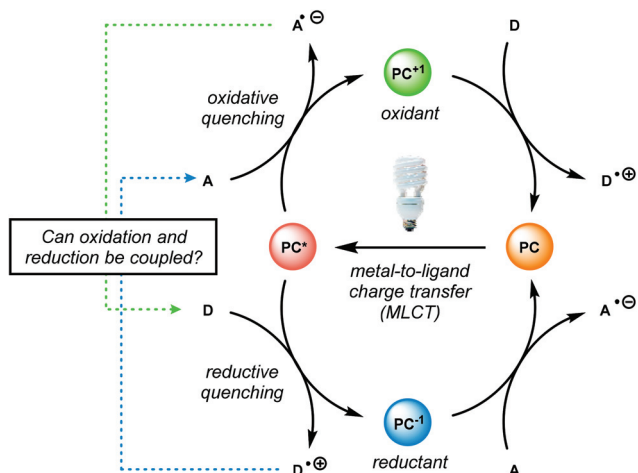
Fig. 19 Oxidative and reductive quenching cycle of photocatalysts (PCs). A = acceptor. D = donor.

oxo-piperidinium tetrafluoroborate (Bobbitt's Salt,[100] [4-NHAc–TEMPO]BF$_4$) to obtain the necessary phenyl ketone motif.[101] Interestingly, the benzylic oxidation concomitantly formed a reducible PRC functionality (phenyl ketone), decreasing the β-O-4 bond strength by ~10 kcal mol^{-1} (see Fig. 35).[102] While this approach was not a one-pot redox neutral sequence, batch

oxidation using Bobbitt's salt was shown to oxidize the lignin model systems in an efficient and operationally simple manner. Additionally, Bobbitt's salt proved ideal, as it is recyclable by stoichiometric oxidation with store bought bleach.[100]

Subsequently, the β-O-4 reduction was realized with catalytic [Ir(ppy)$_2$(dtbbpy)]PF$_6$ (**146**), three equivalents of *N,N*-diisopropylethylamine (DIPEA) and formic acid. Under these conditions a variety of model lignin substrates were observed to fragment (Fig. 20). This substrate scope supported the mechanistic hypothesis of fragmentation to give a carbon radical (**157**) and an oxyanion (**158**), as the substrate reactivity correlated with the pK_a values of the leaving group. Additionally, this method was selective for phenyl ketones and aldehydes, as the corresponding aliphatic ketones and esters could not be reduced under the employed reaction conditions (see Fig. 20). Interestingly, the commercially available benzyloxyacetaldehyde (**152**) underwent efficient reductive cleavage, yielding benzyl alcohol in 83% isolated yield. Not only does this demonstrate that aldehydes were sufficient electrophiles for this reaction but also that these reaction conditions are amenable to the reduction of stronger C–O bonds of unactivated ethers. This result suggests that this chemistry has potential application in the degradation of other biomass derived polymers such as polysaccharides. Substrates **147**, **148**, and **149** are model compounds for coumaryl, coniferyl, and sinapyl β-O-4 linkage motifs commonly found in lignin. These substrates were found to effectively undergo reductive fragmentation

1870 | *Org. Biomol. Chem.*, 2016, **14**, 1853–1914

This journal is © The Royal Society of Chemistry 2016
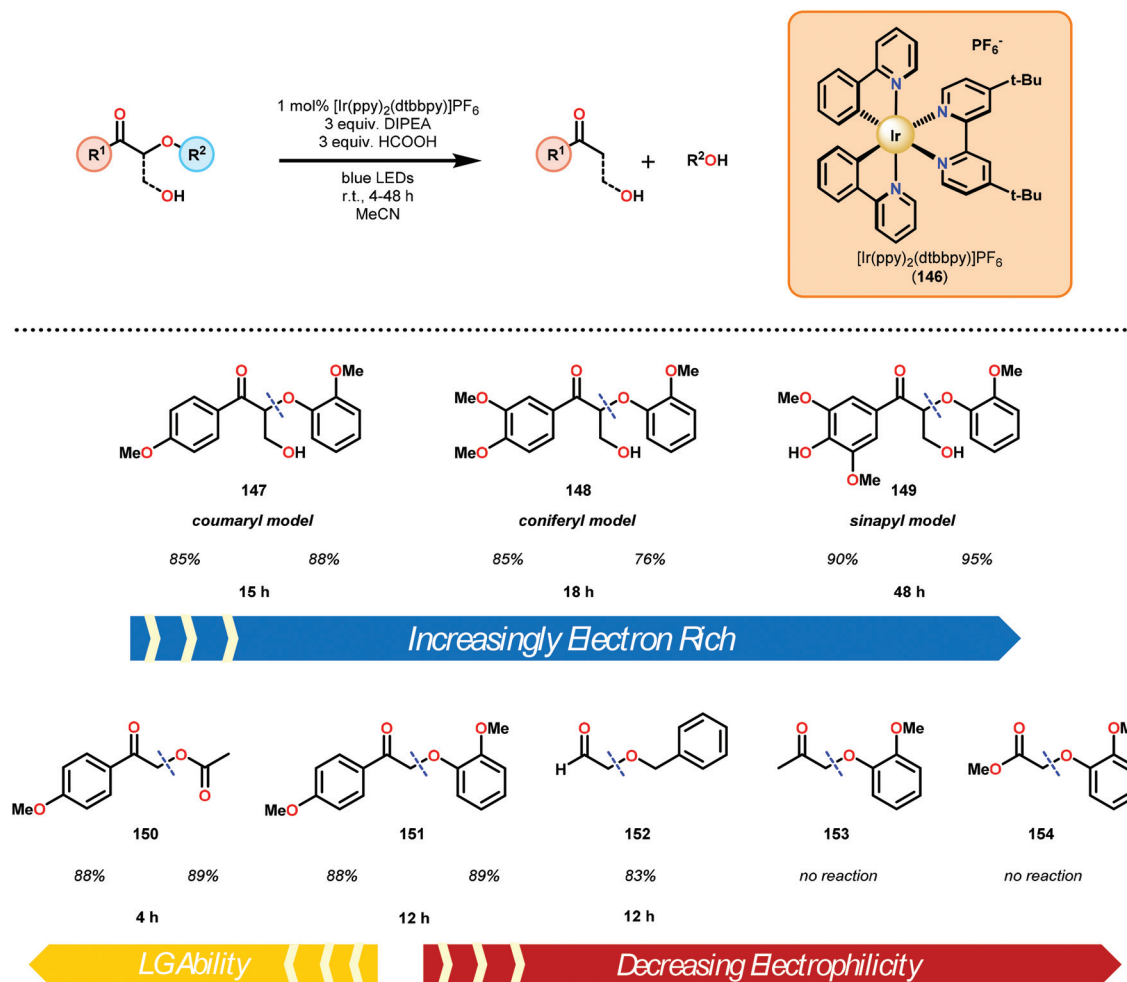
Fig. 20 Visible-light-mediated C−O bond cleavage of oxidized lignin model systems.

yielding the β-hydroxyl ketones in 85%, 85%, and 90% yield, respectively. These generated hydroxyketones were stable under the reaction conditions and did not undergo significant side reactions such as retro-aldol, pinacol coupling or oxidation.[101] They are also unique fragmentation products which had only previously been observed in minute quantities.

Consistent with the corresponding electron transfer reduction literature,[103–109] Stephenson and co-workers proposed a reaction mechanism in which the reaction is initiated by visible-light excitation of the Ir[III] photocatalyst (**146**) to generate an excited state, Ir[III]*. From this excited state, the photocatalyst is reductively quenched by the single-electron oxidation of DIPEA. The generated Ir[II] species is now an excellent reductant and reduces the oxidized lignin model substrates. Electron transfer most likely proceeds through the carbonyl functionality, generating an anionic ketyl radical (**156**) which can intramolecularly fragment to afford the corresponding α-keto radical (**157**) and phenoxide anion (**158**). Subsequent hydrogen atom transfer (HAT) to the α-keto radical generates the desired ketone (**159**) and completes the catalytic cycle (Scheme 9).

With the success of the two-step batch-to-batch process, Stephenson and co-workers were interested in exploring the reaction within a continuous flow reactor. Indeed a simple batch-to-flow protocol where the oxidation occurred in batch and the photochemical reduction occurred within a continuous flow reactor effectively caused the β-O-4 cleavage to occur.[101] Previous reports by the groups of Stephenson and Seeberger had demonstrated that the use of a flow reactor can greatly accelerate photocatalyzed reactions due to an efficient irradiation of the reaction solution.[110,111] Thus, performing the reaction in the flow reactor greatly accelerated the reaction rate when compared to the analogous batch-to-batch reaction.[101] Collectively, this batch-to-flow processing of lignin model substrates demonstrated the potential for future photoredox technologies for biomass conversion applications.

3.   Oxidative conversion of lignin

From the previous chapter it is obvious that several methods have been investigated for the reductive transformation of

This journal is © The Royal Society of Chemistry 2016

Org. Biomol. Chem., 2016, **14**, 1853–1914 | **1871**
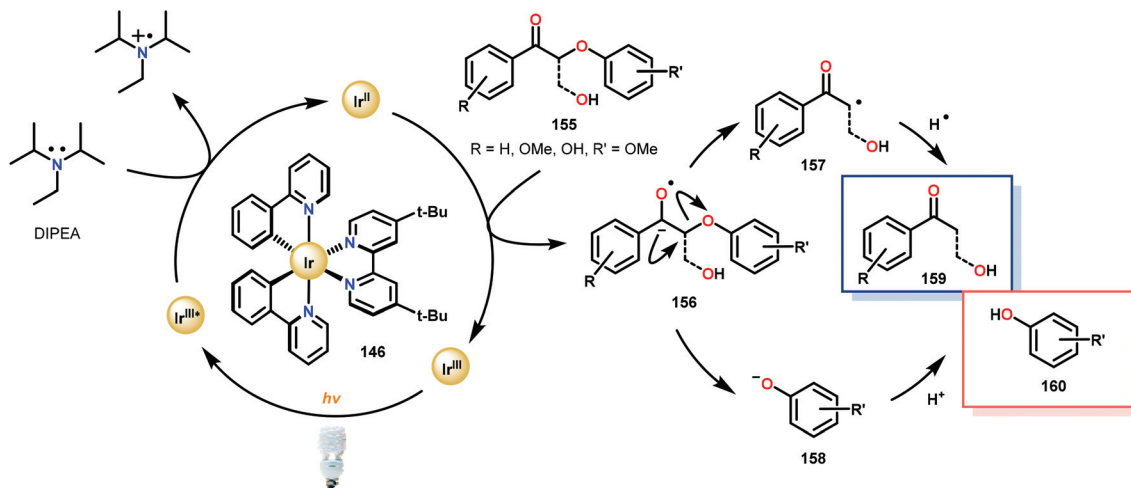
Scheme 9 Proposed mechanism for the photocatalytic reductive cleavage of oxidized lignin model systems.
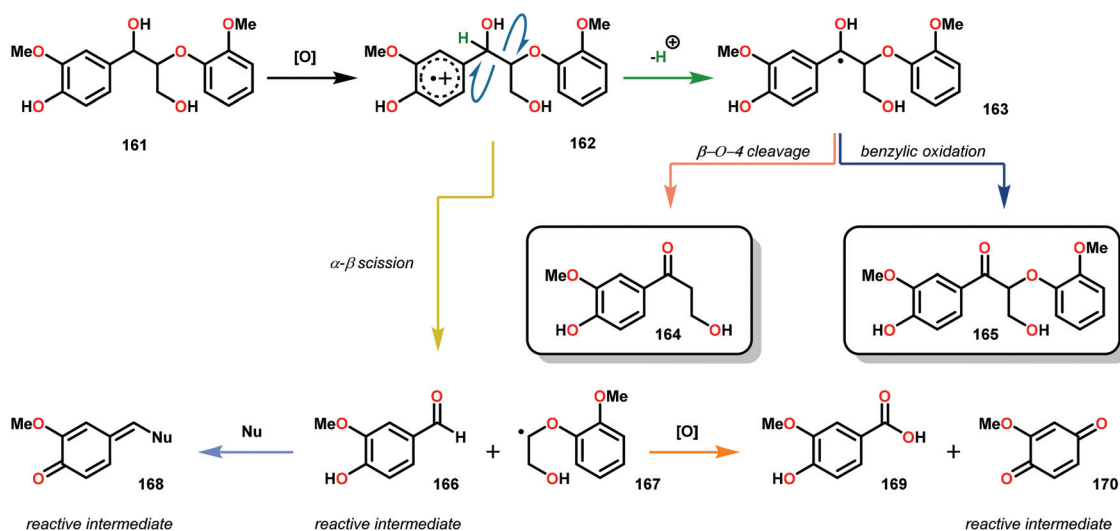
Scheme 10 Depolymerization mechanism of lignin by delignifying enzymes. Nu = nucleophile.

lignin and lignin model systems. Another approach that has been widely explored is the oxidative conversion. In nature, there are several species of white-rot fungi that are capable of degrading lignin through the action of peroxide dependent ligninase or laccase.[112,113] These enzymes work through the single-electron oxidation of the aromatic groups found in lignin, generating arene radical cations, such as radical **162** (Scheme 10) upon oxidation of **161**. This reactive intermediate can either undergo α–β cleavage, causing a break in the polymeric backbone yielding the corresponding aldehyde **166** and radical **167**. Alternatively, deprotonation of $H_α$ from intermediate **162** generates ketyl radical **163**, which can undergo β-O-4 fragmentation to yield β-hydroxyketone **164** or undergo direct oxidation to the benzylic ketone **165**. Under these oxidative conditions, the cleaved

products readily undergo further oxidation chemistry yielding carboxylic acid (**169**) and quinones (**170**). The relatively stable radical cations formed during arene oxidation by enzymes can also undergo reversible intramolecular or intermolecular electron transfer. This charge transfer phenomena allows the ligninase to initiate degradation at multiple sites within the polymer matrix despite having low surface contact with the substrate. The overall delignification process is relatively slow, taking many months to fully degrade higher molecular weight lignin, since the depolymerization process occurs on the heterogeneous surface of the wood itself. Despite the low contact surface area the fungi have to degrade lignin, especially in the early stages of wood decay, the depolymerization of lignin occurs efficiently.[114–116]

3.1 Biomimetically inspired catalysts for oxidative fragmentation of lignin model systems

Early reports on the oxidative degradation of lignin model systems centered on the use of biomimetic catalysts, such as metal porphyrins.[117] Analogous to the hemo-protein ligninase, isolated from the white-rot fungus, which are enzymes that catalyze the oxygenative C–C bond cleavage of lignin model systems,[112,113] Shimada and co-workers reported on the first example of an unprecedented C–C bond cleavage reaction of a lignin model compound.[118] It was found that employing tetra-phenylporphyrinatoiron(III) chloride (177) as a biomimetic catalyst, 1,2-bis(4-ethoxy-3-methoxyphenyl) propane-1,3-diol (171) was oxidatively cleaved to produce a variety of products where 4-ethoxy-3-methoxybenzaldehyde (172) was found to be the major product (Scheme 11).[118] Although this study showed that it was possible to mimic the function of the lignin degrading enzymes, the oxidation of model system 171 was not selective and resulted in an array of products.

Further studies by Shimada, Higuchi and co-workers explored the use of hemin, a Fe–porphyrin complex, to study the C_α–C_β bond cleavage of model compound 178.[119] It could

be established that hemin (181) efficiently degraded model system 178 at ambient temperature in the presence of 5 equivalents ^{t}BuOOH to afford aldehyde 179 as the major product, along with the hydroxylated product 180 (Scheme 12). Diol 180 was also shown to undergo C_α–C_β bond cleavage to yield aldehyde 179.

A one-electron transfer mechanism was invoked in these C_α–C_β bond cleavage reactions where the catalytically active intermediate was proposed to be an Fe^V-oxo species. It was proposed that a one-electron abstraction by Fe^V-oxo from the substrate generates a radical cation, which fragments in a manner analogous to 162 (cf. Scheme 10).[119,120] The proposed mechanism is in good accordance with earlier C–C bond cleavages observed for electrochemical oxidations[121] and ligninase.[122] A related report by Crawford and co-workers made use of a variety of Fe^{III} porphyrins to study the delignification of wood pulps. It could be demonstrated that the treated wood chips were extensively delignified and examination of the treated chips by transmission electron microscopy revealed morphological alterations similar to that of white rot fungi.[123]

In a related study, Meunier and Labat studied the conversion of 1-(3,4-dimethoxyphenyl)-2-(2-methoxyphenoxy)
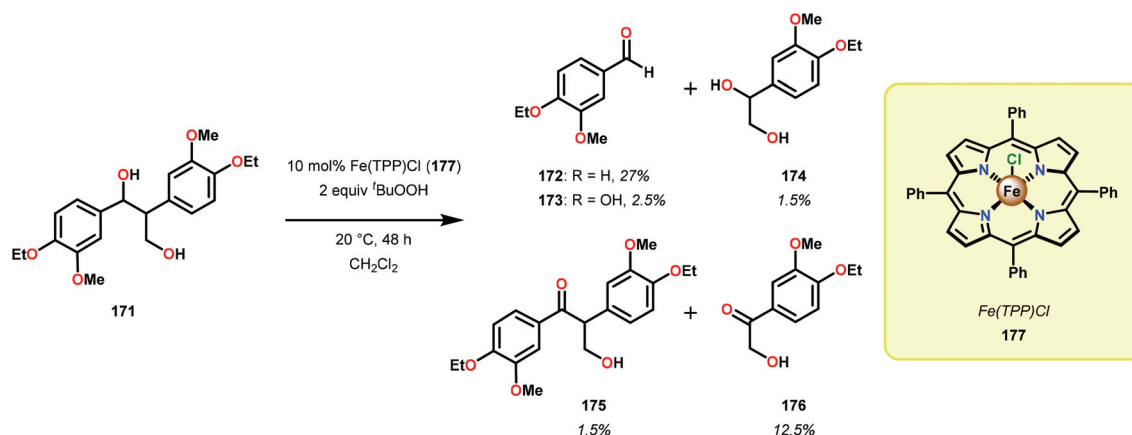
Scheme 11 Oxidation of lignin model system 171 by Fe(TPP)Cl (177).
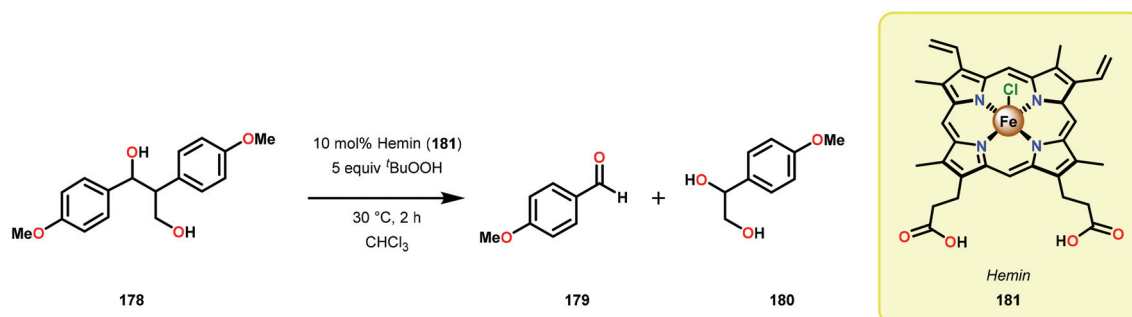
Scheme 12 Oxidative C_α–C_β bond cleavage of lignin model system 178 by hemin 181.

This journal is © The Royal Society of Chemistry 2016

Org. Biomol. Chem., 2016, 14, 1853–1914 | 1873
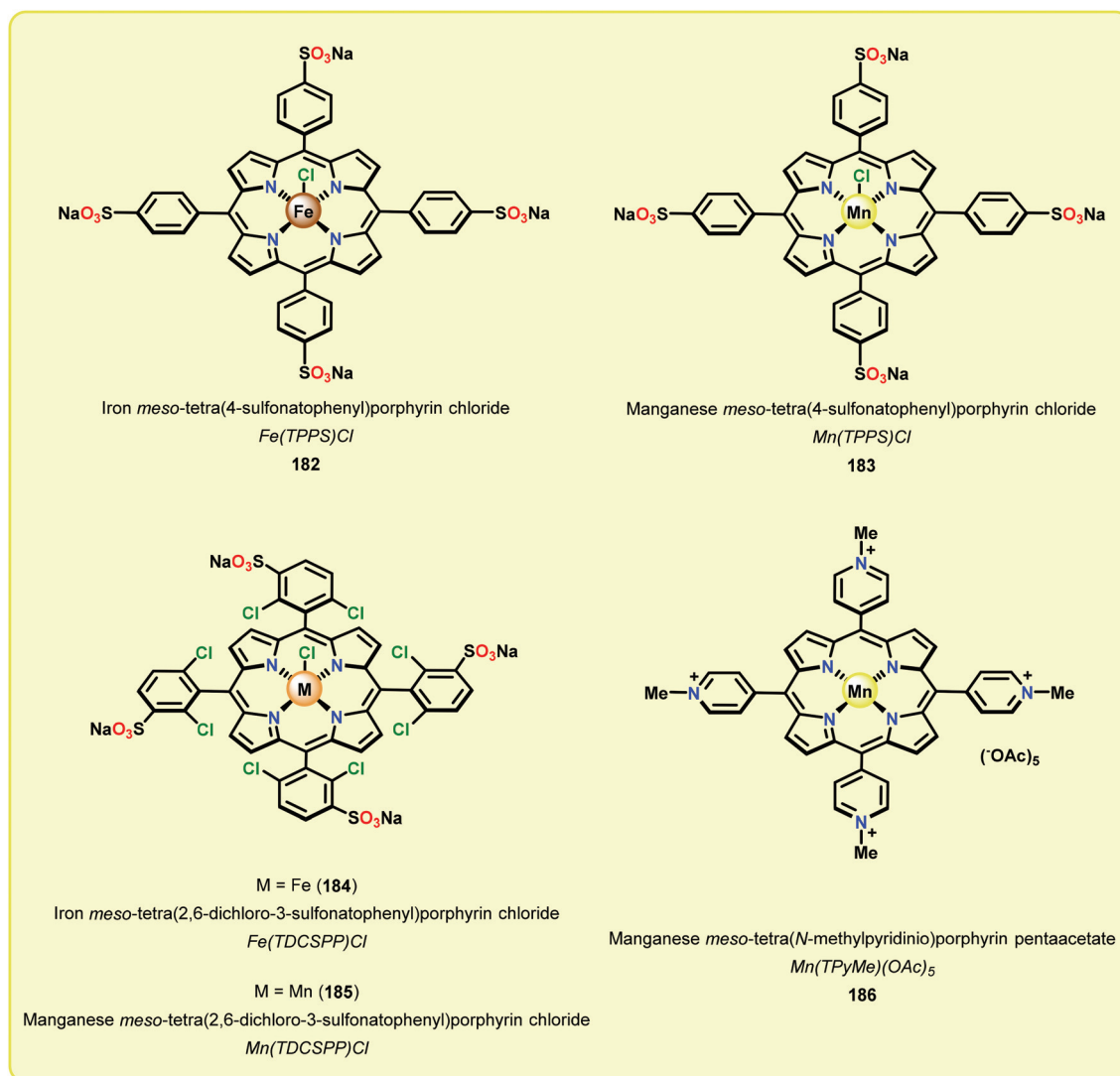
Fig. 21 Water soluble porphyrin complexes **182**–**186** employed for degradation of lignin model systems.

propane-1,3-diol (**61**) for both homogeneous and resin-immobilized Fe and Mn derivatives of sulfonated tetraphenyl-porhyrins (TPPS) (**182**–**186**, Fig. 21). It could be established that the homogeneous catalysts displayed higher catalytic activity compared to the corresponding immobilized catalysts. Here the influence of pH was also investigated and the authors found that the Fe catalysts were more efficient at pH < 3 while an opposite effect was observed for the Mn(TPPS) catalyst (**183**), which showed an optimum between pH 4.5 and 6.0. For the Fe(TPPS) catalysts, it was reasoned that the acidic medium favored the cleavage of the inactive μ-oxo Fe porphyrin dimers, which are known to be generated during the oxidations, and represent a deactivation pathway for these Fe complexes.[124] Crestini and co-workers,[125] and Dolphin and co-workers[126–128] have also used cationic and anionic water soluble metal porphyrin complexes (Fig. 21) for the degradation of lignin model systems. Additional investigations on immobilized metal por-

phyrins as lignin-peroxidase biomimetic catalysts include the studies by Sanjust[129,130] and Crestini.[131,132]

Although the early examples on the use of metal porphyrins resulted in unselective degradation of lignin model systems and rather low yields of the desired products, a recent study by Ying and co-workers highlighted that further progress in this area is achievable. Ying and co-workers employed metallo-deuteroporphyrins (Fig. 22) as biomimetic catalysts for the oxidative depolymerization of lignin model systems. Although the corresponding Fe- and Mn-based deuteroporphyrin complexes were not efficient in catalyzing the oxidation of the lignin model system, the Co-deuteroporphyrins were shown to efficiently convert the lignin model system in the presence of Oxone® (2 KHSO$_5$·KHSO$_4$·K$_2$SO$_4$).[133]

When using the Co(DPCys) catalyst **192** on phenolic lignin model substrate **161**, full conversion was observed within 15 min at room temperature. This reaction yielded the three

1874 | *Org. Biomol. Chem.*, 2016, **14**, 1853–1914

This journal is © The Royal Society of Chemistry 2016
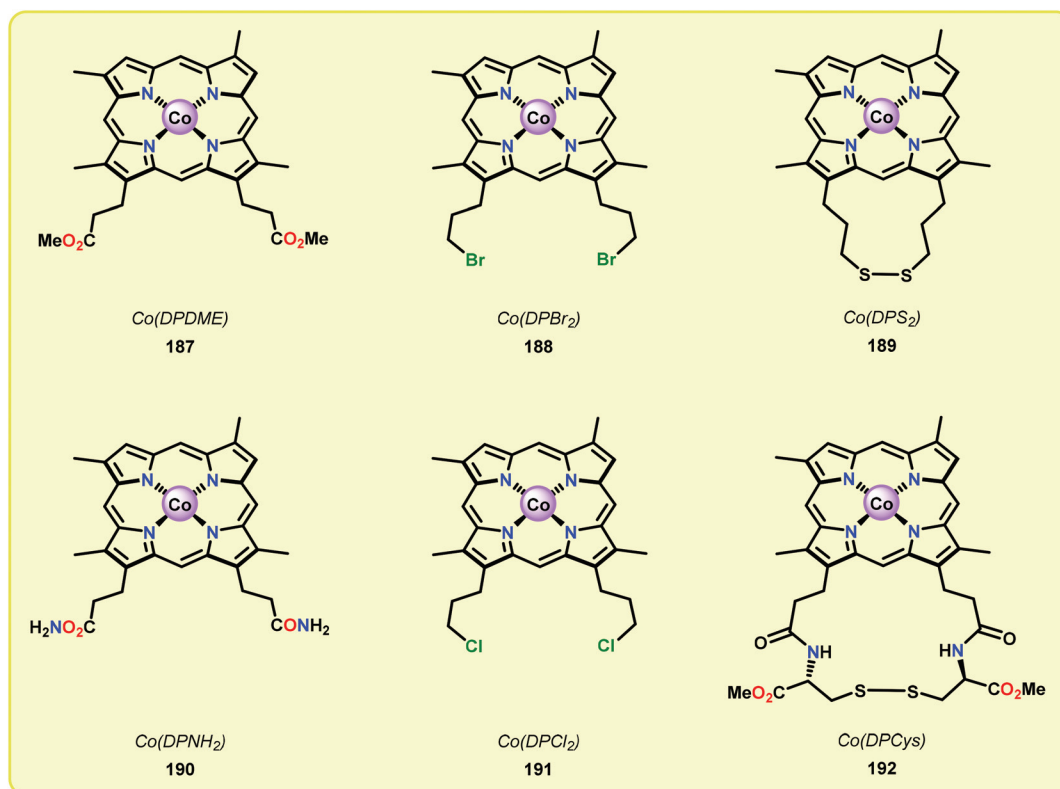
Fig. 22 Structure of Co deuteroporphyrins **187–192**.
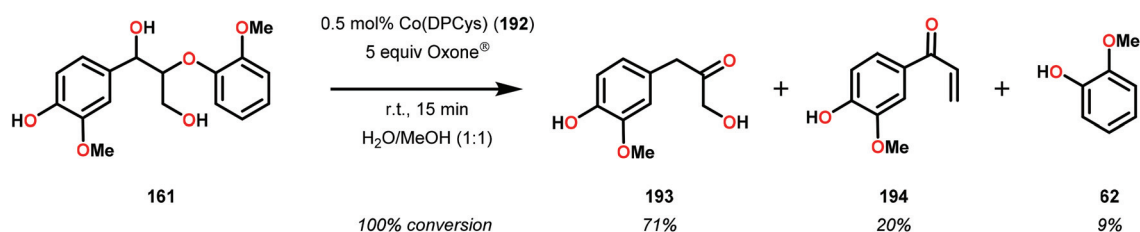
Scheme 13 Oxidative degradation of lignin model system **161** by the Co deuteroporphyrin catalyst Co(DPCys) (**192**).

compounds **193**, **194** and **62**, where product **193** was obtained in 71% yield (see Scheme 13). In the absence of the Co-catalyst, 91% of the starting material was recovered, highlighting the need for the catalyst. The proposed mechanism for the formation of products **194** and **62** is depicted in Scheme 14. These products were proposed to form through the activated Co^{IV}-oxo species, which initially abstracts the benzylic hydrogen atom of substrate **161**, resulting in a Co^{III}-bound ketyl radical species (**195**). Elimination of a phenoxyl radical (**197**) generates Co^{III}-hydroxo intermediate **196**, which is subsequently dehydrated to liberate product **194** and a Co^{III}-hydroxo species. This Co^{III}-hydroxo is concomitantly oxidized by the phenoxyl radical (**197**), which regenerates the high-valent Co^{IV}-oxo catalyst and closes the catalytic cycle.[133]

Attempts of employing the Co(DPCys) catalyst **192** on enzymolysis lignin (*i.e.* lignin obtained after enzymatic hydrolysis) revealed that almost no conversion occurred at room temperature. The temperature had to be increased to 120 °C to significantly improve the conversion and under optimized conditions, 31.2 wt% of discrete monomeric aromatic products could be obtained. The authors also investigated if the catalytic procedure could be applied on other types of lignin. When applying the catalytic protocol on organosolv lignins, such as ethanosolv lignin from bagasse, dioxasolv lignin from bagasse and ethanosolv lignin derived from pine sawdust, it was found that the source of the lignin had a dramatic effect on the conversion and the distribution of products. Although the solvent employed in the organosolv derived lignin from
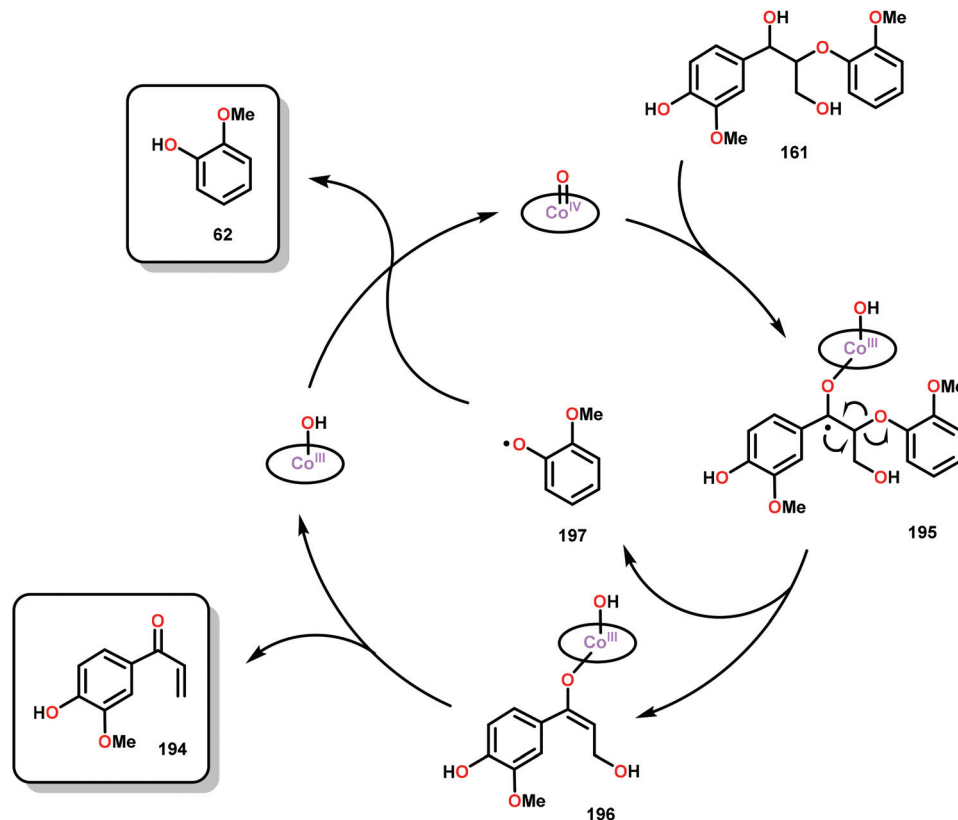
Scheme 14 Proposed mechanism for the Co deuteroporphyrin catalyzed formation of products **194** and **62** from substrate **161**.

bagasse did not significantly alter the outcome of the Co-catalyzed degradation, the use of grass biomass lignin and ethanosolv lignin derived from pine only resulted in low yield of monomeric aromatics.[133] These findings strongly imply that the source of the lignin has a crucial impact on the studied catalytic system.

It should also be mentioned that water soluble metallophthalocyanines (Fig. 23) have also been evaluated as lignin peroxidase models for the oxidative conversion of simple lignin model systems.[134,135] However, these complexes were in general found to suffer from oxidative degradation and have therefore not received any widespread attention.

3.2   Cobalt-Schiff base complexes for catalytic oxidative degradation of lignin model systems

Analogous to metalloporphyrins and metallophthalocyanines, Co-Schiff base complexes are well-known to activate O_2[136,137] and have been used to catalyze a plethora of transformations.[138] Co-Schiff base complex (**203**) and related complexes reversibly react with O_2 to give an equilibrium mixture of the Co-superoxo species (**204**) and the dimeric peroxo species (**205**) (Fig. 24), where the equilibria of these species is dependent on the nature of the Schiff-base complex and the specific reaction conditions.[139] The efficiency of activating O_2 by Co-Schiff base complexes may be strongly dependent on the coordination environment around the Co center, where the
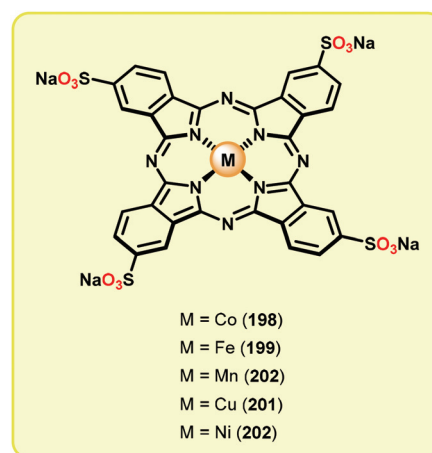
Fig. 23 Water soluble metallophthalocyanines (**198–202**) employed for studying oxidative conversion of lignin model systems.

four-coordinated Co–salen complex **208** (Fig. 25) binds O_2 poorly at room temperature, thus resulting in a low concentration of the Co-superoxo species **204**. On the other hand, the presence of a donor ligand in the axial position stabilizes the Co–O_2 bond, making the five-coordinated Co-Schiff complexes, such as **206** and **207** (Fig. 25), more efficient in binding O_2.[140]
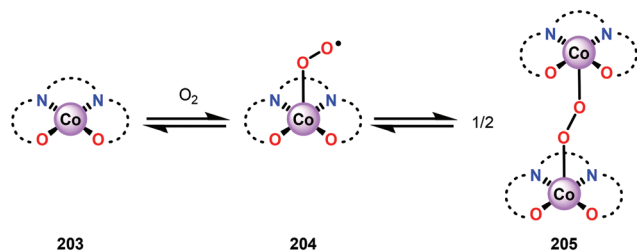
Fig. 24 Activation of O_2 by Co-Schiff base complexes.

Catalyst **206**: *71% yield*

Catalyst **207**: *86% yield*

Scheme 15 Aerobic oxidation of syringyl alcohol **209** to 2,6-dimethoxybenzoquinone (**210**) catalyzed by Co-Schiff base complexes **206** and **207**.

Early support suggested that Co-Schiff base complexes could be used for the oxidative conversion of lignin-like model systems.[141] Bozell and co-workers found that treatment of syringyl alcohol (**209**) with 10 mol% of the five-coordinate Co-Schiff base complexes **206** and **207** (Fig. 25), in the presence of O_2, afforded 2,6-dimethoxybenzoquinone (**210**) in 71% and 86% yield, respectively (Scheme 15). Competitive deactivation of the Co catalyst was found to occur with substrates of lower reactivity. It was also established that guaiacyl-type model substrates only afforded <20% of the methoxybenzoquinone product, probably because of the reduced ability of these model substrates to generate the essential intermediary phenoxyl radical.[142] Related studies have also been conducted by Canevali,[143] Sippola[144] and Repo[145–147] where Co(salen)-type catalysts such as complex **208** was employed as the oxygen-activating catalyst. Heterogeneous systems where Co–salen was immobilized on SBA-15 have also been employed for the oxidative conversion of lignin model systems.[148,149]

Bozell and co-workers subsequently discovered that the stoichiometric addition of a sterically encumbered aliphatic nitrogen base could yield the methoxybenzoquinone product in 51% yield.[150] The authors therefore designed a new family of unsymmetrical Co-Schiff base catalysts that housed a sterically hindered base within the ligand scaffolds (Fig. 26).[151,152] Several of the unsymmetrical catalysts were capable of oxidizing syringyl alcohol **209** to afford 2,6-dimethoxybenzoquinone **210** in good yield. It was established that the unsymmetrical Co-Schiff base complexes did not require the addition of an external axial ligand. Of the synthesized catalysts, *N*-benzyl catalyst **215** displayed the highest activity, giving 2,6-dimethoxybenzoquinone **210** in 74% yield after only 1 h. After identifying catalyst **215** as the optimal catalyst, several lignin model systems containing a phenolic OH were evaluated under the
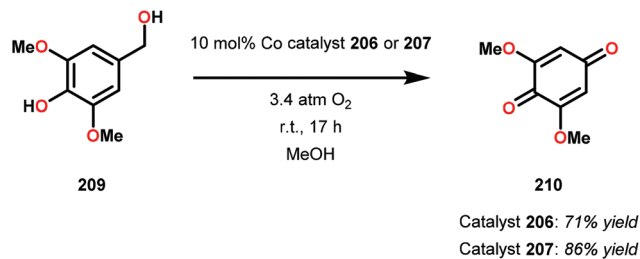
optimal conditions (Table 1). In general, high yields of the corresponding benzoquinone products were obtained through conversion of the studied lignin models.[151]

The Co-based system was subsequently applied on organosolv lignin, derived from tulip poplar. Treating this lignin with *N*-benzyl catalyst **215** and O_2 for 72 h at room temperature produced 2,6-dimethoxybenzoquinone **210** as well as benzaldehydes.[151] However, the absolute yields of monomeric aromatic species from this reaction were rather low, merely 3.5%, highlighting the difficulties when attempting to implement the developed catalytic systems on native lignin.

3.3 Vanadium-catalyzed aerobic oxidation of lignin model systems

Vanadium complexes have proven to be useful catalysts in various oxidative transformations. Oxidative cleavage of C–C bonds in 1,2-diols has been investigated with various transition metals including V,[153] Ru,[154,155] and Mn.[156,157] However, less is known about the oxidative C–C bond cleavage of 1,2-hydroxyethers. A variety of V complexes are able to affect oxidative transformations, and their reactivity can be greatly modified depending on the substrate and ligand or if reacted under photoirradiation, aerobic or anaerobic conditions.[158–160]

Inspired by the reactivity associated with V complexes, Baker and co-workers investigated the aerobic oxidation of four different 1,2-hydroxyether model systems (**116** and **227–229**, Fig. 27) using a base metal V catalyst, V^V(pda)(O)(O^{i}Pr) (**230**; H_2pda = pyridine-2,6-dicarboxylic acid). These substrates allowed the authors to elucidate the effects and reactiv-
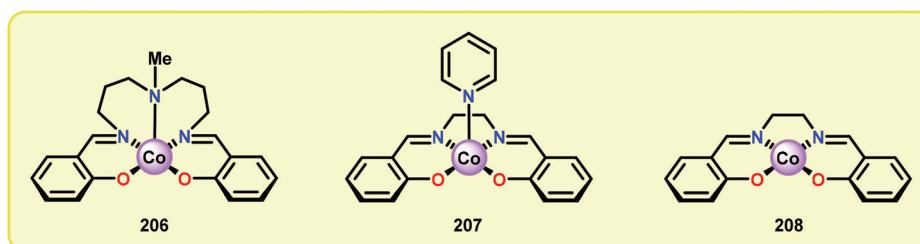
Fig. 25 Co-Schiff base complexes used for oxidative degradation of lignin model systems.

This journal is © The Royal Society of Chemistry 2016

Org. Biomol. Chem., 2016, **14**, 1853–1914 | **1877**
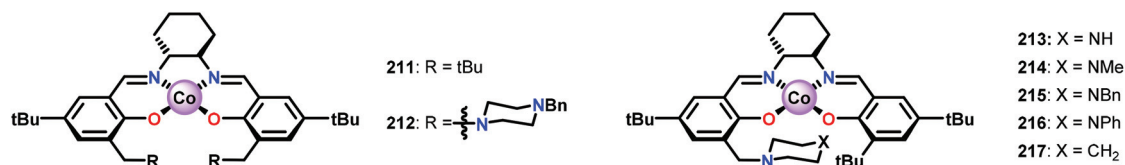
Fig. 26 Symmetrical (**211** and **212**) and unsymmetrical (**213–217**) Co-Schiff base complexes developed for studying the oxidative conversion of lignin models.

ity of the β-O-4 and β-1 lignin motifs, and the effects of the substituted backbones.[161]

Initial studies consisted of using stoichiometric amounts of V complex **230**. When complex **230** was reacted with the different model systems, new V^V complexes were isolated in good yields in which the alcohol–ether ligand was bound in a chelating fashion.[161] Heating the pinacol monomethyl ether complex **231** in pyridine-d_5 solution (6 h at 100 °C, or 3 weeks at 25 °C) the previously reported V^{IV} complex (**232**) was generated,[162] alongside acetone (**233**), 2-methoxypropene (**234**), and pinacol monomethyl ether (**227**) (Scheme 16).[161]

When substrates with secondary C–H bonds were subjected to these conditions, C–H bond cleavage was observed when using stoichiometric amounts of the V complex. Heating V complex **235** in pyridine-d_5, afforded aldehyde **236** and the original lignin model (**228**) (Scheme 17a). Analogous to complex **235**, complexes **237** and **238** also underwent C–H bond cleavage; however, for these complexes the cleavage occurred at room temperature (Scheme 17b and c).[161]

In the absence of pyridine, V complex **238** exhibited different reactivity. Not only did the complex mediate C–H bond cleavage, it also carried out C–C bond cleavage (Scheme 18). The products observed from heating complex **238** in DMSO included a V^{IV} complex (**240**), benzoin methyl ether (**239**) together with methanol, benzaldehyde (**241**) and 1,2-diphenyl-2-methoxyethanol (**229**).[161]

The mechanism of the C–C bond cleavage is not fully understood, but the authors proposed that V complex **238** reacts to produce an aldehyde and a methoxybenzyl radical. The methoxybenzyl radical can subsequently react with water and a second equivalent of complex **238** to generate methanol, a second equivalent of benzaldehyde (**241**), with the release of 1,2-diphenyl-2-methoxyethanol (**229**). Attempts were made to evaluate the proposed mechanism by reacting V complex **238** in the presence of a radical trap, BHT (2,6-di-*tert*-butyl-4-methylphenol), and triphenyl phosphine. However, this reaction was inconclusive and the products could not be characterized. When adding 9,10-dihydroanthracene to the reaction mixture only trace amounts of anthracene (<1%) was detected, with the reaction course being unaffected. With a basic understanding of the reactivity of the V-based catalysts, attempts were made to run the reactions with catalytic amounts of V^V(pda)(O)(O^{i}Pr) (**230**). These results are summarized in Table 2.[161]

Consistent with the results from the stoichiometric oxidations, the substrates with substituted phenyl groups on the carbon backbone facilitated oxidation more efficiently. However, substrate **229** showed different product distributions when changing the solvent from DMSO to pyridine (*cf.* Table 2, entries 3 and 4). The generated benzoic acid (**243**) and methyl benzoate (**245**) are most likely oxidation products derived from the intermediate benzoin methyl ether (**239**).[161]

Control experiments were run under anaerobic conditions with DMSO to investigate the possible role of DMSO as an oxidant. A mixture of V^{IV}(pda)(O)(pyr)$_2$ and 1,2-diphenyl-2-methoxyethanol (**229**) in d_6-DMSO after 1 week at 100 °C showed no turnover, suggesting that DMSO does not act as an oxidant in the catalytic cycle. Performing the reactions with V^{IV}(pda)(O)(DMSO)$_2$ (**240**) and 2-phenoxyethanol (**228**) or 1-phenyl-2-phenoxyethanol (**116**) as substrates also displayed no conversion after heating at 100 °C for 1 week in DMSO-d_6. The selectivity of the stoichiometric reactions compared to the catalytic reactions with the V^{IV} complexes is not well understood and is still the subject of ongoing experimental and computational investigations. The stoichiometric reactions afforded a mixture of C–H and C–C bond cleavage products while the catalytic reactions afforded only products derived from C–C bond fragmentation.[161] Collectively, this method provides a proof of principle for the oxidation and cleavage of lignin models. The homogeneous nature of the catalyst provides opportunities for exploring new ligand designs in order to optimize the activity and selectivity for the oxidative disassembly of lignin model systems and native lignin.

Inspired by previous work on using 8-quinolinate ligands for the oxidation of benzylic, allylic, and propargylic alcohols in air,[163,164] Hanson and co-workers explored the electron-donating nature of the ligand scaffolds on the catalytic oxidative cleavage of lignin models. They envisioned that a tridentate scaffold with phenolate donors could provide a more electron-rich environment and an additional open coordination site to facilitate the reaction of V^{III} or V^{IV} with O$_2$. A bis(phenolate)-pyridine ligand (**246**; H$_2$BPP = 2,6-(HOC$_6$H$_2$-2,4-^{t}Bu$_2$)$_2$NC$_5$H$_4$), and a bis-(phenolate)amine ligand (**247**; H$_2$BPA = *N,N*-bis(2-hydroxy-4,5-dimethylbenzyl)propylamine) (Fig. 28A) were identified as promising ligands and the corresponding V complexes (**248** and **249**) are depicted in Fig. 28B.[165]

In initial experiments, complexes **248** and **249** were tested stoichiometrically with pinacol to probe the reactivity of the complexes. These stoichiometric reactions were shown to afford the reduced V^{IV} species in 95% and 97% yield from complexes **248** and **249**, respectively. Acetone was also estab-

1878 | *Org. Biomol. Chem.*, 2016, **14**, 1853–1914

This journal is © The Royal Society of Chemistry 2016

Table 1 Co-Schiff base catalyzed aerobic oxidation of lignin model systems

Entry	Substrate	Time (h)	Yield[a] (%)		
			170	**210**	**218/219**
1	**220**	16	—	72	11
2	**221**	16	83	—	—
3[b]	**222**	24	51	—	22
4[c]	**223**	16	—	81	Traces
5	**224**	16	17	86	Traces
6[b]	**225**	48	21	64	Traces
7[b]	**226**	48	0[d]	10	0[e]

[a] Isolated yields. [b] 10 mol% of Co catalyst used. [c] Yields relative to 2 equivalents of product formed. [d] 14% 2,5-dimethoxybenzoquinone was isolated. [e] 30% aldehydes was observed.

This journal is © The Royal Society of Chemistry 2016

Org. Biomol. Chem., 2016, **14**, 1853–1914 | **1879**
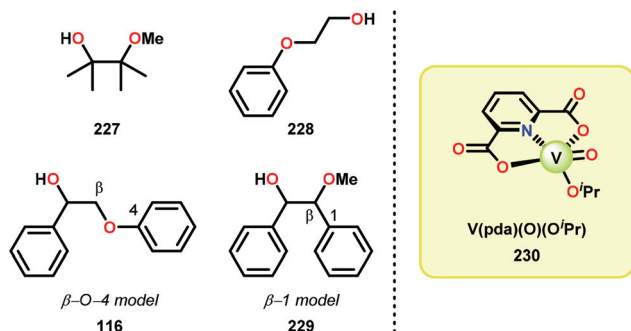
Fig. 27 (Left) Model systems **116** and **227–229** and (right) V complex **230**.

lished as a product in these reactions. The V^{IV} complexes were therefore isolated and exposed to air in CD_2Cl_2 to produce the corresponding V^V complexes, an essential element that is required for the catalytic oxidative cleavage of C–C and C–O bonds. These initial reactions were optimized for the catalytic aerobic oxidation of 4-methoxybenzyl alcohol. Reacting V complex **248** (2 mol%) with 4-methoxybenzyl alcohol at 60 °C under air in 1,2-dichloroethane did not result in significant oxidation. Increasing the temperature to 80 °C under air, with Et_3N (10 mol%) as an additive, in toluene afforded 4-methoxybenzaldehyde in 99% yield after 65 h. Complex **249** was also able to oxidize 4-methoxybenzyl alcohol but afforded lower yields (80%) of the oxidized product. After determining the optimized catalytic conditions, the oxidation of lignin model compounds was investigated using complexes **248** and **249**. When non-phenolic lignin model **250** was subjected to V catalyst **248** (10 mol%) in toluene at 100 °C for 48 h, 84% conversion occurred with the formation of various oxidized products (Scheme 19).[165]

The product mixture obtained was similar to that obtained from the previously reported V catalyst **230**, consisting mostly of C–O and C–H bond cleavage products.[165] It should be noted that these results contrast the results observed by Son and Toste using V catalyst **256** (Fig. 29) in which high C–O bond cleavage selectivity was observed.[166] These results also contrast the C–H bond cleavage selectivity for the previously reported

8-quinolinate catalyst **257** (Fig. 29).[167] In Son and Toste's work, it was proposed that the selectivity for C–O vs. C–H bond cleavage depends on the bite angle of the ligand framework.[166] However, the preference for C–O vs. C–H cleavage is still not fully understood and the two cleavage pathways most likely go through different mechanisms as noted by the different selectivities for the different V catalysts.[167]

V complex **248** was also used catalytically in the oxidation of substrate **250** at 100 °C for 48 h but afforded low conversion. Decomposition of the catalyst was suggested by the appearance of NMR signals corresponding to 4,5-dimethylsalicylaldehyde. The presence of 4,5-dimethylsalicylaldehyde could also be confirmed by GC-MS analysis, showing a peak with an expected $m/z = 150$. Phenolic lignin model systems have proven to be more difficult substrates to perform chemoselective reactions on, meriting separate investigation of reactivity with aerobic oxidations. Attempts to oxidize various phenolic lignin model systems with V complex **248** afforded low conversions (~20%) and yielded mostly the oxidized ketone product with only trace amounts of cleavage products (Scheme 20). These results were surprising since complex **248** afforded C–O bond cleavage products of the non-phenolic lignin model but did not efficiently mediate C–O bond cleavage when employing the phenolic model system.[165]

These results are also perplexing considering that the 8-quinolinate V catalyst **257** was previously reported to afford the alkyl–phenyl bond cleavage products **210** and **258** as major products together with ketone **149** when reacted with the phenolic substrate **225**.[167] Realizing how different ligands give rise to different selectivities highlights the complexity involved in devising a reasonable mechanism for these V-catalyzed oxidations.

Having made these observations, Hanson and co-workers subsequently went on to explore the reactivity of V catalysts **256** and **257** with diastereomerically pure *erythro* and *threo* phenolic and non-phenolic β-1 lignin models **259** and **263**. Aerobic oxidation of *threo* lignin model system **259** (**259T**) afforded the various oxidation products shown in Table 3, entry 1. Additional screening of the V-catalyzed cleavage of the *erythro* isomer (**259E**) with complex **257** was also carried out, as summarized in Table 3.[168]
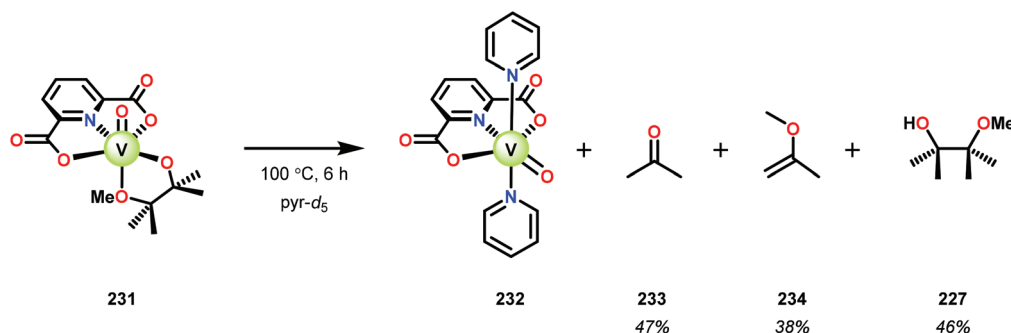
Scheme 16 Stoichiometric C–C bond cleavage by V complex **231**.

a)

b)

c)
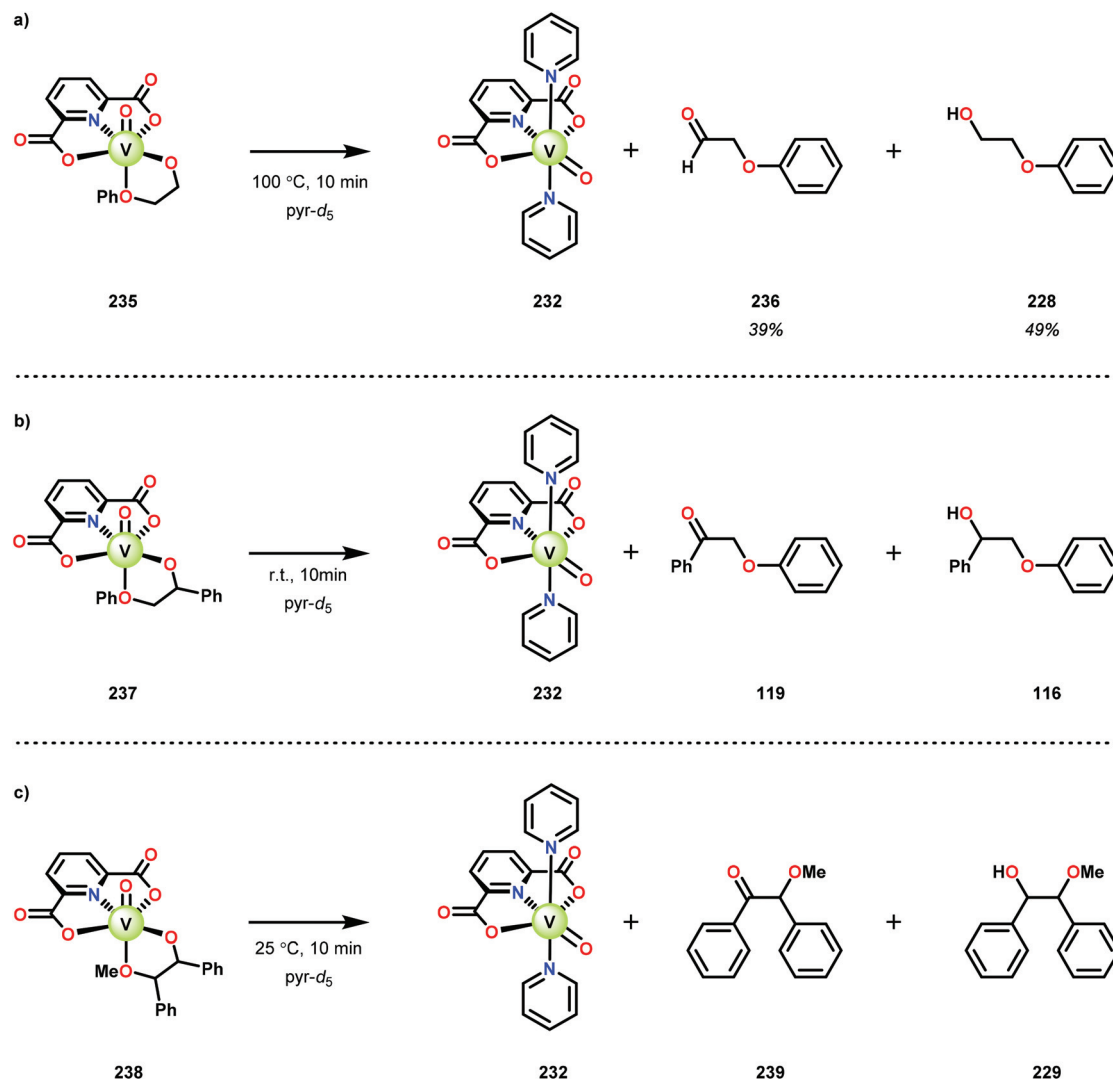
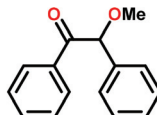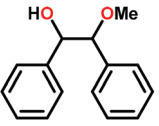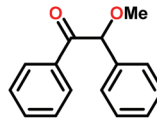**Scheme 17** Alcohol oxidation by V complexes (a) **235**, (b) **237** and (c) **239**.
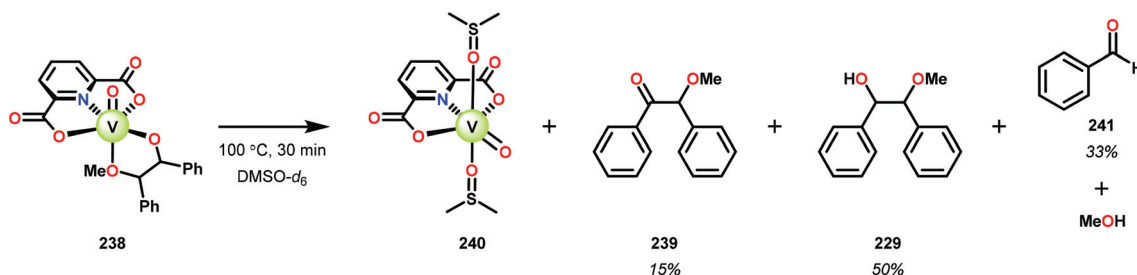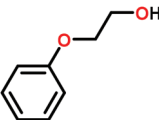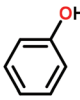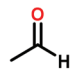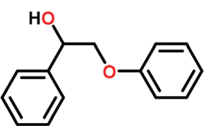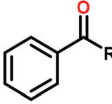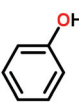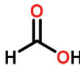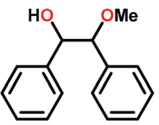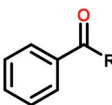
Scheme 18 Heating of V complex **238** in DMSO-d_6.

The phenolic substrate **263T** was also reacted but afforded an incomplete mass balance (see Scheme 21).[168] Mass balance inconsistencies have been previously reported on the oxidation of lignin models and are most likely attributed to polymerization or other reactions involving radical intermediates.[169,170]

To elucidate possibilities for loss of mass, aerobic oxidation of 2,6-dimethoxyphenol was carried out with the $V^V(HQ)_2(O)$ (O^iPr) catalyst (**257**) in the presence of Et_3N (10 mol%). After 48 h of heating at 80 °C, 98% of the 2,6-dimethoxyphenol had reacted to produce a dark brown solid. An aliquot was removed

This journal is © The Royal Society of Chemistry 2016

Org. Biomol. Chem., 2016, **14**, 1853–1914 | **1881**

Table 2 Catalytic oxidation of lignin model systems **116**, **228** and **229**[a]

Entry	Substrate	Conversion (%)	Products (%)
1[b]	**228**	20%	**66** 18% + **242** 6% + unidentified 2-5%
2[b]	**116**	95%	**243**: R = OH, 81% / **119**: R = CH$_2$OPh, 9% + **66** 77% + **244** 46%
3[c]	**229**	94%	**241**: R = H, 73% / **243**: R = OH, 5% / **245**: R = OMe, 5% + MeOH 69% + **239** 13%
4[d]	**229**	99%	**241**: R = H, 9% / **243**: R = OH, 85% / **245**: R = OMe, 84% + MeOH 6% + **239** 9%

[a] Reactions were carried out at 100 °C under an atmosphere of air in d_6-DMSO if not otherwise stated. [b] 10 mol% V(pda)(O)(O^{i}Pr) (**230**), 7 days. [c] 5 mol% V(pda)(O)(O^{i}Pr) (**230**), 20 h. [d] 10 mol% V(pda)(O)(O^{i}Pr) (**230**), 6 days. Reaction was carried out in pyridine-d_5.
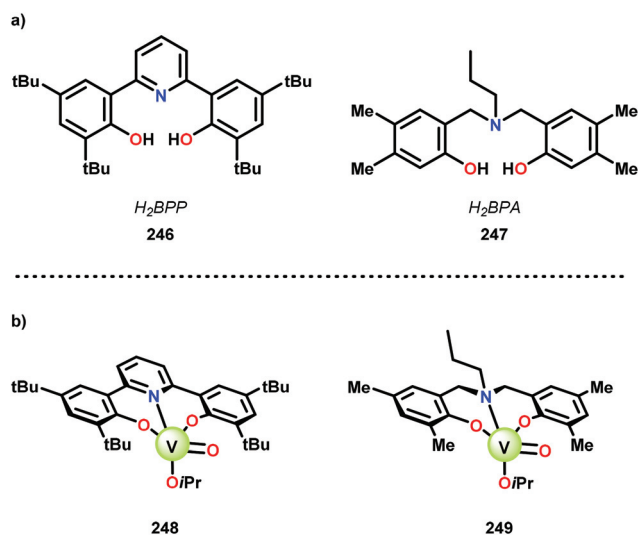
Fig. 28 Structure of (a) ligands H$_2$BPP (**246**) and H$_2$BPA (**247**), and (b) the corresponding V complexes (**248** and **249**).

and analyzed by NMR to show no soluble organics in the sample, consistent with polymerization or other reactions to afford recalcitrant byproducts.[168]

It is apparent that this catalyst system mediates the benzylic oxidation preferentially over other oxidized products. However, the phenolic containing substrates afford slightly different product distributions and selectivities.[168] This is consistent with the oxidative experiments of the phenolic and non-phenolic β-O-4 lignin models using the V^V(HQ)$_2$(O)(O^{i}Pr) catalyst (**257**).[167]

Based on the aforementioned results, it is evident that tuning the selectivity and reactivity with V catalysts is possible, although the outcome is rather difficult to predict. There are no established mechanisms for these oxidations but the selectivity and reactivity are greatly affected by the choice of ligand. The homogeneous nature of the various V catalysts has made them an attractive target for studying the oxidative degradation of lignin model systems. However, the evaluated V catalysts afford mainly oxidized ketone products in contrast to Cu and TEMPO-mediated oxidations that form mostly C–C bond cleavage products, implying that different mechanisms are operating (see section 3.4).

1882 | *Org. Biomol. Chem.*, 2016, **14**, 1853–1914

This journal is © The Royal Society of Chemistry 2016
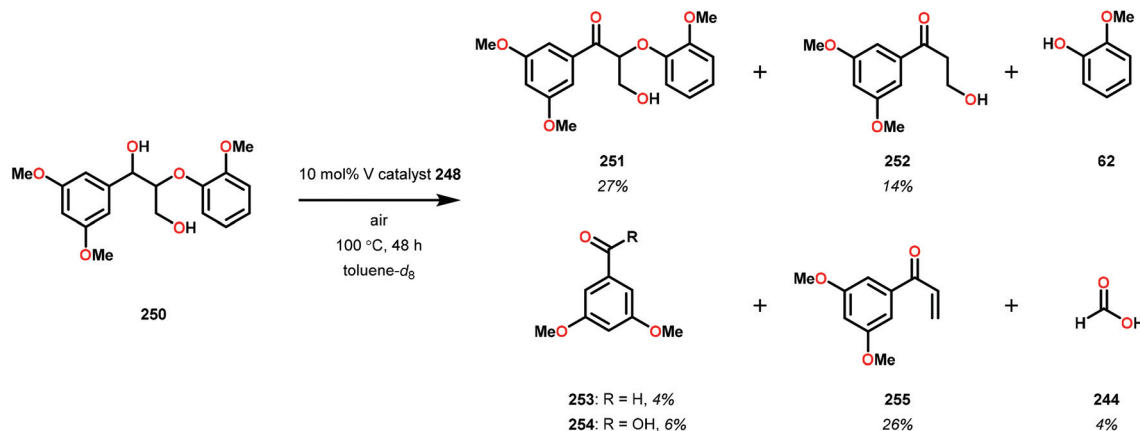
Scheme 19 Catalytic aerobic oxidation of lignin model system **250** with V complex **248**.
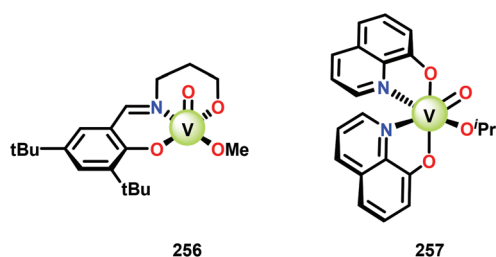
Fig. 29 (a) Previously reported V catalyst **256** that mediates C−O bond cleavage of non-phenolic lignin models and (b) the previously reported 8-quinolinate-based V catalyst **257** (V^V(HQ)$_2$(O)(O^{i}Pr)) that promotes C−H bond cleavage products of non-phenolic lignin model systems.

3.4 TEMPO-based catalytic system for oxidation and degradation of lignin models

N-Oxyl radicals have provided great utility for the oxidation of numerous functional groups. Commonly used oxidants are TEMPO (TEMPO = 2,2,6,6-tetramethylpiperidine-*N*-oxyl) and ABNO (ABNO = 9-azabicyclo[3.3.1]nonane *N*-oxyl) derived reagents. *N*-Oxyl based oxidants are widely applicable in the field of organic oxidations and have proven to be excellent choices for the selective oxidation of primary alcohols, secondary alcohols, primary amines and aldehydes.[171–176]

As previously stated, the primary pathway for degradation of lignin in nature is believed to occur *via* oxidative single-electron transfer (see Scheme 10).[114,115] Inspired by nature,

several research groups have turned their attention to developing methods for the oxidative degradation of lignin models using TEMPO-mediated oxidation protocols. Coupling such protocols with aerobic procedures is desirable since O$_2$ is a bountiful, inexpensive and an environmentally benign terminal oxidant. Hanson and co-workers therefore compared the aerobic oxidation of lignin models using homogeneous Cu- and V-based catalysts. The Cu catalysts used in this study consisted of a Cu/TEMPO system,[177] originally developed by Sheldon and co-workers, which was shown to mediate the aerobic oxidation of primary alcohols at room temperature.[178,179]

Hanson and co-workers began their investigations with a simple β-1 containing lignin model (**229**) where the catalytic system consisted of O$_2$, catalytic amounts of CuCl (20 mol%) and catalytic amounts of TEMPO (30 mol%) in pyridine at 100 °C for 48 h. In the Cu/TEMPO systems, Cu is believed to activate O$_2$, and Cu and TEMPO achieves the oxidation of the alcohol. This system was shown to afford benzaldehyde (**241**) and methyl benzoate (**245**) in good yields (Scheme 22).[177]

The authors found that the active Cu species was not stable under the reaction conditions, which prompted for portion-wise additions of CuCl and TEMPO to achieve 92% conversion after 48 h.[177] In contrast to the CuCl/TEMPO system, the V-catalyzed aerobic oxidation afforded benzoin methyl ether (**239**), which could subsequently undergo C–C bond cleavage and further oxidation to benzoic acid (**243**) and methyl benzoate (**245**) (Table 2, entry 4). With the V system, benzaldehyde
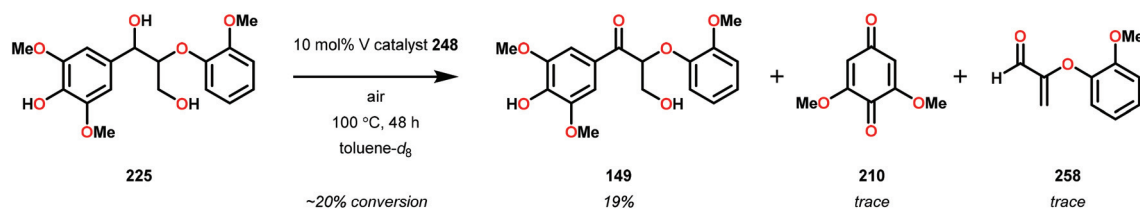
Scheme 20 Aerobic oxidation of phenolic lignin model **225** catalyzed by V complex **248**.

This journal is © The Royal Society of Chemistry 2016

Org. Biomol. Chem., 2016, **14**, 1853–1914 | **1883**

Table 3 Aerobic oxidation of the *erythro* and *threo* isomers of non-phenolic lignin model system 259. Italic columns represent C−H bond cleavage products[a]

Entry	Substrate	Solvent	Conversion (%)	Yield[b] (%)					
				260	*261*	253	179	254	262
1	**259T**	Pyridine-d_5	100	*34*	*57*	3	3	3	4
2	**259T**	DMSO-d_6	91	*66*	*6*	3	3	4	11
3[c]	**259E**	Toluene	100	*72*	*<1*	7	2	<1	<1

[a] Reaction conditions: V complex **257** (10 mol%), substrate, air, 100 °C, 48 h. [b] Yield determined by ^{1}H NMR using internal standard. [c] Reaction run in the presence of Et$_3$N (15 mol%).
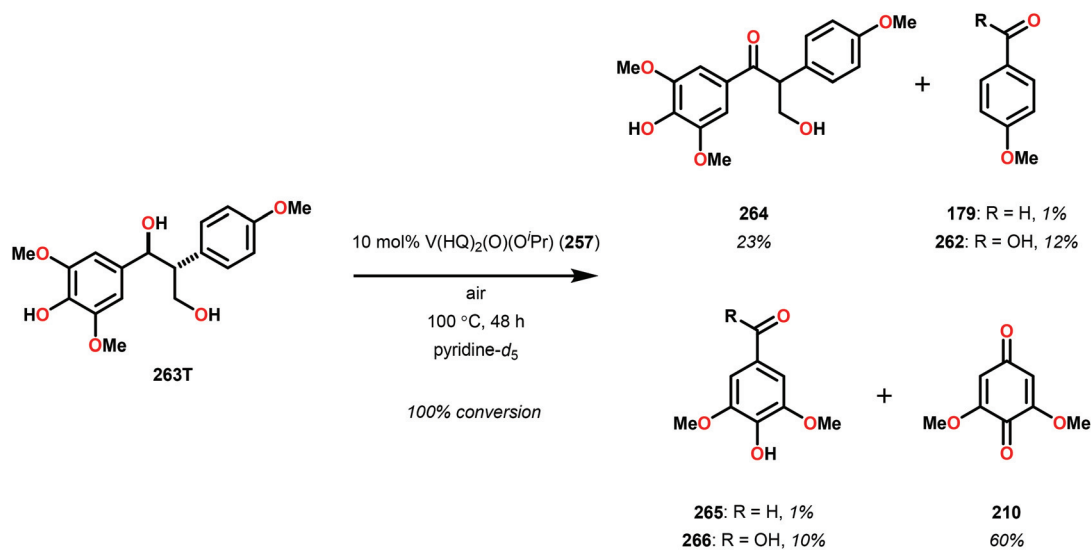
Scheme 21 Aerobic oxidation of the *threo* isomer of phenolic lignin model system 263 by V complex 257.

(**241**) (9%), methanol (6%), benzil (<5%), and benzoin (<5%) could also be observed as minor products.[161] To investigate the intermediacy of benzoin methyl ether (**239**) with the CuCl/TEMPO system, benzoin methyl ether (**239**) was subjected to the catalytic CuCl/TEMPO conditions for 18 h. The reaction afforded methyl benzoate (**245**) (85%), benzoic acid (**243**)

(76%), and benzaldehyde (**241**) (5%) (Scheme 23), implying that ketone **239** is indeed an intermediate.[177]

With the success of oxidizing **229**, the authors subsequently applied the Cu/TEMPO system on more complex lignin model systems. Considering the instability and limited lifetime of the CuCl/TEMPO system, the authors decided to use stoichio-

1884 | *Org. Biomol. Chem.*, 2016, **14**, 1853–1914

This journal is © The Royal Society of Chemistry 2016
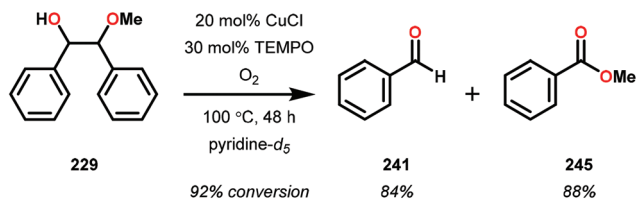
Scheme 22 Aerobic oxidation of 1,2-diphenyl-2-methoxyethanol (**229**).
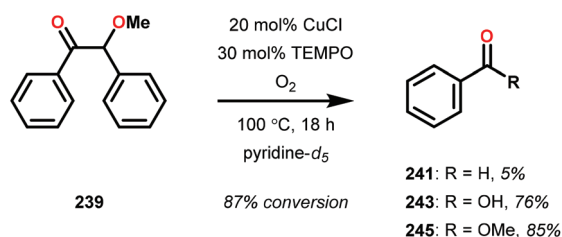
Scheme 23 CuCl/TEMPO catalyzed oxidation of benzoin methyl ether (**239**).

metric amounts of the CuCl/TEMPO system on lignin model system **250** (Scheme 24).[177]

The stoichiometric reaction afforded a mixture of products including C–C bond cleavage products (**253** and **254**), the oxidized ketone (**251**), the dehydrated ketone (**268**), and C–O bond cleavage products (**62** and **267**). The authors also observed the formation of condensation products by NMR. This was later confirmed using LC-MS analysis after observing higher molecular weight compounds in the reaction mixture. In order to determine whether ketone **251** was an intermediate, substrate **250** was treated with 10 mol% CuCl/TEMPO at 100 °C under an O$_2$ atmosphere for 18 h. This resulted in 48% conversion along with the dehydrated ketone **268** (18%) and other unidentified products; however, the aldehyde products

could not be detected. When subjecting model system **229** to ceric ammonium nitrate, a strong single-electron oxidant, a similar product distribution was observed as when compound **229** was subjected to the CuCl/TEMPO system, implying a single-electron mechanism followed by direct C–C bond cleavage.[177]

Subsequently, Hanson and co-workers proceeded to further investigate a Cu(OTf)/2,6-lutidine/TEMPO catalyst system for the degradation of β-1 lignin models. Non-phenolic lignin models were initially investigated with the Cu(OTf)/2,6-lutidine/TEMPO system. Substrate **259T**, a non-phenolic β-1 lignin model, was heated at 100 °C in the presence of 10 mol% Cu(OTf)/TEMPO, O$_2$ and 2,6-lutidine (10 equiv.) for 48 h to afford 3,5-dimethoxybenzaldehyde (**253**) (81%) and 4-methoxybenzaldehyde (**179**) (69%) as major products (Scheme 25, top).[168] These conditions afforded C–C bond cleavage products, similar to the previous CuCl/TEMPO system.[177] This mode of reactivity resembles the observed reaction pattern from Stahl and co-workers in which a Cu(OTf)(MeCN)$_4$/bpy/TEMPO/N-methylimidazole system afforded veratryl aldehyde (**269**) as the major product, resulting from initial oxidation of the primary alcohol followed by a retro-aldol reaction to cleave the C$_\alpha$–C$_\beta$ bond (Scheme 25, bottom).[180]

Following the Cu(OTf)/TEMPO results on the non-phenolic lignin model (**259T**), Hanson and co-workers proceeded to apply these conditions on a phenolic lignin model system (**263T**), still containing the β-1 connectivity. To investigate the selectivity of the Cu system, a catalytic reaction using 10 mol% of Cu(OTf)/TEMPO and a stoichiometric reaction was carried out on the phenolic lignin model (Scheme 26).[168] These results highlight that the aerobic oxidation of the phenolic β-1 lignin models afford mostly products derived from cleavage of the C$_{aryl}$–C$_\alpha$ bond, whereas oxidation of non-phenolic β-1 lignin models afford C$_\alpha$–C$_\beta$ bond cleavage products. This change in selectivity additionally emphasizes the challenges in catalyst development for the degradation of lignin models.
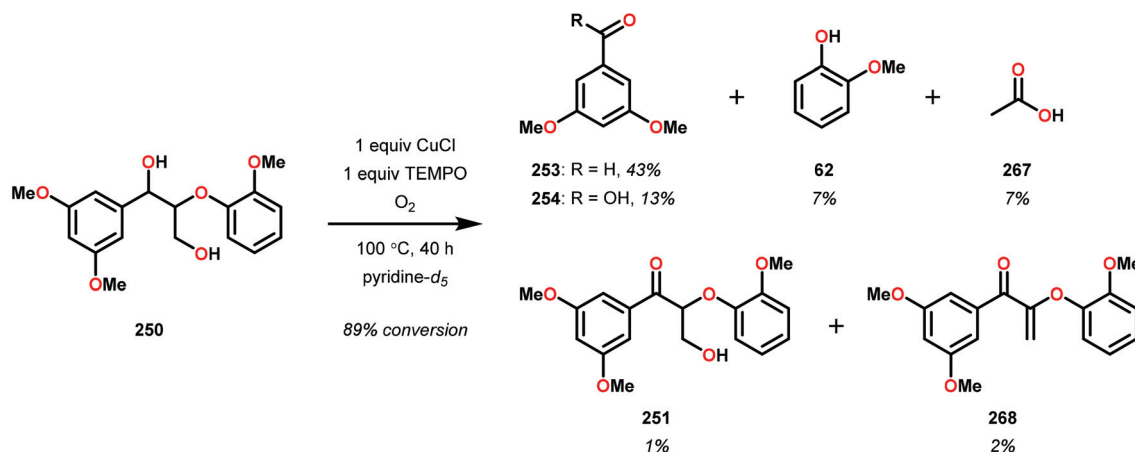
Scheme 24 Stoichiometric oxidation of lignin model system **250** with CuCl/TEMPO.
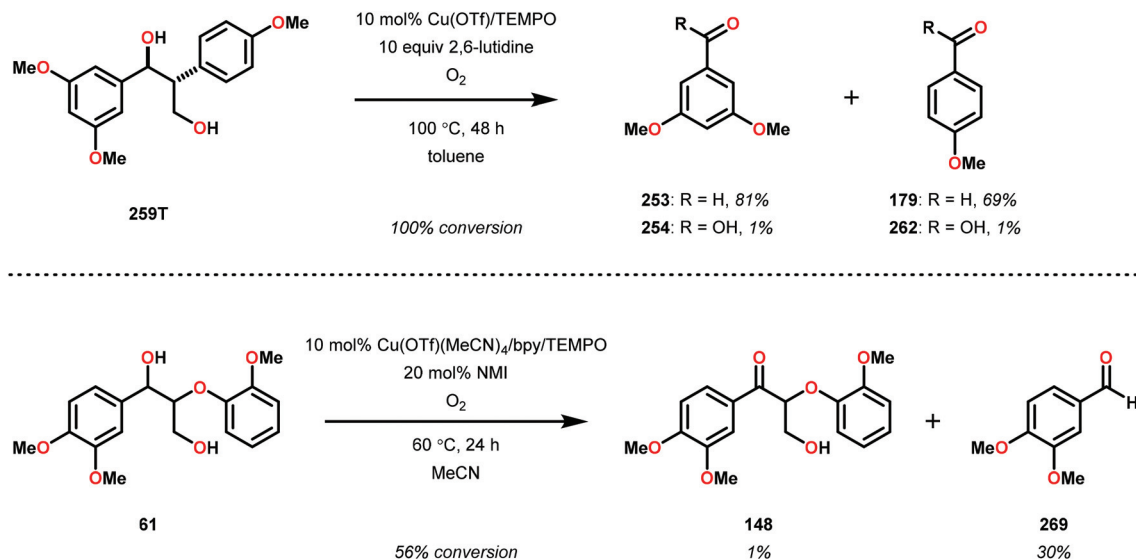
Scheme 25 (Top) Oxidation of the non-phenolic lignin model **259T** with the Cu(OTf)/2,6-lutidine/TEMPO system. (Bottom) Oxidation of non-phenolic lignin model **61** with the Cu(OTf)(MeCN)$_4$/bpy/TEMPO/NMI system.
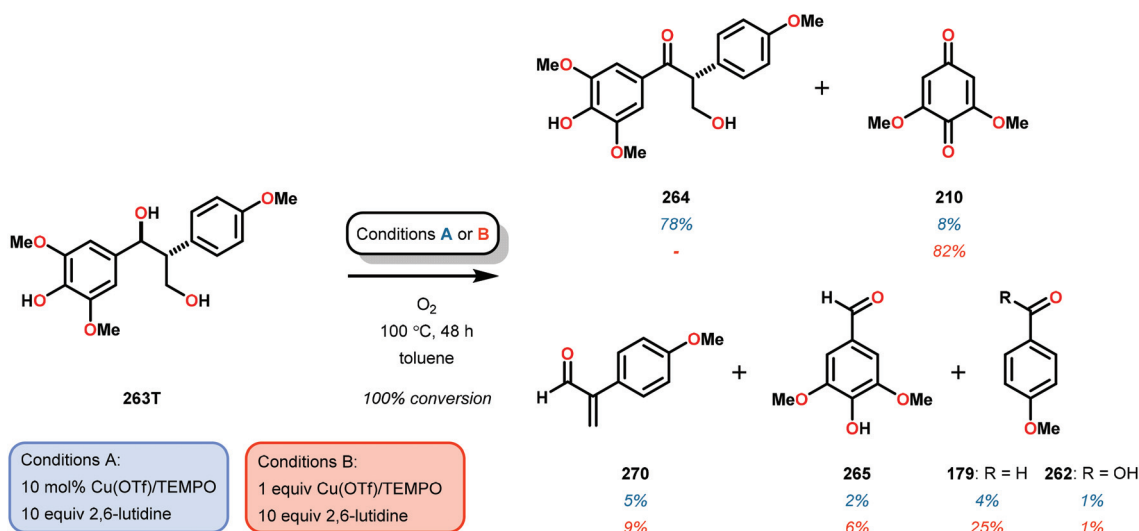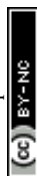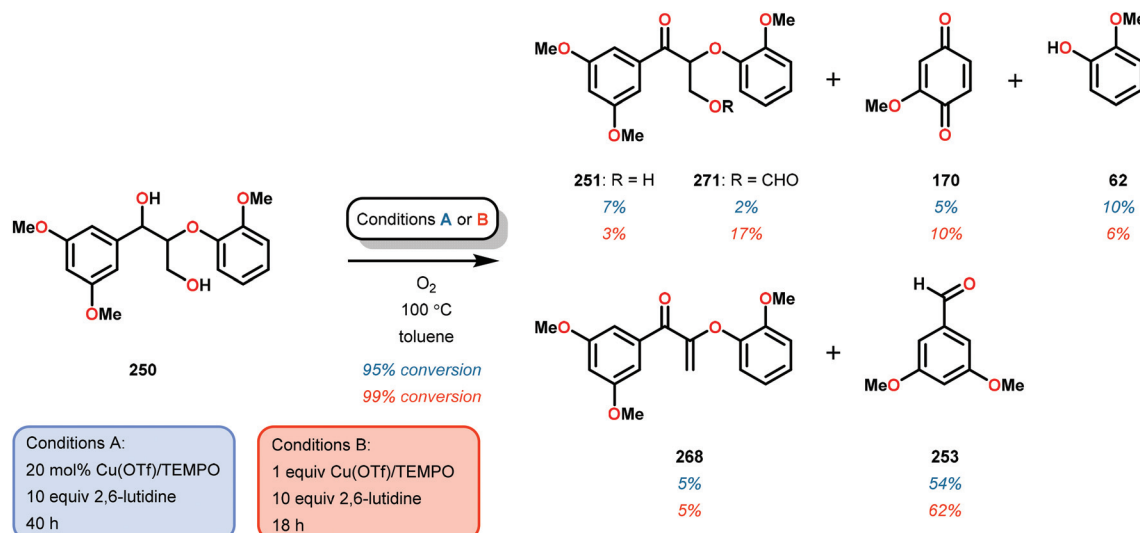

Scheme 26 Catalytic and stoichiometric oxidation of lignin model system **263T** by the Cu(OTf)/TEMPO system.

Baker and co-workers continued working with the Cu/TEMPO system and applied it to β-O-4 lignin model systems. The authors first focused on optimizing the catalyst system with non-phenolic substrate **250** in order to maximize the yield of the aldehyde product. Optimization began using stoichiometric amounts of Cu and TEMPO where a variety of N-donor ligands, Cu catalysts, time, and solvents were screened. It was noted that applying bulkier N-donor ligands generally increased the selectivity and the yield of the aldehyde product (**253**). Using pyridine and 2,6-lutidine as solvents showed moderate yields but were not as efficient as when using toluene with 2,6-lutidine as an additive (10 equivalents). The authors finally settled on a Cu(OTf)/TEMPO system, 2,6-lutidine

(10 equivalents) in toluene. Heating this reaction mixture at 100 °C gave 99% conversion and 62% yield of aldehyde **253** (Scheme 27).[181]

After determining suitable conditions for the stoichiometric oxidation of non-phenolic lignin model system **250**, the authors attempted to devise a catalytic procedure. A plethora of oxidation products were generated, with 3,5-dimethoxybenzaldehyde (**253**) being the major product (Scheme 27). Gratifyingly, improved selectivity was observed when applying the catalytic conditions to the phenolic β-O-4 lignin model **225** (Scheme 28). However, the reason for this change in selectivity when changing from non-phenolic to phenolic models is not fully understood.[181]

Scheme 27 Stoichiometric and catalytic oxidation of non-phenolic β-O-4 lignin model **250** by the Cu(OTf)/TEMPO/2,6-lutidine system.
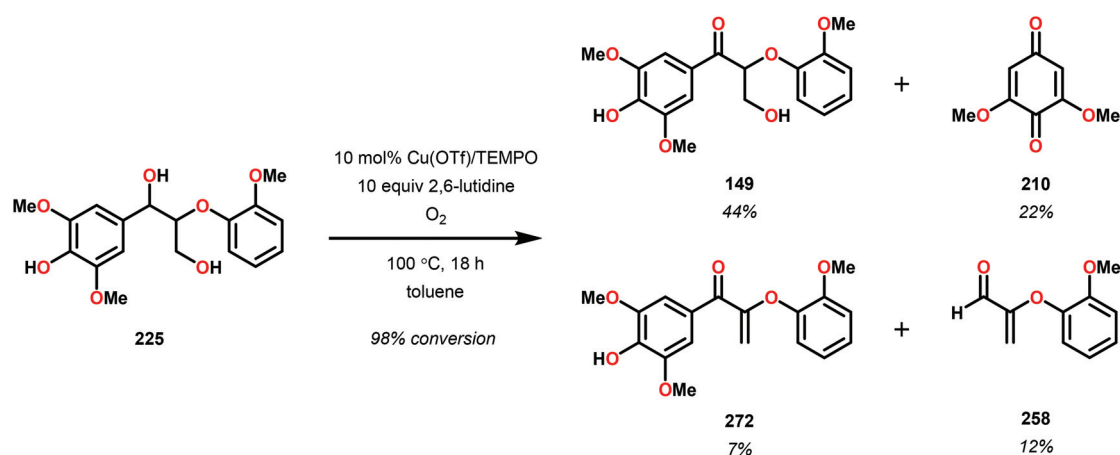
Scheme 28 Catalytic oxidation of phenolic lignin model system β-O-4 lignin model **225** by the Cu(OTf)/TEMPO/2,6-lutidine system.

Control reactions were run to highlight the importance of the TEMPO and 2,6-lutidine. Omitting both Cu(OTf) and TEMPO afforded only 2% conversion. In the absence of TEMPO, 60% conversion was observed after 18 h, indicating that oxidation can proceed without TEMPO, although it is evident that the TEMPO has a crucial role as a co-catalyst.[181]

Several catalytic systems have been developed for the aerobic oxidation of alcohols, lignin models, and diols, employing Cu and TEMPO.[182–184] Although different mechanisms have been proposed for Cu/TEMPO based oxidations,[185–189] Stahl and co-workers have proposed a mechanism relevant to the Cu(OTf)/TEMPO/2,6-lutidine reactions.[190,191] Oxidation of alcohols by the oxoammonium salt is a well-understood process and this possibility has been probed by kinetic studies. However, Stahl and co-workers noticed a

significant rate increase when switching from a Cu^{II} to a Cu^{I} source. For the mechanistic studies, Stahl and co-workers settled for a Cu^{I}(bpy)/TEMPO system where this system was compared to the TEMPO-catalyzed oxidation of alcohols. Monitoring of these reactions by *in situ* IR showed that the oxidation reactions employing stoichiometric oxoammonium (TEMPO) salts proceeded at a slower rate for both benzylic and aliphatic alcohols, implying that the oxoammonium cation is not the catalytically competent species in the TEMPO-catalyzed oxidation of alcohols, regardless of the 20-fold increase of the TEMPO reagent (Fig. 30).[190]

From the spectroscopic studies, rate law calculations, kinetic isotope effect and Hammett studies, a mechanism was proposed and is depicted in Fig. 31. The authors proposed two separate half-reactions: (1) activation of O₂ by the reduced

This journal is © The Royal Society of Chemistry 2016

Org. Biomol. Chem., 2016, **14**, 1853–1914 | **1887**
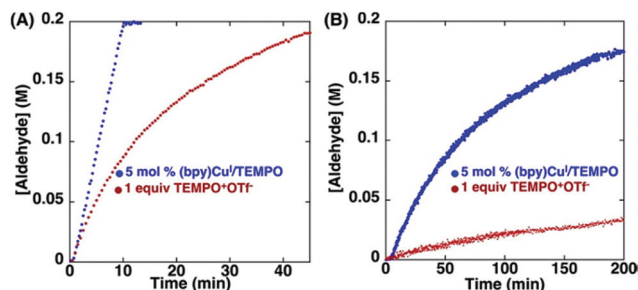
Fig. 30 Monitoring of the formation of aldehyde by *in situ* IR. Oxidation of (A) benzyl alcohol and (B) cyclohexylmethanol by 5 mol% Cu^I(bpy)/ TEMPO (blue) and stoichiometric TEMPO$^+$OTf$^-$ (red). Reprinted with permission from ref. 190. Copyright 2013 American Chemical Society.

Cu catalyst (Cu^I) (**273** → **274**), and (2) concerted oxidation of the alcohol where both Cu^{II} and TEMPO act as one-electron oxidants to achieve the overall two-electron conversion of the alcohol to the corresponding aldehyde (**278** → **273**).[190]

Baker and co-workers noted that the mechanism outlined by Stahl and co-workers pertains to several key steps that may be occurring in the Cu(OTf)/TEMPO oxidation of lignin model systems. However, in contrast to the proposed mechanism in Fig. 31, which is proposed to be the fundamental mechanism operating under ambient temperatures, the Cu(OTf)/TEMPO experiments were conducted at elevated temperatures (100 °C). The increased temperatures most likely creates conditions where both Cu^I and Cu^{II} complexes with N-donor ligands are more labile, hence reducing the potential for achieving higher reactivity and selectivity.[181] Additionally, Chiba and co-workers have also employed Cu for the aerobic oxidative cleavage of lignin model systems.[192]

In light of the potential for using oxoammonium salts as oxidants, Stahl and co-workers set out to develop a selective method for the aerobic oxidation of lignin model systems containing the β-O-4 linkage. Here, oxidation of the benzylic alcohol to produce the corresponding ketone was the desired transformation and their investigation started with β-O-4 lignin model system **61** (Fig. 32).[180]
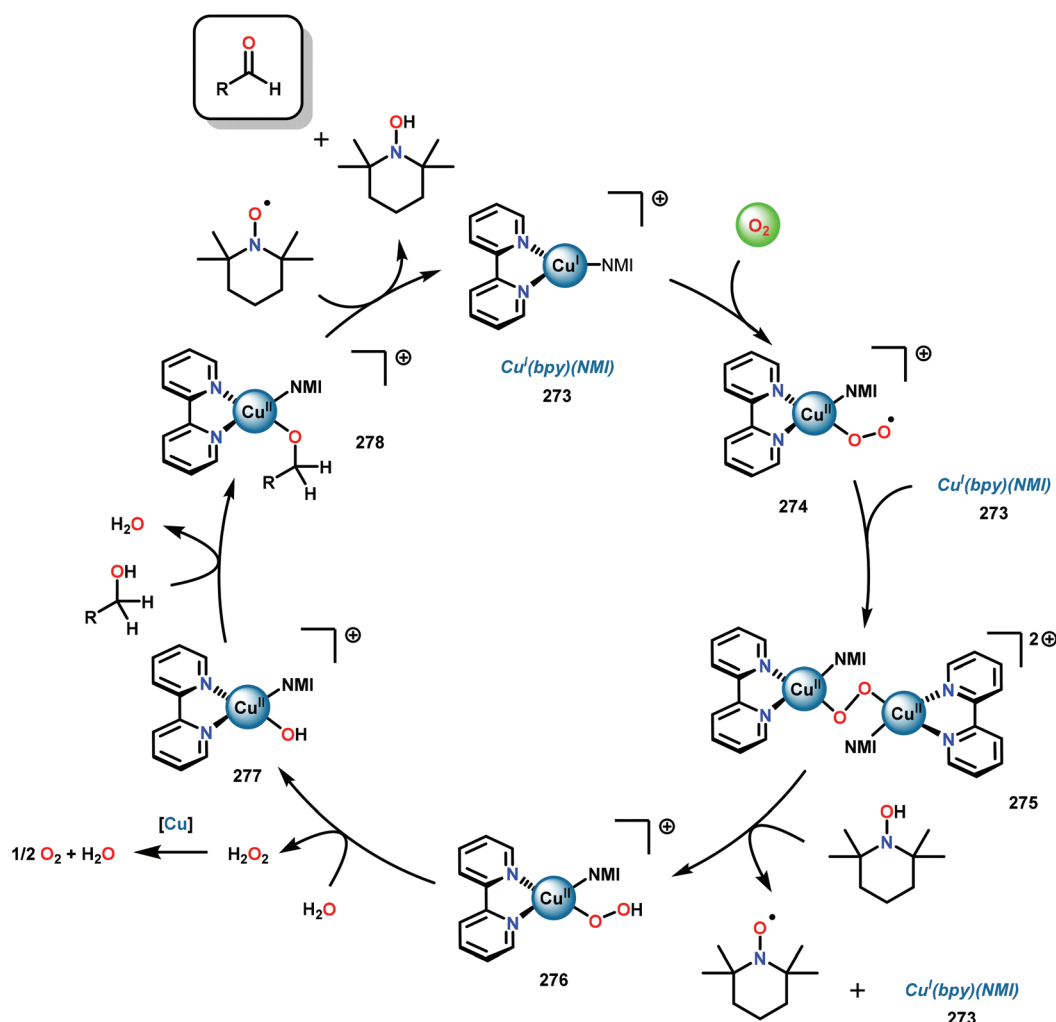
Fig. 31 Proposed mechanism for catalytic Cu^I/TEMPO mediated oxidation of alcohols. NMI = *N*-methylimidazole. R = alkyl, aryl.
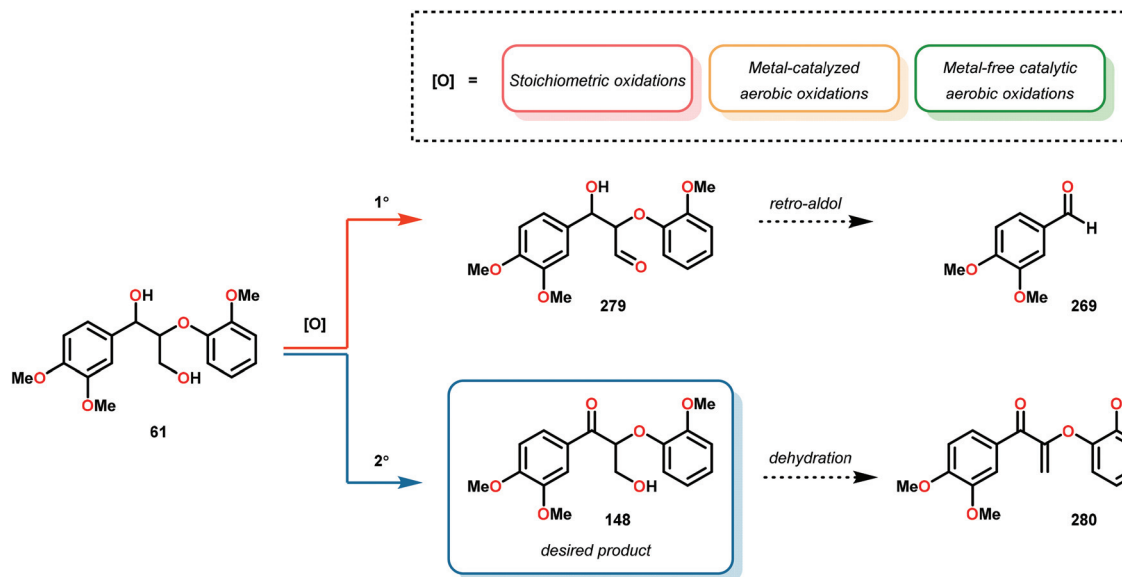
Fig. 32 Possible product distribution for oxidation of lignin model system **61** by TEMPO-based catalytic protocols.

An assortment of oxidation methods was investigated on model system **61** to identify suitable conditions for achieving high selectivity for the benzylic oxidation. In some of the applied catalytic systems, oxidation of the primary alcohol unit could also be observed and produced a "byproduct" (**269**), which is presumably the result of a retro-aldol reaction. In addition to these two oxidation products, the dehydrated ketone **280** was also isolated in certain cases. A CuBr/bpy/DABCO/TEMPO (10 mol%) system afforded 86% conversion but unfortunately afforded the dehydrated ketone **280** (23%) and aldehyde **269** (31%) as major products with the desired ketone **148** in merely 6% yield after 24 h at 60 °C using O_2 as the terminal oxidant. Removal of DABCO increased conversion to 89% but afforded ketone **148** in only 10% yield and aldehyde **269** in 37% yield, together with other unidentifiable products. An aerobic system consisting of Pd(OAc)$_2$/DMSO (5 mol% Pd(OAc)$_2$) gave excellent selectivity, producing ketone **148** exclusively but in a modest yield of 42%. This could be slightly improved by employing Pd(OAc)$_2$ (5 mol%) in a DMSO/H$_2$O mixture (4:6) with added 2,9-dimethyl-1,10-phenanthroline (10 mol%) as a ligand. This combination produced 87% conversion of substrate **61** with the exclusive formation of ketone **148** in 56% yield. A TEMPO-based system using Fe(NO$_3$)$_3$ (5 mol%) and TEMPO/NaCl (10 mol%) in DCE afforded 100% conversion and produced the desired ketone **148** in 79% yield, but all metal-catalyzed oxidations paled in comparison to the final conditions, which consisted of AcNH–TEMPO (5 mol%), HNO$_3$/HCl (10 mol% each), 1 atm O_2 at 45 °C. These conditions were subsequently used on a variety of lignin model systems and generally afforded the desired ketones in high yields and excellent selectivity (Fig. 33).[180] Even oxidized lignin, derived from aspen, could be depolymerized when

treated with formic acid to afford >61 wt% of low-molecular-mass aromatics (Scheme 29).[193]

Stephenson and co-workers subsequently designed a two-step, overall redox-neutral approach to the degradation of lignin model compounds containing β-O-4 linkages. This method employed a recyclable oxidant, [4-AcNH-TEMPO]BF$_4$, to carry out the oxidation of the benzylic alcohols with a subsequent photochemically-mediated reduction step to afford β-O-4 cleavage products (see also section 2). Stephenson and co-workers targeted the oxidation of the C$_\alpha$–O in order to weaken the C$_\beta$–O bond (see Fig. 35) for a subsequent photochemical reduction of the β-O-4 linkage using 1 mol% [Ir(ppy)$_2$(dtbbpy)]PF$_6$ (**146**) as the photocatalyst. 1 equivalent of Bobbitt salt in the presence of an equimolar amount of silica afforded the oxidized products in high yields for a variety of lignin model systems (Table 4).[101] Additionally, a similar two-step approach has been reported by Westwood and co-workers where DDQ/t-BuONO was employed to affect the initial oxidation and stoichiometric amounts of Zn were used to carry out the subsequent reductive cleavage.[194]

The extensive work with TEMPO-mediated oxidations of lignin model systems highlights that homogeneous catalysis with TEMPO reagents is indeed suitable for affecting the oxidation of lignin models. Selective oxidation of the benzylic alcohol as well as oxidative degradation of lignin models has shown how catalyst choice and catalyst amount can affect the efficiency and selectivity of the studied reaction. The knowledge acquired from this body of work is rapidly increasing as more advanced methods are being developed towards the depolymerization of more sophisticated lignin model systems and native lignin itself.
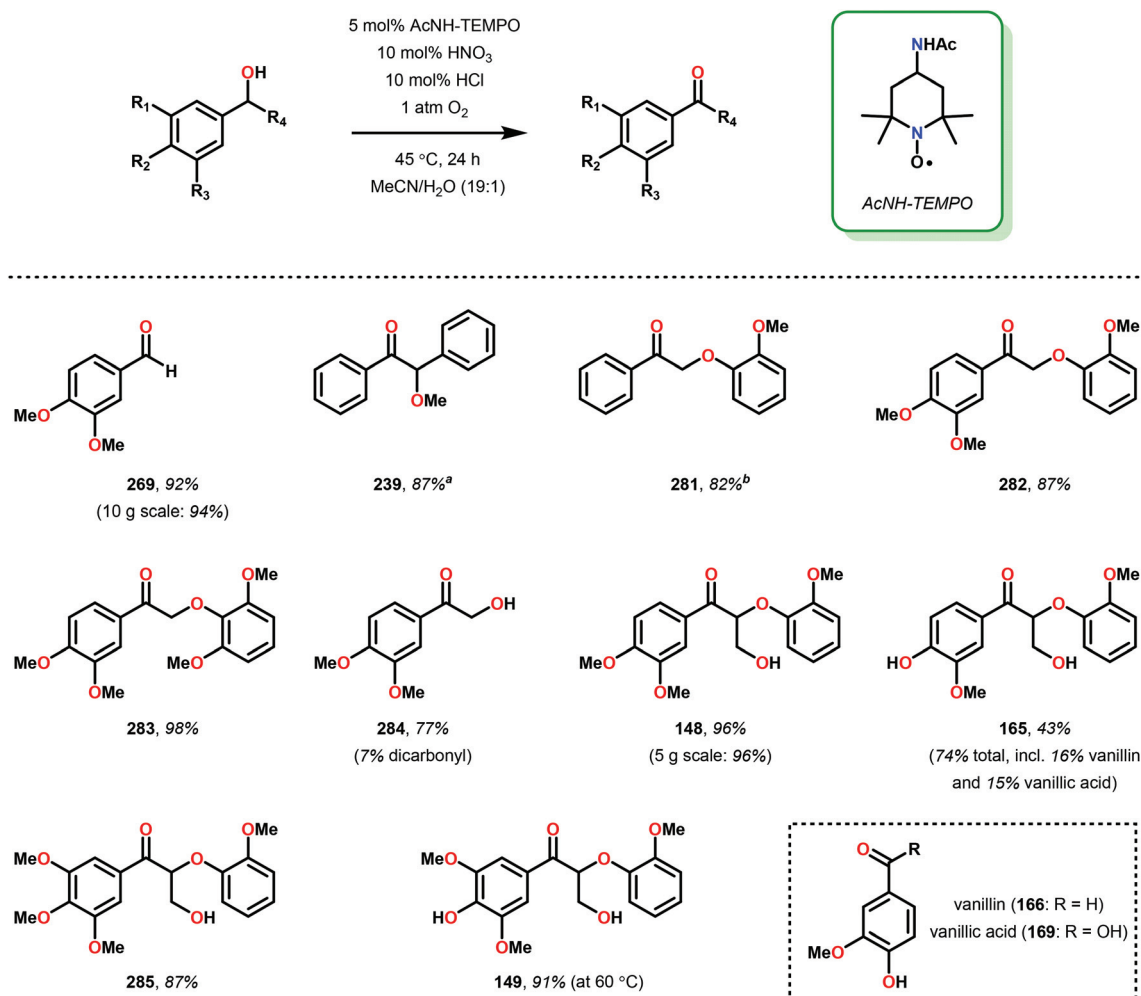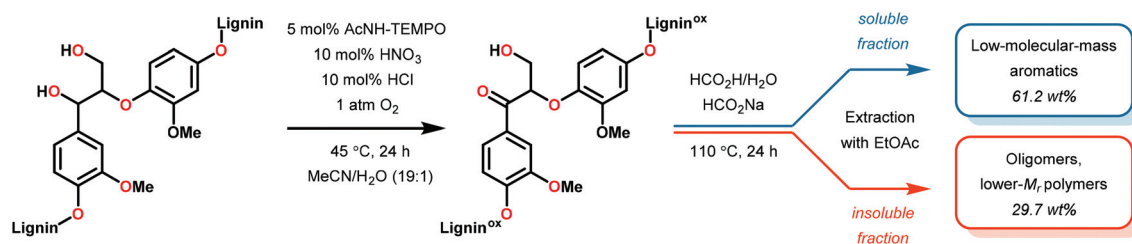
This journal is © The Royal Society of Chemistry 2016

Org. Biomol. Chem., 2016, **14**, 1853–1914 | **1889**

Fig. 33 Metal-free aerobic oxidation of lignin models using the AcNH–TEMPO/HNO$_3$/HCl catalyst system. Reaction conditions: 1 mmol of alcohol (0.2 M in MeCN/H$_2$O 19 : 1). [a] 10 mol% AcNH–TEMPO, 36 h. [b] Yield after 36 h.
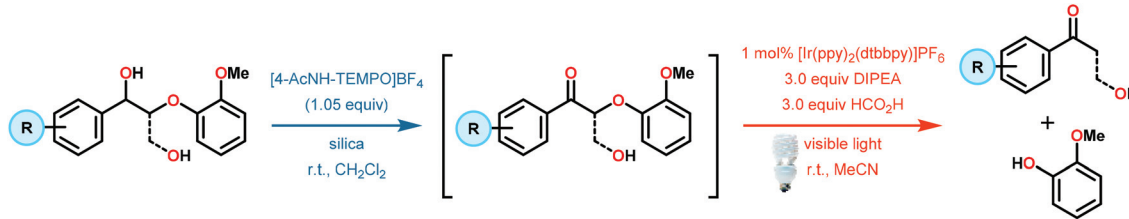

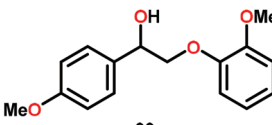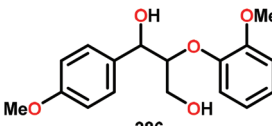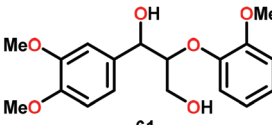**Scheme 29** Two-step approach for depolymerization of aspen lignin.

4. Redox-neutral conversion of lignin

The ultimate atom-economical route for valorization of lignin would be to design a pathway where lignin is fragmented in a redox-neutral fashion. In this approach, the generated reductive equivalents stemming from the initial oxidation step would subsequently be used to reductively cleave the β-O-4 bond of the oxidized lignin fragment (see Fig. 34). This would allow carrying out the overall depolymerization of lignin through a one-pot tandem cleavage process without the use of stoichiometric additives or reagents. Although the two-step fragmentation process is formally redox-neutral, an initial oxidation step followed by a reduction step, the ideal redox-neutral transformation would utilize the same catalyst to perform both the oxidation and the reduction step and such catalytic systems are certainly not elementary to design.

Table 4 Two-step TEMPO/photochemical β-O-4 degradation of lignin model systems

Substrate	Oxidation time (h)	Reduction time (h)	Yield[a] (%)	
			Oxidation	Reduction
99	15	12	85%	83%
286	18	15	81%	80%
61	15	18	84%	93%

[a] Yields of products isolated *via* column chromatography and based on an average of two runs.
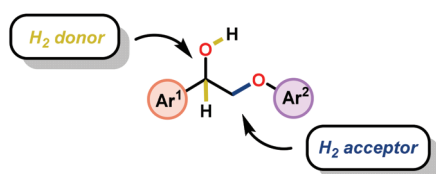
Fig. 34 Principle for redox-neutral conversion of lignin and lignin model systems.

Beckham and co-workers recently examined the bond dissociation energies (BDEs) of common bonds that are prevalent in native and oxidized lignin model dimers. By use of density functional theory (DFT) calculations the authors were able to quantitatively predict the relative BDEs for C–C and C–O bonds in an expanded range of lignin model compounds.[102]

It could be predicted that oxidation of the lignin model system (**287**) at either the γ-carbon (primary alcohol) or α-carbon (secondary alcohol) to an aldehyde or ketone, respectively, would significantly reduce the bond energy for C–O bond cleavage at the β-position (*i.e.* β-O-4 linkage). The BDEs for the ketone form (**288**) was shown to be on average 3 kcal mol^{-1} lower than the aldehyde form (**289**) (see Fig. 35).[102] These results suggest that routes for depolymerization of lignin involving initial oxidation of either of the alcohol

units in native lignin could lead to enhanced catalytic rates for the subsequent β-O-4 cleavage step.

4.1 Ruthenium-promoted cleavage of lignin and β-O-4 model compounds

An elegant approach for the redox-neutral conversion of lignin model compounds was reported by Ellman, Bergman and co-workers.[195] Ru(H)$_2$(CO)(PPh$_3$)$_3$ and related complexes have previously been reported to be competent in affecting both dehydrogenation[196,197] and C–O activation[198,199] and thus seemed as a prominent starting point. Their approach utilized a Ru catalyst, produced *in situ* from Ru(H)$_2$(CO)(PPh$_3$)$_3$ in combination with xantphos ((9,9-dimethyl-9H-xanthene-4,5-diyl)bis (diphenylphosphane)). The generated catalyst was able to affect the tandem catalytic dehydrogenation/C–O bond cleavage in a redox-neutral fashion without any additional reagents.[195]

Initial experiments consisted of using 2-phenoxy-1-phenylethan-1-ol (**116**) as the model system to screen a variety of monodentate and bidentate ligands. In the absence of any ligand, catalytic amounts of Ru(H)$_2$(CO)(PPh$_3$)$_3$ only resulted in minor amounts of cleaved products. Addition of monodentate phosphine ligands gave even lower conversion and use of bidentate ligands with a wide range of bite-angles were able to affect the dehydrogenation step to afford α-phenoxyacetophe-
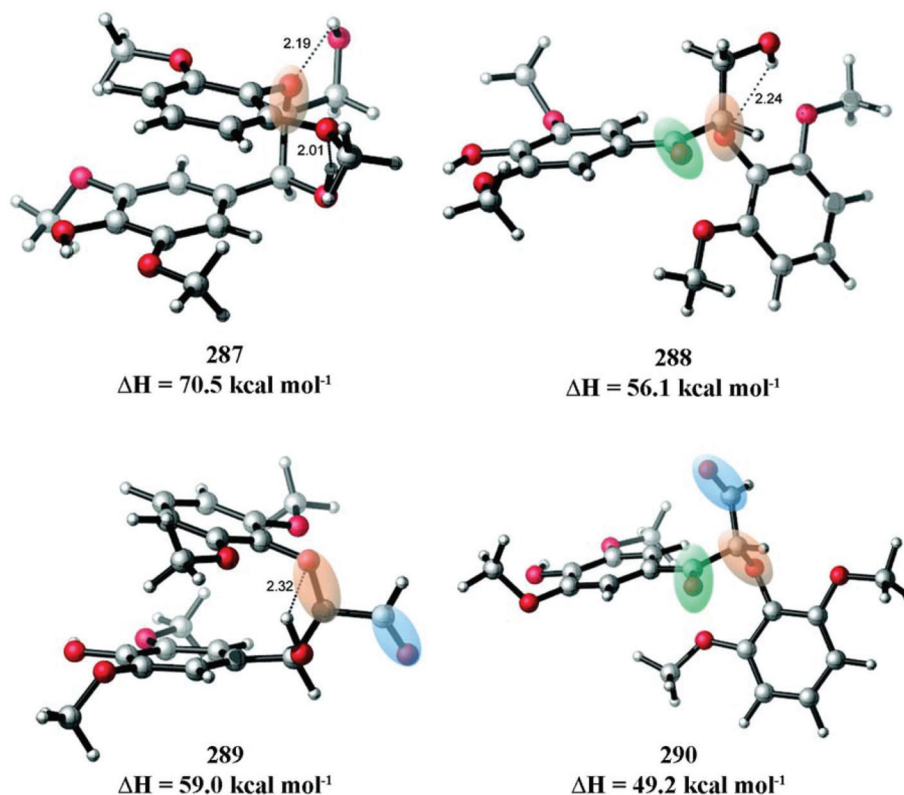
This journal is © The Royal Society of Chemistry 2016

Org. Biomol. Chem., 2016, **14**, 1853–1914 | **1891**

287
ΔH = 70.5 kcal mol⁻¹

288
ΔH = 56.1 kcal mol⁻¹

289
ΔH = 59.0 kcal mol⁻¹

290
ΔH = 49.2 kcal mol⁻¹

Fig. 35 Comparison of β-O-4 in a native lignin model compound (**287**) and β-O-4 in various oxidized systems (**288–290**) for C−O bond cleavage at the β-position. Bond lengths are given in Å. The β-O-4 linkages (red) and the oxidized alcohol unit(s) (blue and green) have been highlighted for clarity. Adapted with permission from ref. 102. Copyright 2011 American Chemical Society.

none but were ineffective in promoting the subsequent β-O-4 reductive cleavage. However, quantitative yield of the cleaved products were obtained when using the wide bite-angle ligand xantphos, highlighting that a catalytic redox-neutral strategy is indeed achievable. A small set of lignin model systems were applied to the catalytic system and afforded in general high yields of the cleaved products (Table 5). However, a slight decrease in yield was observed when using a 2,6-dimethoxy substituted phenol (**292**).[195]

The authors subsequently applied the developed Ru-based catalytic system on an actual polymer of 2-aryloxy-1-arylethanol. Gratifyingly, the Ru-xantphos system was capable of providing quantitative depolymerization of poly(4′-hydroxy-1-phenethanol) to 4′-hydroxyacetophenone (**107**) by slightly modifying the reaction conditions (Scheme 30) in order to account for the poor solubility of the as-synthesized polymer. This result demonstrates the power of the designed catalytic system for redox-neutral cleavage of a lignin model polymer.[195]
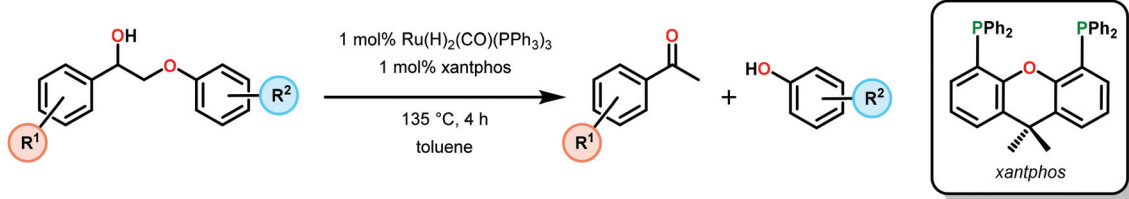
Mechanistic studies revealed that blocking the dehydrogenation process inhibited the subsequent C–O bond cleavage (Scheme 31, top). In addition, the use of silane as a surrogate for molecular hydrogen successfully reduced the proposed intermediate **119** to afford the C–O bond cleaved products in 89% yield (Scheme 31, low). Lastly, deuterium labeling experiments using Et₃SiD resulted in the formation of 55%

deuterium incorporation at the α-keto position of the produced acetophenone. Collectively, these findings support the depicted mechanism in Fig. 36 where the Ru catalyst dehydrogenates the benzylic alcohol (**116**) to give the corresponding ketone (**119**). This is followed by C–O bond activation to produce a Ru-enolate (**297**), which upon hydrogenation results in a Ru-phenolate species (**298**), from which reductive elimination generates the phenol (**62**) to close the catalytic cycle.[195] The group of Beckham subsequently performed DFT calculations on the Ru-xantphos system, which supported the suggested catalytic mechanism and further elucidated the kinetic and thermodynamic preferences of the Ru-based system.[200]

Although the discovery that the Ru-xantphos system was able to fragment lignin model compounds in a redox-neutral fashion, the necessity to implement the catalytic system on more complex and closely related native lignin systems should also be addressed. Inspired by Ellman, Bergman and co-workers, James and co-workers investigated the Ru-xantphos redox capability on more intricate model systems.[201–203] Although the Ru(H)₂(CO)(PPh₃)₃-xantphos system was applied to the efficient depolymerization of a synthetic polymer,[195] James and co-workers found that the incorporation of a γ-OH functionality into the "simple" lignin model systems dramatically inhibited the formation of the hydrogenolysis products.[201] When attempting to cleave the γ-OH containing

1892 | *Org. Biomol. Chem.*, 2016, **14**, 1853–1914

This journal is © The Royal Society of Chemistry 2016

Table 5 Tandem alcohol dehydrogenation and β-O-4 reductive cleavage of various 2-aryloxy-1-arylethanols by the Ru(H)$_2$(CO)(PPh$_3$)$_3$-xantphos system

Entry	Substrate	R^1	R^2	Yield^a (%)
1	**116**	H	H	98
2	**291**	H	2-(MeO)	88
3	**292**	H	2,6-(MeO)$_2$	62
4	**293**	4-(MeO)	H	98
5	**294**	3,4-(MeO)$_2$	2-(MeO)	89

^{a} Isolated yields of the corresponding ketone based on two duplicate experiments.
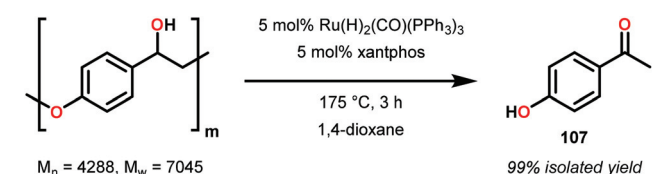
Scheme 30 Redox-neutral depolymerization of lignin model polymer by the Ru(H)$_2$(CO)(PPh$_3$)$_3$-xantphos system.

compounds **299** and **300**, only minor amounts of the hydrogenolysis product guaiacol were detected (Table 6). In addition to guaiacol, ketones **281** and **301** were observed, which most likely are formed by loss of formaldehyde. The conversions of compounds **299** and **300** under the studied conditions ranged from 10% up to 81%; however, the (by)products along with guaiacol and ketones **281** and **301** remain to be identified. Similar reactivity was also observed when using the reduced substrate **302**, resulting in high conversion but with low yields of guaiacol and ketones **281** and **299** (Table 7).[201] These findings clearly highlight that the inclusion of the γ-OH functionality severely restricts the catalytic hydrogenolysis reaction and limits the substrate scope of the Ru-xantphos system.

To probe the possible deactivation pathways, a scaled up reaction of ketone **299** and the Ru(H)$_2$(CO)(PPh$_3$)$_3$-xantphos catalyst, resulted in the isolation of two white colored products, which were found to be Ru complexes **303** and **304** (Fig. 37). The structures of these complexes imply that substrate **299** has undergone a dehydrogenation accompanied by the formation of a stable Ru species where both α- and γ-carbons are coordinated to the metal center. Both of the isolated Ru complexes **303** and **304** were essentially inactive towards the β-O-4 cleavage of substrate **299**. Interestingly, Ru complex **303** could not be interconverted to complex **304**, implying that the two complexes originate from a common catalytic entity.[201]
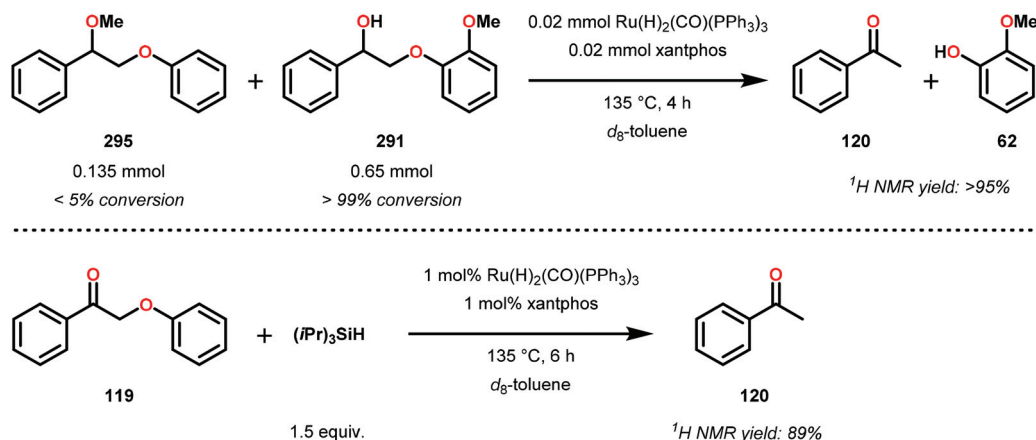
Scheme 31 Mechanistic experiments conducted on the Ru(H)$_2$(CO)(PPh$_3$)$_3$-xantphos system.

This journal is © The Royal Society of Chemistry 2016

Org. Biomol. Chem., 2016, **14**, 1853–1914 | **1893**
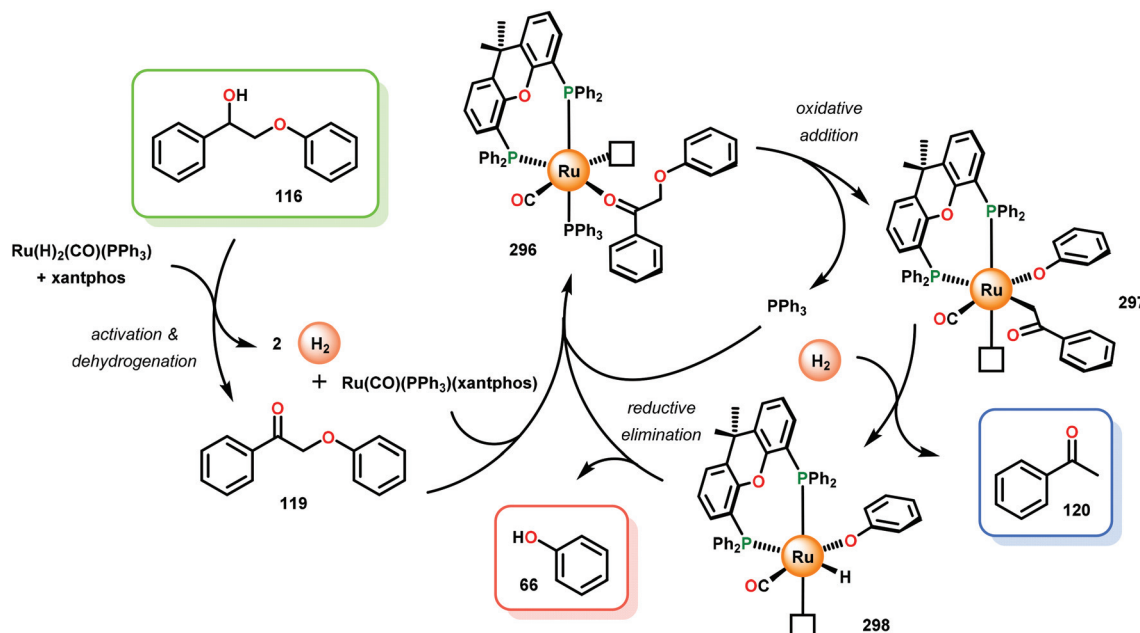
Fig. 36 Proposed catalytic cycle for C–O bond cleavage by the Ru(H)₂(CO)(PPh₃)₃-xantphos system.

Table 6 Redox-neutral attempts to cleave γ-OH containing lignin model compounds **299** and **300** by the Ru(H)₂(CO)(PPh₃)₃-xantphos catalyst
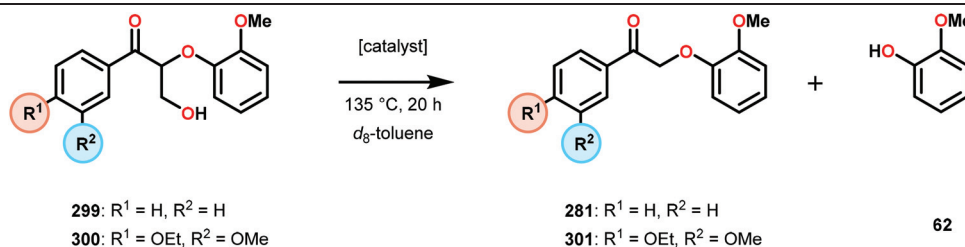
Entry	Substrate	Catalyst (5 mol%)	Atmosphere[a]	Conversion[b] (%)	Yield[b] (%)	
					281/301	62
1	299	Ru(H)₂(CO)(PPh₃)₃-xantphos	Ar or H₂	71–81	17–23	11–15
2	300	Ru(H)₂(CO)(PPh₃)₃-xantphos	Ar or H₂	68–70	5–11	7–8
3	299	—	Ar or H₂	9–12	3–7	0
4	299	Xantphos	Ar or H₂	24–32	9–13	0
5	299	Ru(H)₂(CO)(PPh₃)₃	Ar or H₂	51–59	16–24	3–5

[a] 1 atm. [b] Yields and conversions were determined by ¹H NMR based on two duplicate experiments.

A tentative mechanism explaining the formation of Ru complexes **303** and **304** from reaction with ketone **299** is depicted in Scheme 32. It is assumed that the Ru(H)₂(CO)(PPh₃)₃-xantphos catalyst dehydrogenates the primary alcohol moiety to form a Ru⁰-aldehyde species (**307**) with concomitant loss of H₂. Such electron-rich Ru⁰-carbonyl intermediates have been documented to facilitate oxidative addition of the aldehyde unit to afford Ruᴵᴵ-acyl-hydrido species.[204] Oxidative addition of Ru⁰-aldehyde species **307** subsequently generates intermediate **308**. The Ruᴵᴵ-acyl-

hydrido species **308** is proposed to be the common intermediate from which the two Ru complexes **303** and **304** are derived from. Loss of H₂ from intermediate **308** would deliver Ru complex **303**, or alternatively, if the H₂ is used to hydrogenolyze the aryl ether moiety affords complex **304**.[201] This work highlights the deactivation pathways for the Ru (H)₂(CO)(PPh₃)₃-xantphos system and that implementing redox-neutral fragmentation of simple lignin related compounds on more functionalized substrates housing the γ-OH unit is not straightforward and requires additional studies

1894 | *Org. Biomol. Chem.*, 2016, **14**, 1853–1914

This journal is © The Royal Society of Chemistry 2016

Table 7 Tandem dehydrogenation/hydrogenolysis reaction with lignin model system **302**

Entry	Catalyst (5 mol%)	Atmosphere[a]	Conversion[b] (%)	Yield[b] (%)		
				281	**299**	**62**
1	Ru(H)$_2$(CO)(PPh$_3$)$_3$-xantphos	Ar or H$_2$	73–82	3–7	7–11	11–15
2	Ru(H)$_2$(CO)(PPh$_3$)$_3$	Ar or H$_2$	57–73	3–4	2–5	2–6

[a] 1 atm. [b] Yields and conversions were determined by ^{1}H NMR based on two duplicate experiments.
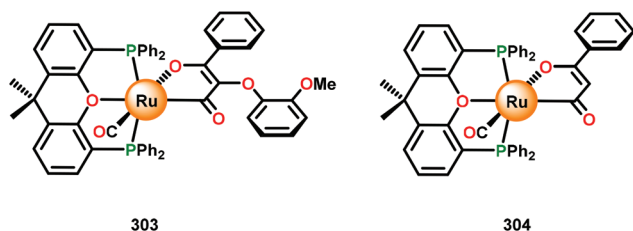
Fig. 37 Structures of Ru complexes **303** and **304** generated after reaction with ketone **299**.

before redox-neutral conversion of native lignin can be carried out.

Subsequent studies by James and co-workers tried to address this lack of activity by modifying the γ-OH functionality to give model systems that would not irreversibly ligate to the Ru center.[203] The γ-OH entity was therefore acetylated, a technique commonly employed to study and characterize lignin by NMR[205] and mass spectrometry.[206] Treating the acetylated compound **309** with the Ru(H)$_2$(CO)(PPh$_3$)$_3$-xantphos catalyst under the previously established reaction conditions, resulted in complete conversion to hydrogenolysis products (see Table 8). However, attempts to transfer this methodology to acetylated native lignin were not successful.[203] Although not being able to apply the strategy to native lignin, these findings are in sharp contrast to the studies with the non-acetylated substrates. Overall, the seminal studies on the Ru-xantphos system by Ellman, Bergman and James highlight the difficulties in identifying competent catalysts capable of mediating redox-neutral C–O bond activation of more complex systems that do not irreversibly ligate to the substrates.

A subsequent study on the Ru(H)$_2$(CO)(PPh$_3$)$_3$-xantphos system was carried out by Li and co-workers who demonstrated that RuHCl(CO)(PPh$_3$)$_3$ and Ru(H)$_2$(CO)(PPh$_3$)$_3$ in the presence of inorganic bases, such as KOH, could be used in place of xantphos to affect the cleavage of β-O-4 lignin systems.[207] In the absence of KOH, no product formation was observed when using pristine RuHCl(CO)(PPh$_3$)$_3$, which is in accordance with the earlier studies conducted by Ellman, Bergman and co-workers.[195] Addition of KOH to either the RuHCl(CO)(PPh$_3$)$_3$ or Ru(H)$_2$(CO)(PPh$_3$)$_3$ system had a dramatic impact on the catalytic activity. It is clear that KOH converts the inactive Ru precursors to active species *in situ*, which are responsible for the cleavage of the model substrates (Table 9). When applying the developed RuHCl(CO)(PPh$_3$)$_3$-base catalytic system on a lignin model compound housing a γ-OH unit, four products were observed (see Table 10). Relatively low yields of the corresponding veratryl-based products were obtained but with higher yields of guaiacol. A similar mechanism for the tandem dehydrogenation/hydrogenolysis was proposed as for the Ru-xantphos system (see Fig. 36).[207]

Since RuCl$_2$(PPh$_3$)$_3$[208] and related Ru complexes[209,210] are known to mediate the direct alkylation of ketones with alcohols, *via* a so-called hydrogen borrowing strategy,[211] Plietker and Weickmann recently coupled the redox-neutral β-O-4 cleavage to a sequential alkylation step where the derived acetophenone-based products could be alkylated with alcohols as the alkylating agent.[212] The combination of the two processes allowed the formation of a variety of new structural motifs. Initial screening of the reaction conditions employed a variety of different Ru precursors (see Table 11). Simple Ru precursors such as RuCl$_2$(PPh$_3$)$_3$ was found to efficiently cleave the β-O-4 linkage after activation with KO^{t}amylate (Table 11, entry 2). It was revealed that a catalytic amount of EtOAc was necessary to obtain catalytic turnover (Table 11, entry 3). Thermal conditions, in the absence of any catalyst, did not yield any significant amounts of the cleaved products (Table 11, entry 1). Besides RuCl$_2$(PPh$_3$)$_3$, several other common Ru precursors also gave the desired fragmented products in good to high yields (Table 11, entries 5–11). The influence of the monodentate phosphine ligands was also investigated and it could be concluded that more electron-donating phosphine ligands facilitated the cleavage (Table 11, entries 12 and 13), whereas more electron deficient and mixed alkyl–aryl phosphines were less effective (Table 11, entries 14 and 15).[212]

With the optimized reaction conditions in hand, a variety of lignin model systems were evaluated (Table 12). Model systems derived from the three different monolignols cou-

This journal is © The Royal Society of Chemistry 2016

Org. Biomol. Chem., 2016, **14**, 1853–1914 | **1895**
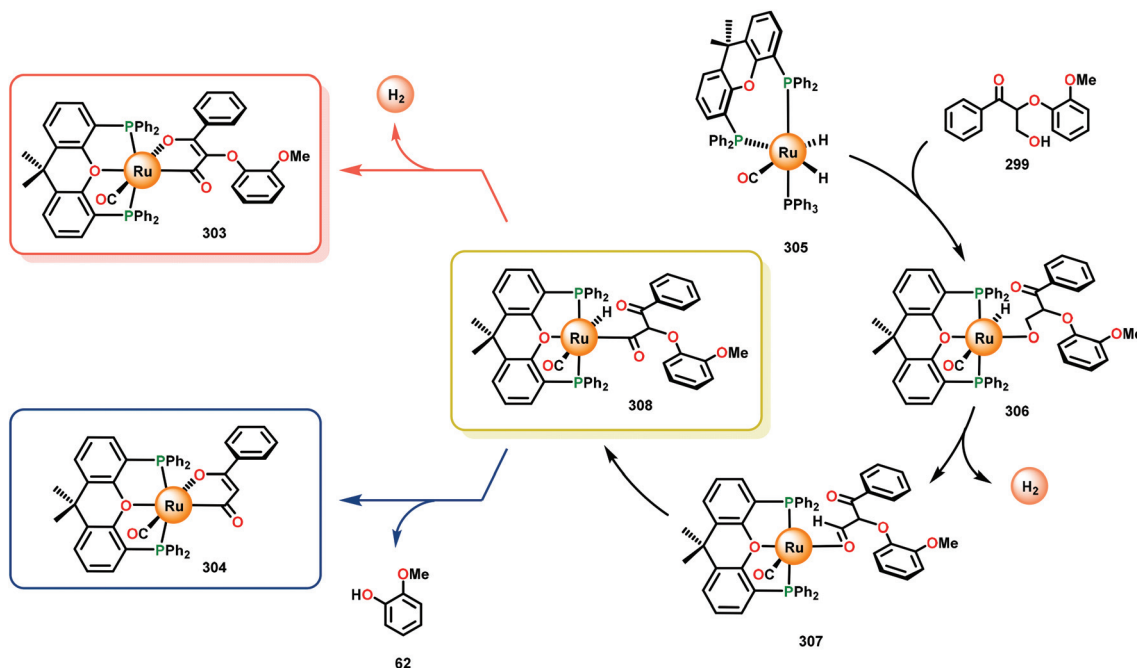
Scheme 32 Proposed mechanism for formation of inactive Ru complexes **303** and **304** from reaction with lignin model compound **299**.

Table 8 Catalytic hydrogenolysis of acetylated compound **309** with the Ru(H)$_2$(CO)(PPh$_3$)$_3$-xantphos catalyst

Entry	Atmosphere[a]	Conversion[b] (%)	Yield[b] (%)				
			310	**311**	**62**	**312**	**280**
1	Ar	100	25	9	20	24	17
2	H$_2$	100	19	27	42	18	9

[a] 1 atm. [b] Yields and conversions were determined by ^{1}H NMR based on two duplicate experiments.

maryl-, coniferyl- and sinapyl alcohol were all successfully cleaved to the corresponding acetophenone and phenol products in good to excellent yields.[212]
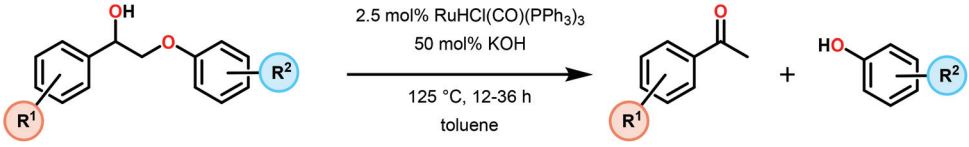
After completion of the β-O-4 cleavage of the lignin model systems, benzyl alcohol and a stoichiometric amount of KOH were added to the reaction mixture. Heating the resulting mixture for 16 h afforded the desired benzylated product in 71% yield (Table 13, entry 1). The Ru-catalyzed sequential β-O-4 cleavage/α-alkylation protocol was found to tolerate a wide variety of alcohols, such as benzylic-, heterobenzylic- and aliphatic alcohols (Table 13, entries 2–13). A tentative mechanism for the sequential β-O-4 cleavage/α-alkylation process is depicted in Scheme 33.[212] Coupling the β-O-4 cleavage with a

subsequent dehydrative α-alkylation process highlights that further *in situ* functionalization of the products stemming from cleavage of lignin model systems is viable for generation of a diverse array of lignin-derived value-added aromatic products.

Leitner, Klankermayer and co-workers reported on an even more active Ru-based complex for the redox-neutral β-O-4 bond cleavage of lignin model system **116**. By combining the Ru precursor [Ru(cod)(methallyl)$_2$] (cod = 1,5-cyclooctadiene; methallyl = η^3-C$_4$H$_7$) with tripodal phosphine based ligands, highly efficient Ru catalysts were obtained. Initial screening showed that monodentate and bidentate ligands such as PPh$_3$ and dppp (dppp = 1,3-bis(diphenylphosphino)propane)
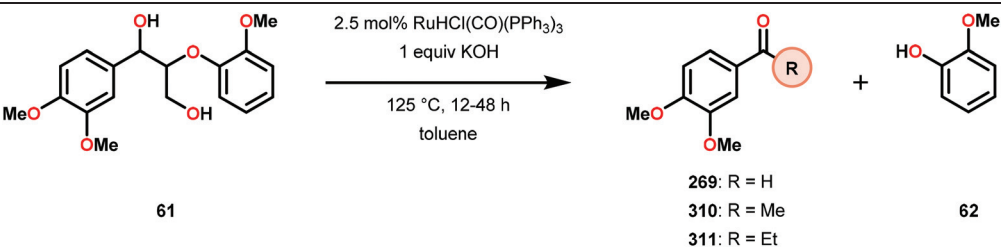
1896 | *Org. Biomol. Chem.*, 2016, **14**, 1853–1914

This journal is © The Royal Society of Chemistry 2016

Table 9 Ru-catalyzed redox-neutral conversion of β-O-4 lignin systems in the presence of KOH[a]

Entry	Substrate			Time (h)	Conversion[b] (%)	Yield[b] (%)	
		R[1]	R[2]			Ketone	Phenol
1	**116**	H	H	12	99	86	84
2	**291**	H	2-MeO	36	93	80	75
3	**292**	H	2,6-(MeO)$_2$	24	41	30	4
4	**293**	4-MeO	H	12	91	80	77
5	**294**	3,4-(MeO)$_2$	2-MeO	24	95	66	45
6	**313**	3-OH-4-MeO	2-MeO	24	89	—	14

[a] Reactions were run with 0.8 mmol of the substrate in a Schlenk flask under an atmosphere of argon. [b] Yields and conversions were determined by GC relative to an internal standard.

Table 10 Ru-catalyzed redox-neutral conversion of γ-OH containing lignin system **61** in the presence of KOH[a]

Entry	Time (h)	Conversion[b] (%)	Yield[b] (%)			
			269	**310**	**311**	**62**
1	12	95	5	4	—[c]	18
2	24	94	7	6	—[c]	26
3	36	89	8	6	—[c]	26
4	48	91	11	4	—[c]	53

[a] Reactions were run with 0.4 mmol of the substrate in a Schlenk flask under an atmosphere of argon. [b] Yields and conversions were determined by GC relative to an internal standard. [c] Minor product and not quantified.
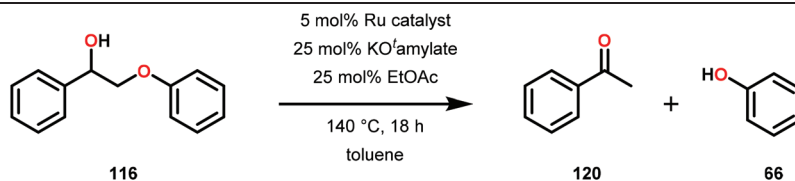
resulted in low yields (Table 14, entries 1 and 2). However, when using the tripodal phosphine ligand 1,1,1-tris(diphenyl-phosphinomethyl)ethane (**L1**), a highly active catalytic system was obtained, affording the cleaved products **120** and **66** in 65% and 67% yield, respectively (Table 14, entry 4). Increased activity was observed with bis(diphenylphosphinoethyl)phenyl-phosphine (**L2**) where substrate **116** was selectively fragmented to produce acetophenone and phenol in 93% and 84% yield, respectively (Table 14, entry 5).[213]

The unique activity prompted the authors to further study the catalytic system. A crystal structure of the Ru-tripodal phosphine complex showed that the structure was comprised of a doubly anionic [η^3-C$_4$H$_6$]$^{2-}$ ligand where all three phosphorus atoms were coordinated to the Ru^{II} center to give complex **323** (Fig. 38). Conducting the catalytic experiments with isolated

complex **323**, cleavage was observed even at temperatures as low as 60 °C (Table 15).[213] These results show that enhanced activity for the cleavage of lignin model substrates can be achieved by appropriate tailoring of the ligand scaffold.
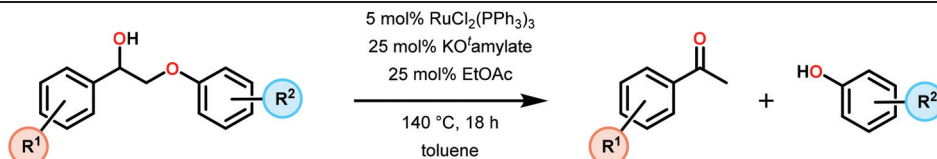
A follow-up study by Klankermayer and co-workers on these Ru-triphos systems revealed an unprecedented reactivity and selectivity of these complexes. The authors were able to carry out redox-neutral C–C bond cleavage on γ-OH containing lignin model substrates. Initial screening experiments using different tripodal-based phosphine systems showed that the use of Ru catalyst **329** afforded the C–C bond cleavage product **324** in 66% yield whereas the C–O bond cleavage product **62** was only detected in 4% yield (Table 16, entry 5). It could also be concluded that the catalyst had a strong influence on the catalytic activity (Table 16, entries 1–4).[214]

This journal is © The Royal Society of Chemistry 2016

Org. Biomol. Chem., 2016, **14**, 1853–1914 | **1897**

Table 11 Ru-catalyzed cleavage of lignin system **116**[a]

Entry	Catalyst	Yield[b] (%) 120	66
1	—	2	13
2	$RuCl_2(PPh_3)_3$	94	94
3	$RuCl_2(PPh_3)_3$[c]	23	27
4	$RuCl_2(PPh_3)_3$[d]	68	74
5	$[Ru(p\text{-cymene})Cl_2]_2$	70	70
6	$[Ru(p\text{-cymene})Cl_2]_2/PPh_3$	80	81
7	$Ru(OAc)_2(PPh_3)_3$	80	89
8	$Ru(OAc)_2(PPh_3)_3$[c]	53	47
9	$Ru(dmso)_4Cl_2$	52	58
10	$RuH_2(PPh_3)_4$	80	99
11	$RuHCl(CO)(PPh_3)_3$	79	75
12	$RuCl_2(P(p\text{-MeC}_6H_4)_3)_3$[d]	78	85
13	$RuCl_2(P(p\text{-MeOC}_6H_4)_3)_3$[d]	72	84
14	$RuCl_2(P(p\text{-FC}_6H_4)_3)_3$[d]	26	20
15	$RuCl_2(PCyPh_2)_3$[d]	47	47

[a] Reactions were carried out in a closed Schlenk tube under a N_2 atmosphere with substrate **116** (0.125 mmol), Ru catalyst (5 mol%), KO[t]amylate (25 mol%) and EtOAc (25 mol%) in toluene (0.25 mL) at 140 °C for 18 h. [b] Determined by GC analysis using dodecane as internal standard. [c] Without EtOAc. [d] Reaction time of 4 h.

Table 12 $RuCl_2(PPh_3)_3$/KO[t]amylate-catalyzed cleavage of lignin model systems[a]

Entry		Substrate R[1]	R[2]	Yield[b] (%) Ketone	Phenol
1	**291**	H	4-MeO	59	53
2	**293**	4-MeO	H	62	82
3	**314**	3,4-(MeO)$_2$	H	98[c]	98
4	**294**	3,4-(MeO)$_2$	4-MeO	81[c]	62
5	**315**	3,4,5-(MeO)$_3$	H	68[c]	65

[a] Reactions were carried out in a closed Schlenk tube under a N_2 atmosphere with lignin model substrate (0.25 mmol), $RuCl_2(PPh_3)_3$ (5 mol%), KO[t]amylate (25 mol%) and EtOAc (25 mol%) in toluene (0.5 mL) at 140 °C for 18 h. [b] Determined by GC analysis using dodecane as internal standard. [c] Isolated yield.

Since Ru complex **329** afforded the desired C–C bond cleavage product in good yield, the RuHCl(PPh₃)₃ precursor was used in combination with selected phosphine ligands (Table 17). When carrying out the catalytic reactions with the bidentate ligands xantphos or dppp, only minor amounts of the C–C bond cleavage products were detected (Table 17, entries 2 and 5); however, use of the tridentate triphos ligand

**L1** afforded the C–C cleavage products in high yields (~76%) after 4 h (Table 17, entry 6). Comparable yields (70%) were observed after merely 1 h (Table 17, entry 7) when performing the reactions at 160 °C. These findings highlight the potential of the Ru-triphos complexes for mediating redox-neutral hydrogen transfer reactions. Different phenyl and phenol substituted lignin model systems were subsequently evaluated

Table 13 RuCl$_2$(PPh$_3$)$_3$/K^{t}amylate-catalyzed sequential β-O-4 cleavage/α-alkylation^a

Entry	Substrate	Alcohol	Yield^b (%)
1	R^1 = H (116)	R^2 = C$_6$H$_5$	71
2	R^1 = H (116)	R^2 = 4-MeO-C$_6$H$_4$	43
3	R^1 = H (116)	R^2 = 4-Cl-C$_6$H$_4$	51
4	R^1 = H (116)	R^2 = 3,4-(MeO)$_2$-C$_6$H$_3$	58
5	R^1 = H (116)	R^2 = 2,4-Cl$_2$-C$_6$H$_3$	47
6	R^1 = H (116)	R^2 = 2-furanyl	40
7	R^1 = H (116)	R^2 = 2-thiophenyl	40
8	R^1 = H (116)	R^2 = CH$_2$CH(CH$_3$)$_2$	47
9	R^1 = H (116)	R^2 = C$_6$H$_{11}$	53
10	R^1 = 4-MeO (293)	R^2 = C$_6$H$_5$	44
11	R^1 = 3,4-(MeO)$_2$ (314)	R^2 = C$_6$H$_5$	53
12	R^1 = 3,4-(MeO)$_2$ (314)	R^2 = C$_5$H$_9$	53
13	R^1 = 3,4,5-(MeO)$_3$ (315)	R^2 = C$_6$H$_5$	37

^{a} Reactions were carried out in a closed Schlenk tube under a N$_2$ atmosphere with lignin model substrate (0.25 mmol), RuCl$_2$(PPh$_3$)$_3$ (5 mol%), KO^{t}amylate (25 mol%) and EtOAc (25 mol%) in toluene (0.5 mL) at 140 °C for 8 h. KOH (0.25 mmol) and alcohol (0.25 mmol) were then added and heated for additional 16 h. ^{b} Isolated yield.
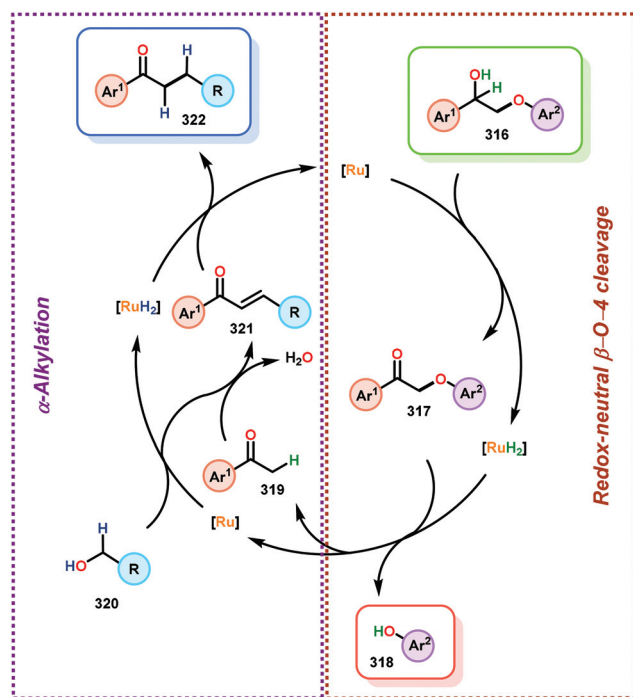

Scheme 33 Plausible mechanism for the sequential β-O-4 cleavage/α-alkylation of lignin model compounds.

with the RuHCl(PPh$_3$)$_3$/triphos ligand **L1** system. It was shown that the substitution pattern of the phenol ring had a moderate effect on the yield of the C–C bond cleavage (Table 18,

entries 1–3 and 5). However, the sterically encumbered *ortho* functionalized substrates **332** only produced aldehyde **269** in 26% yield (Table 18, entry 4). This trend could also be observed with the highly substituted 2,4,5-trimethoxy model system **334**, which yielded its corresponding C–C cleavage product in 14% yield (Table 18, entry 6).[214]

Insight into the catalytic mechanism for these hydrogen transfer reactions was obtained by studying a variety of substituted lignin model systems (Scheme 34). Bis(methyl-ether) substrate **335** and the benzylic ethyl ether compound **336** were practically inactive toward C–C and C–O bond cleavage, giving the fragmented products in <2%. However, substrate **337** containing the benzylic alcohol and a primary methyl ether unit yielded the C–O bond cleavage product in 39% yield. This reactivity pattern suggests that both alcohol moieties need to be present in order for efficient C–C bond cleavage to occur, whereas C–O bond fragmentation only requires the benzylic alcohol. Additional support for this hypothesis was given from the catalytic activity of lignin model systems **338** and **339** containing tertiary alcohol units where exclusive formation of the C–O cleavage product was observed with substrate **339**. Furthermore, species **344** (Scheme 35) was successfully characterized by NMR spectroscopy and was also formed upon reacting the substrate with RuHCl(CO)(**L1**), implying that this species is a potential resting state of the Ru-triphos system.[214] In contrast to the catalytically inactive Ru species **303** (Fig. 37),[201] isolated by James and co-workers, the pentacoordinated intermediate **344** maintains a vacant coordination site, which may in part account for this catalytic improvement.

This journal is © The Royal Society of Chemistry 2016

Org. Biomol. Chem., 2016, **14**, 1853–1914 | **1899**

**Table 14** Ru-catalyzed cleavage of 2-phenoxy-1-phenylethanol **116** using [Ru(cod)(methallyl)₂] as Ru precursor[a]
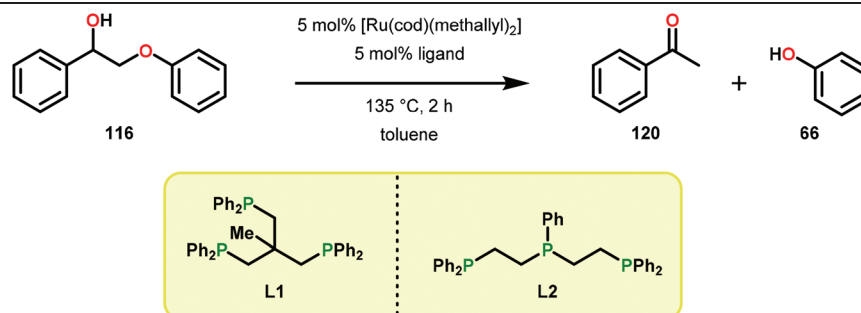
Entry	Ligand	Yield[b] (%)	
		120	**66**
1	PPh₃[c]	5	5
2	DPPP	2	1
3	Xantphos	11	12
4	**L1**	67	65
5	**L2**	93	84

[a] Reactions were carried out with substrate **116** (0.2 mmol), Ru precursor (5 mol%) and ligand (5 mol%) in toluene (0.5 mL) at 135 °C for 2 h. [b] Determined by GC analysis using dodecane as internal standard. [c] 3 equiv. of PPh₃ with respect to Ru precursor. dppp = 1,3-bis-(diphenylphosphino)propane.
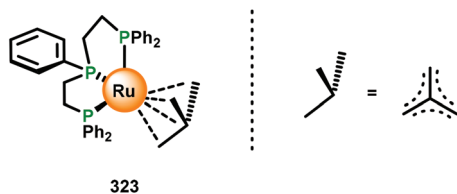
Fig. 38 Molecular structure of Ru complex **323**.

Based on these observations, a mechanistic proposal for the sequential redox-neutral hydrogen transfer/retro-aldol C–C bond cleavage was presented and is outlined in Scheme 35.[214] The initial step in the proposed mechanistic pathway involves coordination of the substrate to the Ru catalyst, with concomitant liberation of H₂ to generate **342**. Subsequent dehydrogenation of intermediate **342** results in species **343**, which undergoes a retro-aldol type C–C bond cleavage to form the product aldehyde **346** and Ru species **345**, where the latter can react with the substrate, closing the catalytic cycle. The generated enol is subsequently hydrogenated under the reaction

Table 15 Catalytic cleavage of 2-phenoxy-1-phenylethanol **116** using Ru complex **323**[a]
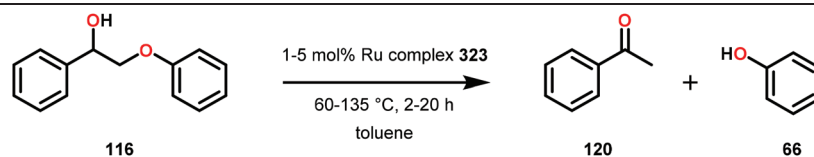
Entry	Ru catalyst **323** (mol%)	T (°C)	Time (h)	Yield[b] (%)	
				120	**66**
1	5	60	20	26	25
2	5	80	20	75	75
3	5	100	20	94	92
4	5	135	2	96	92
5	1	135	2	91	90

[a] Reactions were carried out with substrate **116** (0.2 mmol) and Ru complex **323** (5 mol%) in toluene (0.5 mL) at 60–135 °C for 2–20 h. [b] Determined by GC analysis using dodecane as internal standard.

1900 | *Org. Biomol. Chem.*, 2016, **14**, 1853–1914

This journal is © The Royal Society of Chemistry 2016

Table 16 C−O and C−C bond catalyzed cleavage of substrate **61** by various Ru-triphos complexes[a]
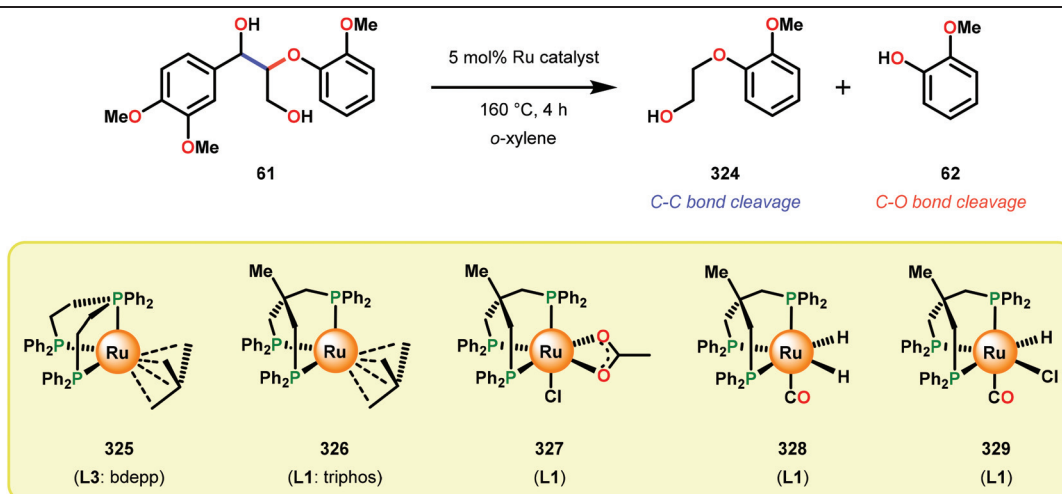
Entry	Complex	Yield[b] (%)	
		324	62
1	325	4	28
2	326	21	14
3	327	24	5
4	328	15	26
5	329	66	4

[a] Reactions were carried out with substrate **61** (0.1 mmol) and Ru catalyst (5 mol%) in *ortho*-xylene (0.5 mL) at 160 °C for 4 h. [b] Determined by GC analysis using dodecane as internal standard.

Table 17 Ligand screening for selective C−C bond cleavage of substrate **61** using the RuHCl(PPh₃)₃ precursor[a]
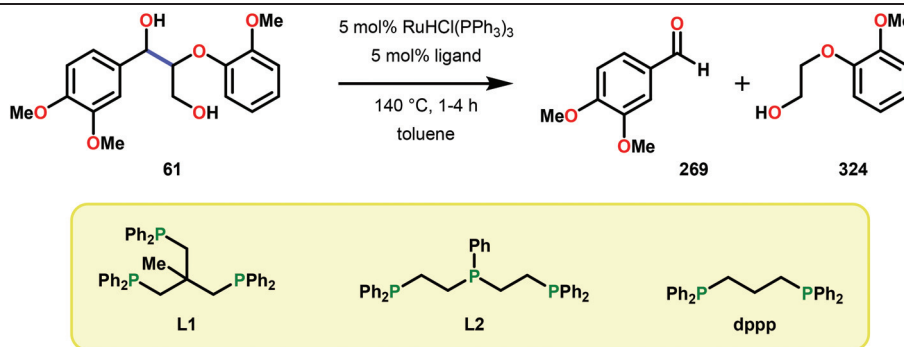
Entry	Ligand	T (°C)	Time (h)	Yield[b] (%)	
				269	324
1	None	140	4	8	3
2	Xantphos	140	4	2	2
3	L1	140	4	64	64
4	L2	140	4	26	31
5	dppp	140	4	8	6
6	L1	160[c]	4	75	77
7	L1	160[c]	1	69	70

[a] Reactions were carried out with substrate **61** (0.1 mmol) and RuHCl(PPh₃)₃ (5 mol%) in toluene (0.5 mL) at 140 °C for 1–4 h. The catalyst precursor/ligand solution was preheated at 140 °C for 2 h. [b] Determined by GC analysis using dodecane as internal standard. [c] Reaction was performed with *ortho*-xylene (0.5 mL) as the solvent.

This journal is © The Royal Society of Chemistry 2016

Org. Biomol. Chem., 2016, **14**, 1853–1914 | **1901**

Table 18 Reactivity pattern of the RuHCl(PPh$_3$)$_3$/triphos ligand **L1** system toward different substituted lignin model substrates[a]

Entry	Substrate	R^1	R^2	Yield[b] (%)	
				Aldehyde	Alcohol
1	**61**	3,4-(MeO)$_2$	2-MeO	75	77
2	**330**	3,4-(MeO)$_2$	3,5-(MeO)$_2$	86	—
3	**331**	3,4-(MeO)$_2$	H	63	—
4	**332**	3,4-(MeO)$_2$	2,6-(MeO)$_2$	26	—
5	**333**	3-MeO-4-EtO	2-MeO	—	75
6	**334**	2,4,6-(MeO)$_3$	2-MeO	—	14

[a] Reactions were carried out with substrate (0.1 mmol), RuHCl(PPh$_3$)$_3$ (5 mol%) and ligand **L1** (5 mol%) in *ortho*-xylene (0.5 mL) at 160 °C for 4 h. The catalyst precursor/ligand solution was preheated at 140 °C for 2 h. [b] Determined by GC analysis using dodecane as internal standard.
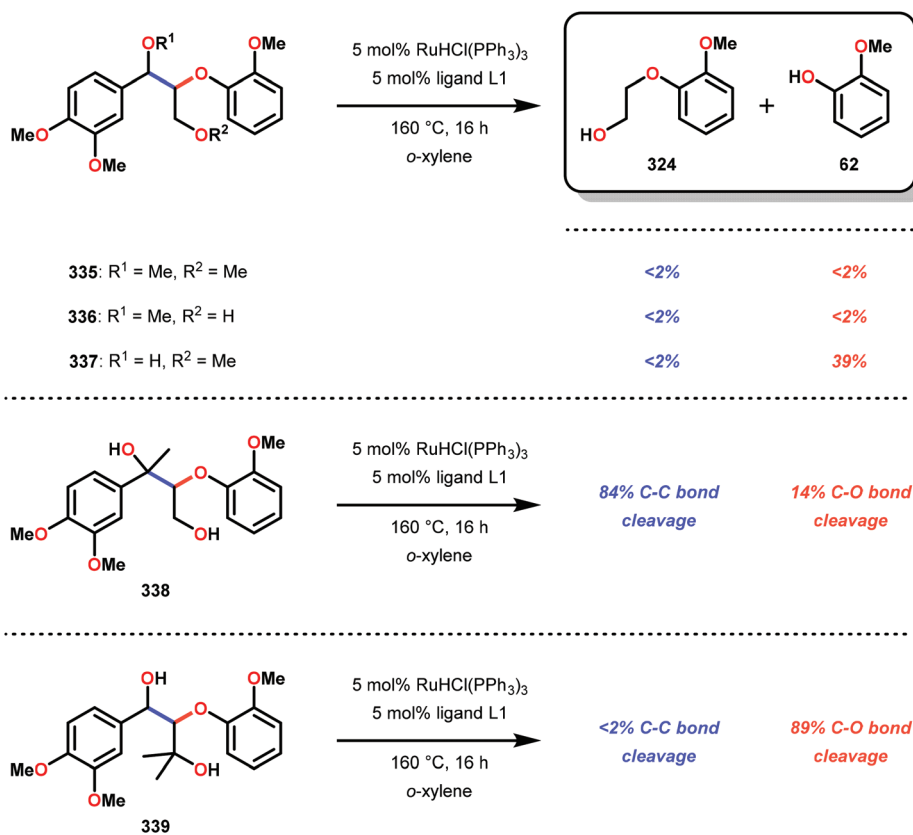
Scheme 34 Reactivity pattern of the RuHCl(PPh$_3$)$_3$/triphos ligand **L1** system.

conditions to yield the observed saturated alcohol moiety.[214] This work emphasizes that simple ligand tuning of homogeneous Ru-based catalytic systems can provide access to systems exhibiting unprecedented catalytic activity and selectivity towards the redox-neutral conversion of lignin model systems.

4.2 Other transition-metal based systems for redox-neutral conversion of lignin and lignin-related substrates

A novel reactivity pattern for carrying out redox-neutral degradation of lignin model systems was reported by Toste and co-workers.[166] This catalytic system utilized a V-based catalyst

1902 | *Org. Biomol. Chem.*, 2016, **14**, 1853–1914

This journal is © The Royal Society of Chemistry 2016
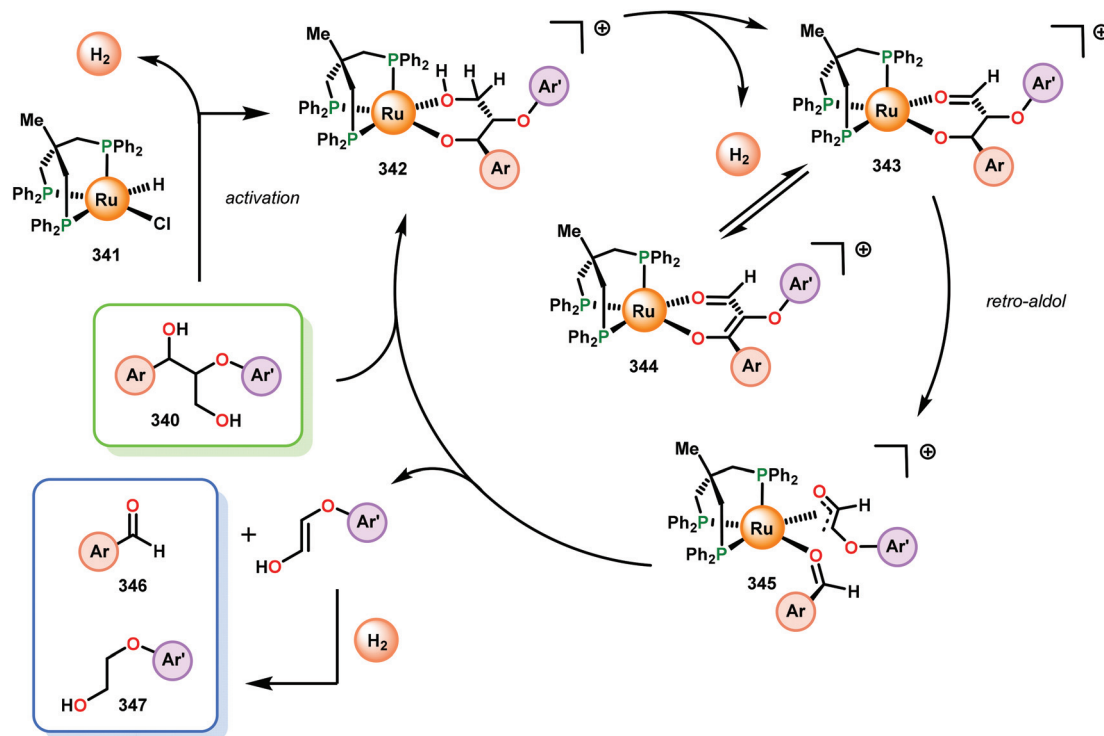
Scheme 35 Proposed redox-neutral hydrogen transfer/retro-aldol mechanism for C−C bond cleavage of lignin model compounds by the Ru-triphos catalytic system.

where the redox-neutral fragmentation was proposed to proceed through a ketyl radical pathway. Initial experiments explored various V-based catalysts to selectively convert the lignin model system. A majority of the tested catalysts gave the oxidized ketone **349** as the major product (Table 19, entries 2–7). However, the use of V complexes with Schiff base ligands was shown to favor C–O bond cleavage over the benzylic oxidation, where ligands with larger bite angles displayed the highest selectivity (Table 19, entries 8–11). As with the Ru-based catalytic systems, subtle modifications in the ligand scaffold were able to change the reactivity of the V system from benzylic oxidation toward promoting C–O bond cleavage.

It was shown that molecular oxygen was not essential to achieve catalytic turnover. When performing the catalytic experiments under anaerobic conditions with V complex **256**, a pale purple precipitate was isolated, which was revealed to be the V^{IV} complex. These results suggest that the initial V^{V} catalyst is reduced to a V^{IV} species during the fragmentation. Fundamental insight into the mechanism of the non-oxidative C–O bond cleavage was obtained from the reactivity of different analogues of the lignin model substrate (Scheme 36, top). Using a substrate where the benzylic alcohol was methylated (**356**), afforded the conjugated aldehyde **357** in low yield, suggesting that ligand exchange with the benzylic hydroxyl moiety is essential for the catalytic reactivity. However, employing the benzyl methyl ether substrate **358**, high conversion was observed to the desired C–O bond cleavage products **348** and **62** (see Scheme 36, lower).[166]

Additional experiments consisted of performing the reaction in another solvent than MeCN. When conducting the cleavage in EtOAc, >95% conversion was observed, affording the cleaved products **348** and **62** in even higher yields (93% and 70%, respectively, *cf.* Table 19, entry 11). The trimeric lignin model compound **359** also underwent clean cleavage to furnish three monomeric species, showing that the V system can be applied on more intricate lignin systems (Scheme 37).[166]

A one-electron catalytic process was invoked and is depicted in Scheme 38. After the initial ligand exchange with the benzylic alcohol unit, the benzylic H_α is abstracted, producing a ketyl radical (**361**) from which subsequent fragmentation occurs to produce an aryloxy radical (**362**) and enolate **363**. Elimination of the hydroxy moiety from the resulting enolate **363** generates the enone product **364** and V^{IV} species **365**, which can be reoxidized to V^{V} by the produced aryloxy radical (**362**).[166] This work demonstrates that the use of V catalysis may dramatically alter the reactivity by which lignin and related compounds can be cleaved. By subtle changes in the ancillary ligands, a novel fragmentation scenario was realized, affording functionalized aryl enones in high yields and good selectivities.

In a subsequent study Toste and co-workers assessed the reactivity of the V-catalyzed redox-neutral depolymerization toward lignin extracted from *Miscanthus giganteus* with various solvents.[215] The plant-derived lignin was extracted using dioxane, acetone and ethanol, affording dioxasolv, acetosolv

This journal is © The Royal Society of Chemistry 2016

Org. Biomol. Chem., 2016, **14**, 1853–1914 | **1903**

Table 19 V-based complexes for promoting C–O cleavage in lignin model system **333**
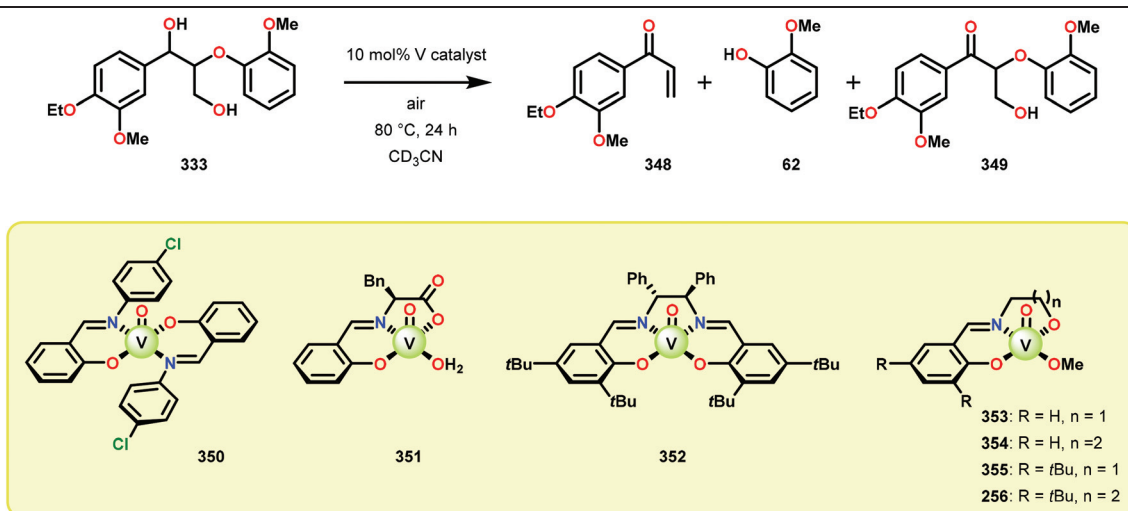
Entry	Catalyst	Conversion^a (%)	Yield^a (%)		
			348	**62**	**349**
1	None	0	—	—	—
2	VOSO$_4$·xH$_2$O	34	2	2	6
3	VO(acac)$_3$	79	13	22	31
4	VO(OiPr)$_3$	82	5	11	45
5	**350**	86	6	6	59
6	**351**	66	13	14	41
7	**352**	55	3	—	37
8	**353**	>95	61	45	27
9	**354**	86	70	62	8
10	**355**	95	65	50	18
11	**256**	>95	82	57	7

^{a} Determined by ^{1}H NMR spectroscopy versus an internal standard.
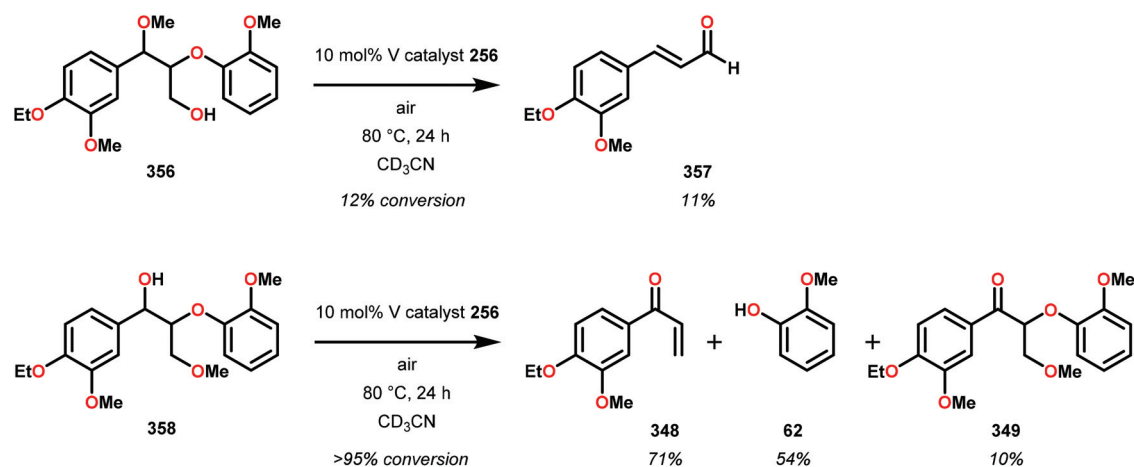
Scheme 36 Reactivity study of V complex **256**.

and ethanosolv lignin, respectively. The degradation studies were carried out at 80 °C for 24 h in MeCN/THF or EtOAc/THF mixtures. For dioxasolv lignin, 24 h treatment with V catalyst

256 lowered the overall molecular weight distribution of the lignin sample, as determined by gel permeation chromatography (GPC) analysis. Similar results were obtained with

1904 | *Org. Biomol. Chem.*, 2016, **14**, 1853–1914

This journal is © The Royal Society of Chemistry 2016
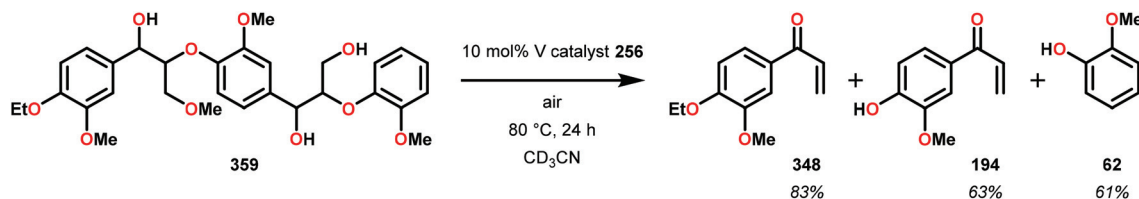
Scheme 37 Redox-neutral cleavage of trimeric lignin model system **359** by V catalyst **256**.
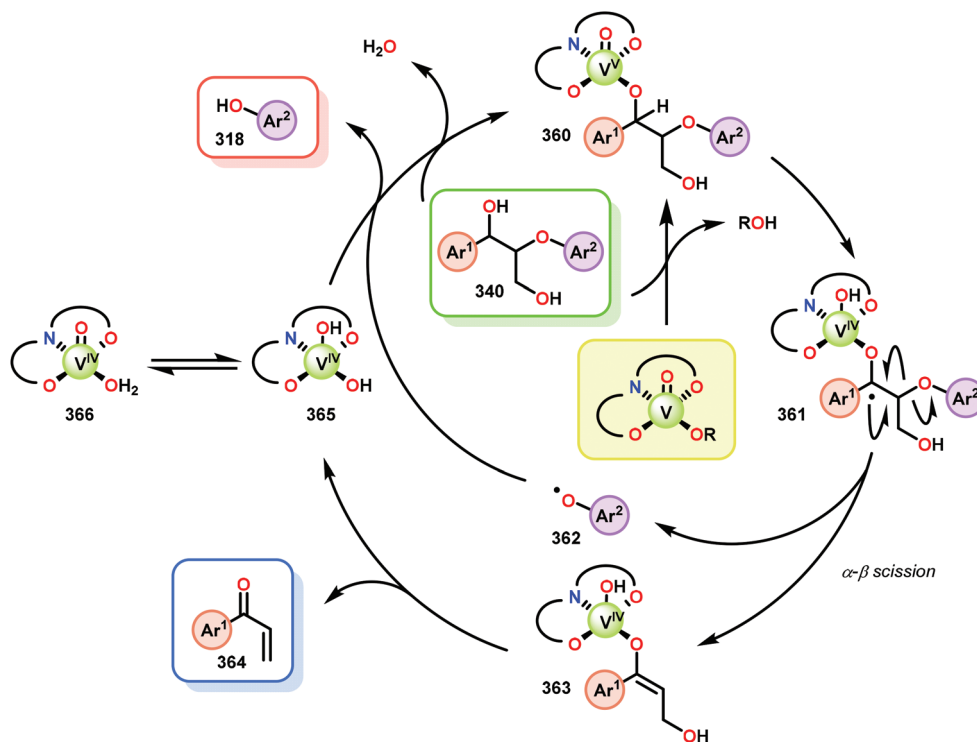
Scheme 38 Proposed mechanism for the V-catalyzed redox-neutral cleavage of lignin model systems.

acetosolv lignin, which produced a shift toward lower molecular weight species after catalysis. However, when using ethanosolv derived lignin, GPC analysis revealed a lesser degree of depolymerization. The lower reactivity of ethanosolv lignin was attributed to the prevalence of ethylated benzylic hydroxyl moieties (*cf.* Scheme 36), which is a result of the acidic pretreatment, thus highlighting that pretreatment and isolation significantly alter the structure of native lignin. The product mixture obtained from V-treated dioxasolv lignin was also analyzed and quantified by GC/MS. The primary phenolic products generated from this reaction are depicted in Fig. 39, where vanillin, syringaldehyde and syringic acid were found to be the most prevalent degradation products.

Methyltrioxorhenium(VII) (MTO) has also been reported to mediate the cleavage of C–O bonds in lignin model systems to yield phenolic- and aldehyde-based products.[216] In these reactions, methyldioxorhenium(V) (MDO), generated *in situ* by reduction from MTO, was proposed to be the catalytically active species. Heating a reaction mixture of MTO and lignin model system **291** at 155 °C afforded phenylacetaldehyde **371** and guaiacol (**62**) in high yields (Scheme 39). Recycling experiments showed that the catalyst could be reused at least five times without any significant loss of conversion or yield of guaiacol. However, attempts to carry out the cleavage on γ-OH functionalized lignin model system **61** proved to be unsuccessful. Although the reaction proceeded with a shorter reaction time and at lower temperature, only 9% yield of aldehyde **373** and 65% yield of guaiacol (**62**) were obtained (Scheme 40). In addition to the formation of compounds **373** and **62**, several other products were detected. The decrease in selectivity for the γ-OH functionalized substrate **61** was not clear and further experiments are needed to explain the unsuccessful cleavage of the γ-OH containing substrate.

Compared to the Ru-catalyzed C–O bond cleavage, the Re-catalyzed cleavage does not afford acetophenone but rather produces phenylacetaldehyde, presumably through a 1,2 shift

This journal is © The Royal Society of Chemistry 2016

Org. Biomol. Chem., 2016, **14**, 1853–1914 | **1905**

367 4-hydroxybenzaldehyde *0.33 wt%*

166 vanillin *0.78 wt%*

265 syringaldehyde *0.59 wt%*

369 3-hydroxy-1-(4-hydroxy-3-methoxy-phenyl)propan-1-one *0.12 wt%*

368 4-hydroxybenzoic acid *0.05 wt%*

169 vanillic acid *0.31 wt%*

266 syringic acid *0.67 wt%*

370 3-hydroxy-1-(4-hydroxy-3,5-dimethoxy-phenyl)propan-1-one *0.08 wt%*

Combined yield of 2.93 wt%

Fig. 39 Identity and yield of products from V-catalyzed degradation of dioxasolv lignin derived from *Miscanthus giganteus*.
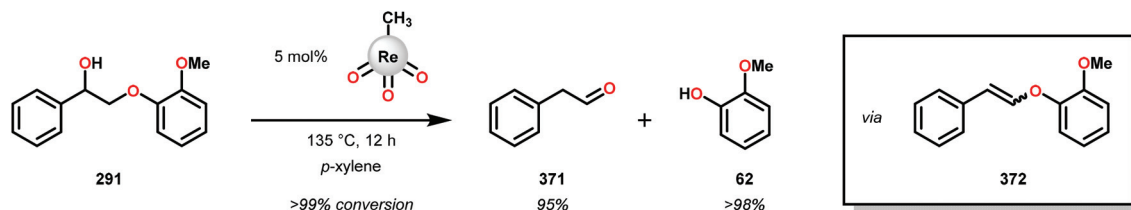
Scheme 39 Methyltrioxorhenium (MTO) catalyzed C−O cleavage of lignin model system **291**.
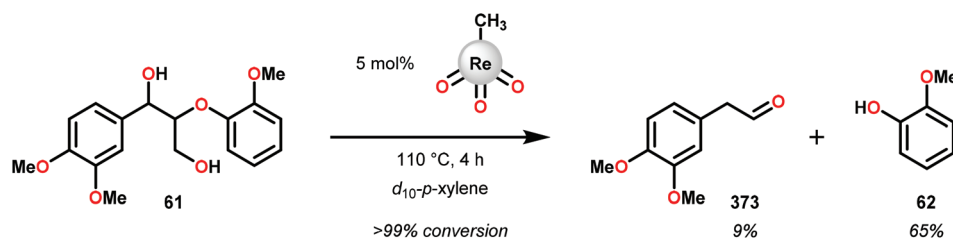
Scheme 40 Re-catalyzed C−O cleavage of γ-OH functionalized lignin model system **61**.

of the O atom. In order to shed some light on the mechanistic pathway, isotopic labeling experiments were performed with ^{17}O and deuterium labeled **291** (see Scheme 41). When using **291-^{17}O** (^{17}O labeled at the benzylic hydroxyl group), complete incorporation of ^{17}O was observed in the phenylacetaldehyde product (Scheme 41, top). For the deuterium labeled compound **291-D**, labeled at the α-carbon, the deuterium labeled

product **371-D** was obtained, showing that the deuterium does not undergo migration. Based on the isotopic labeling studies and the detection of intermediate **372**, a mechanism was proposed and is depicted in Scheme 42. In the proposed catalytic cycle MTO is initially reduced to MDO, which subsequently reacts with a second molecule of the substrate to give the Re-alkoxide species **374**. Elimination from intermediate **374** gen-

1906 | *Org. Biomol. Chem.*, 2016, **14**, 1853–1914

This journal is © The Royal Society of Chemistry 2016

Scheme 41 Isotopic labeling studies of the Re-catalyzed C–O cleavage reaction.
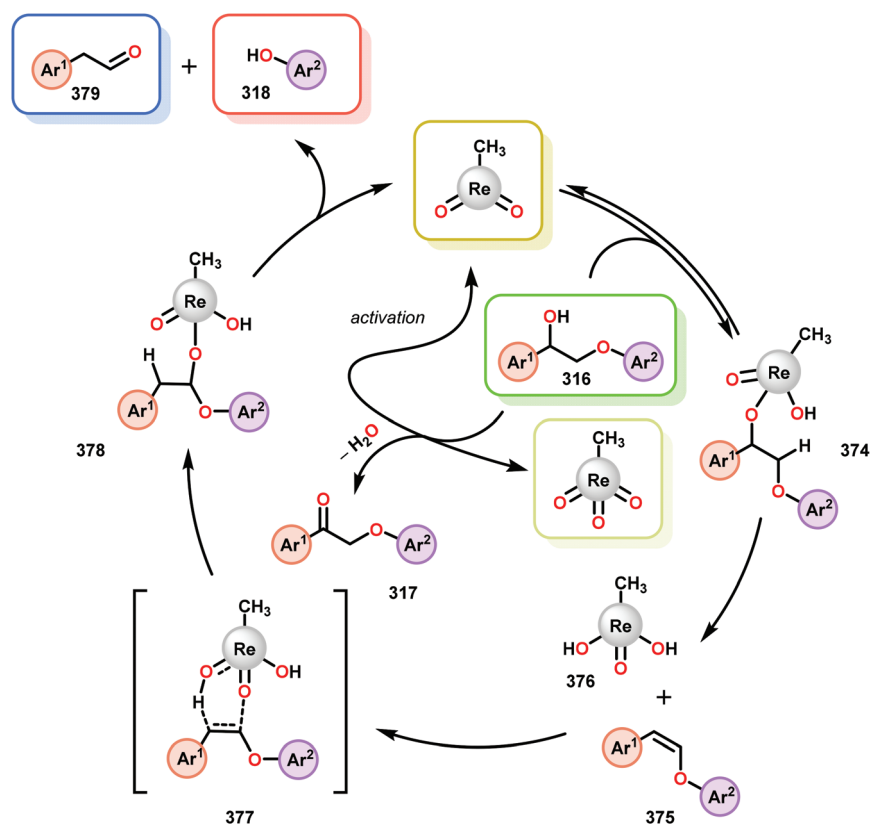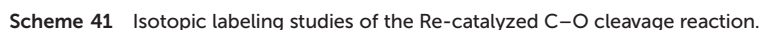
Scheme 42 Proposed mechanism for Re-mediated redox-neutral C–O cleavage of lignin model systems.

erates enol ether **375** and Re^V bis(hydroxo) intermediate **376**, which formally adds an O- and H atom to enol ether **375** to produce an acetal-like Re-alkoxide (**378**). From species **378**, MDO is liberated together with the observed cleavage products.[216] The Re-catalyzed redox-neutral system constitutes a novel route for carrying out C–O cleavage in lignin model systems, however, additional understanding of the mechanistic pathway is vital in order to design improved Re-based systems capable of mediating C–O bond cleavage of γ-OH containing model systems.

This journal is © The Royal Society of Chemistry 2016

Org. Biomol. Chem., 2016, **14**, 1853–1914 | **1907**

Fig. 40 Pd/C catalyzed redox-neutral *vs.* reductive cleavage of β-O-4 lignin model compounds.

Samec and co-workers recently reported on the use of Pd/C as a heterogeneous catalyst for the redox-neutral C–O bond cleavage of various 2-aryloxy-1-arylethanols.[217] The authors reasoned that commercially available Pd/C could indeed be a viable catalyst for mediating the redox-neutral conversion of lignin model systems (Fig. 40) inspired by their previous work on reductive cleavage of lignin model systems[84,85] and because Pd on solid supports is known to be air- and moisture stable in a wide pH range. After initial screening, it could be established that the addition of a substoichiometric amount of NaBH$_4$ in the presence of air resulted in efficient transformation of model system **116** (Table 20). It was reasoned that the required use of NaBH$_4$ was to transform the initial thin Pd oxide layer to produce a reactive Pd surface. The use of 0.1 equivalents of NaBH$_4$ was found to be optimal to efficiently mediate the redox-neutral conversion of model system **116**. Employing <0.1 equivalents of NaBH$_4$ yielded the benzylic oxidized product **119** and the addition of >0.1 equivalents NaBH$_4$ resulted in reduction of the generated ketone **119** to afford 1-phenylethanol (**124**).[217]

The scope of the Pd/C catalyzed redox-neutral reaction was subsequently investigated and it was found that a variety of substituted lignin model systems could be efficiently cleaved,

generating the corresponding acetophenone and phenolic products in excellent yields (Table 20). Phenolic substrates were also tolerated and could be converted to the corresponding products in high yields (Table 20, entries 9 and 10). The Pd/C catalytic system was subsequently applied on a polymeric model substrate to determine the compatibility with 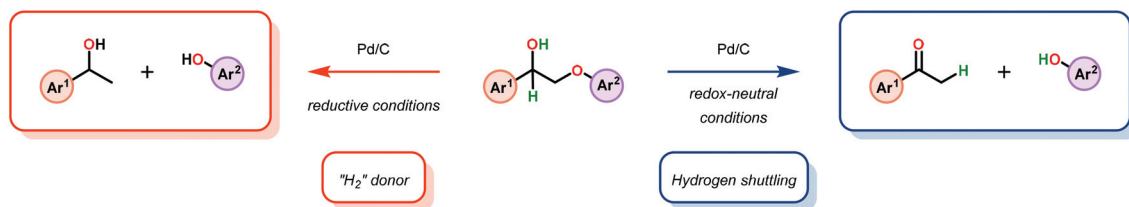more native lignin resembling substrates. The model polymer had a molecular weight of ~6 kDa, similar to that found for native lignin. The model polymer underwent efficient cleavage and ketone **107** was isolated in near quantitative yield (Scheme 43).[217]

To gain insight into the mechanism of the redox-neutral transformation, experiments were performed with methylated substrate **295** and substrate **117**. However, neither of these substrates gave any reaction (Scheme 44). In light of these results the authors proposed a mechanism (Scheme 45) where an initial activation step of the Pd surface occurs to generate the "activated" Pd/C, which subsequently reversibly dehydrogenates the benzylic alcohol unit in the lignin model substrate. The enolate form of the generated ketone is adsorbed to Pd to yield intermediate **383**.[217] The hydride can then be inserted either at the α or β-position, according to a Horiuti–Polanyi-type[218,219] pathway, to give intermediates **385** or **387**, respect-

Table 20 Pd/C catalyzed redox-neutral cleavage of β-O-4 lignin model compounds

Entry	Substrate	R^1	R^2	Yield^a (%)	
				Ketone	Phenol
1	**116**	H	H	95	92
2	**293**	4-MeO	H	98	—
3	**291**	H	2-MeO	94	—
4^b	**314**	3,4-(MeO)$_2$	H	95	—
5	**99**	4-MeO	2-MeO	99	95
6^b	**294**	3,4-(MeO)$_2$	2-MeO	98	—
7	**292**	H	2,6-(MeO)$_2$	97	95
8^b	**380**	3,4-(MeO)$_2$	2,6-(MeO)$_2$	92	—
9^b	**381**	4-OH	2-MeO	97	—
10^b	**382**	3-MeO-4-OH	2-MeO	96	—

^{a} Isolated yield based on two duplicate experiments. ^{b} Reaction was run for 4 h.

1908 | *Org. Biomol. Chem.*, 2016, **14**, 1853–1914

This journal is © The Royal Society of Chemistry 2016
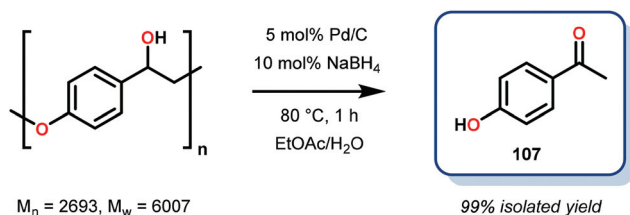
Scheme 43 Pd/C catalyzed redox-neutral depolymerization of lignin model polymer.
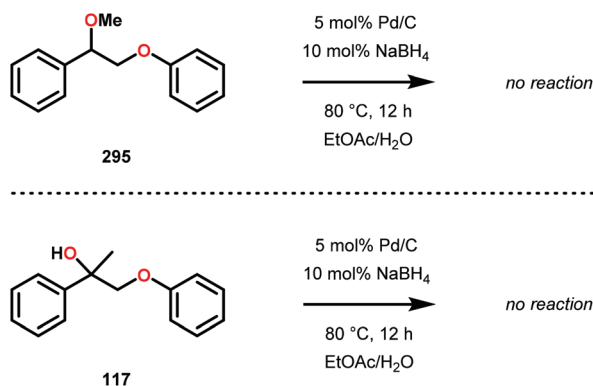
Scheme 44 Redox-neutral C−O bond cleavage attempts of substrates **295** and **117**.

ively. C–O bond cleavage of intermediate **385** produces **386** where the enol moiety and aryloxide are still adsorbed, from which the desired products are subsequently liberated. Alternatively, C–O bond insertion of **387** forms carbene-type intermediate **388**, which can undergo tautomerization to release the acetophenone product (**389**) and phenolic product (**318**).[217]

The ability of Pd/C to mediate redox-neutral cleavage of lignin model systems highlights the implementation and scalability of the reaction. The switch in reactivity is intriguing and may be useful for designing novel catalytic protocols or for improving already existing systems.

5. Conclusions and outlook

The development of a sustainable and carbon-neutral biorefinery has emerged as a prominent scientific and engineering goal of modern society. As petroleum becomes less accessible, biomass-based carbon sources have emerged as potential feedstocks for fuel production and commodity chemical manufacturing. Lignin is the largest source of a renewable material which contains an aromatic skeleton and is the second most abundant component in biomass. While technologies to process cellulose and hemicellulose are well developed, lignin processing constitutes a considerably more challenging task. Lignin is currently regarded as a disposal liability and only used in low-value applications. The fact that lignin is currently
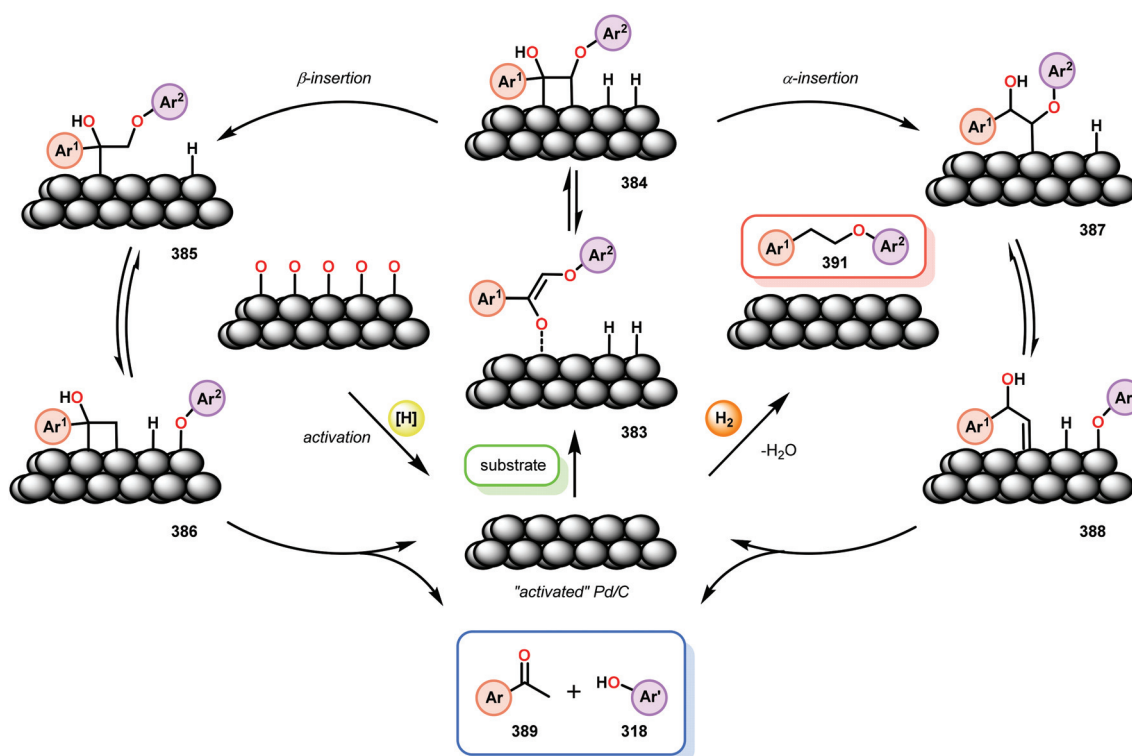
Scheme 45 Proposed mechanism for the Pd/C catalyzed redox-neutral C−O bond cleavage of lignin model systems.

an unexploited resource makes the valorization of lignin an ideal solution for the production of defined aromatic commodity chemicals.

The difficulty in catalytically depolymerizing lignin originates from its highly irregular and complex structure. In this regard, transition metal catalysis constitutes an excellent option for studying the valorization of lignin owing to the relative ease by which these complexes can be accessed in combination with their tunability. Studying lignin valorization constitutes an opportunity for evaluating transition metal catalysis and for method development. From the work described in this review it is clear that three fundamentally distinguishable strategies have emerged for the conversion of lignin and lignin model systems; reductive, oxidative and redox-neutral cleavage.

It is obvious that several intriguing approaches have been devised for the cleavage of lignin model systems, which have had a crucial impact on the field. However, a majority of these methods are not sufficiently selective and low yielding. Several of the prominent pathways developed for fragmenting lignin model systems utilize ketyl radicals as key intermediates. Successfully controlling how these radicals are generated and fragmented could afford novel routes for selectively producing value-added products.

Redox-neutral lignin depolymerization represents an ideal approach to biomass valorization because it does not require a terminal oxidant/reductant. This is a particularly important consideration in the context of commodity chemical/fine chemical synthesis where the cost of stoichiometric reagents becomes prohibitively expensive on scale. Although the redox-neutral approach is certainly appealing, there remains a lack of fundamental knowledge for how to control and govern these catalytic systems to selectively generate aromatic products. To achieve this, it is essential that the scientific field shifts away from employing simple lignin models to more elaborate systems, or even samples of native lignin, to begin to address the compatibility issues encountered already in the elementary stages of catalyst design. Creative solutions based on these advances must be devised to ultimately furnish methods that are industrially applicable for the sustainable production of high-value commodity chemicals. It is clear that a final solution for lignin valorization will most likely utilize a combination of the different approaches highlighted in this review.

Acknowledgements

References

1 P. N. R. Vennestrøm, C. M. Osmundsen, C. H. Christensen and E. Taarning, *Angew. Chem., Int. Ed.*, 2011, **50**, 10502–10509.

2 J. J. Bozell and G. R. Petersen, *Green Chem.*, 2010, **12**, 539–554.

3 J. Zakzeski, P. C. A. Bruijnincx, A. L. Jongerius and B. M. Weckhuysen, *Chem. Rev.*, 2010, **110**, 3552–3599.

4 C. Xu, R. A. D. Arancon, J. Labidi and R. Luque, *Chem. Soc. Rev.*, 2014, **43**, 7485–7500.

5 S. R. Collinson and W. Thielemans, *Coord. Chem. Rev.*, 2010, **254**, 1854–1870.

6 D. M. Alonso, J. Q. Bond and J. A. Dumesic, *Green Chem.*, 2010, **12**, 1493–1513.

7 K. Barta and P. C. Ford, *Acc. Chem. Res.*, 2014, **47**, 1503–1512.

8 S. Dutta, K. C.-W. Wu and B. Saha, *Catal. Sci. Technol.*, 2014, **4**, 3785–3799.

9 H. Lange, S. Decina and C. Crestini, *Eur. Polym. J.*, 2013, **49**, 1151–1173.

10 R. Ma, Y. Xu and X. Zhang, *ChemSusChem*, 2015, **8**, 24–51.

11 M. Zaheer and R. Kempe, *ACS Catal.*, 2015, **5**, 1675–1684.

12 P. J. Deuss and K. Barta, *Coord. Chem. Rev.*, 2016, **306**, 510–532.

13 R. Vanholme, B. Demedts, K. Morreel, J. Ralph and W. Boerjan, *Plant Physiol.*, 2010, **153**, 895–905.

14 W. Boerjan, J. Ralph and M. Baucher, *Annu. Rev. Plant Biol.*, 2003, **54**, 519–546.

15 E. A. Capanema, M. Y. Balakshin and J. F. Kadla, *J. Agric. Food Chem.*, 2004, **52**, 1850–1860.

16 G. Brunow, in *Biorefineries - Industrial Processes and Products*, ed. B. Kamm, P. R. Gruber and M. Kamm, Wiley-VCH Verlag, Weinheim, Germany, 2006, vol. 2, pp. 151–163.

17 J. Ralph, J. Peng, F. Lu, R. D. Hatfield and R. F. Helm, *J. Agric. Food Chem.*, 1999, **47**, 2991–2996.

18 F. S. Chakar and A. J. Ragauskas, *Ind. Crops Prod.*, 2004, **20**, 131–141.

19 J. Ralph, K. Lundquist, G. Brunow, F. Lu, H. Kim, P. F. Schatz, J. M. Marita, R. D. Hatfield, S. A. Ralph, J. H. Christensen and W. Boerjan, *Phytochem. Rev.*, 2004, **3**, 29–60.

20 J. J. Bozell, *Alternative, Renewable, and Novel Feedstocks for Producing Chemicals*, US Dep. Energy Oak Ridge Natl. Lab., Oak Ridge TN, 2006, pp. 204–209.

21 A. J. Ragauskas, G. T. Beckham, M. J. Biddy, R. Chandra, F. Chen, M. F. Davis, B. H. Davison, R. A. Dixon, P. Gilna, M. Keller, P. Langan, A. K. Naskar, J. N. Saddler, T. J. Tschaplinski, G. A. Tuskan and C. E. Wyman, *Science*, 2014, **344**, 1246843.

22 C. O. Tuck, E. Pérez, I. T. Horváth, R. A. Sheldon and M. Poliakoff, *Science*, 2012, **337**, 695–699.

23 M. Besson, P. Gallezot and C. Pinel, *Chem. Rev.*, 2014, **114**, 1827–1870.

24 P. J. Deuss, K. Barta and J. G. de Vries, *Catal. Sci. Technol.*, 2014, **4**, 1174–1196.

25 A. Corma, S. Iborra and A. Velty, *Chem. Rev.*, 2007, **107**, 2411–2502.

26 P. Gallezot, *ChemSusChem*, 2008, **1**, 734–737.

27 P. Anbarasan, Z. C. Baer, S. Sreekumar, E. Gross, J. B. Binder, H. W. Blanch, D. S. Clark and F. D. Toste, *Nature*, 2012, **491**, 235–239.

28 R.-J. van Putten, J. C. van der Waal, E. de Jong, C. B. Rasrendra, H. J. Heeres and J. G. de Vries, *Chem. Rev.*, 2013, **113**, 1499–1597.

29 R. Ahuja, B. Punji, M. Findlater, C. Supplee, W. Schinski, M. Brookhart and A. S. Goldman, *Nat. Chem.*, 2011, **3**, 167–171.

30 M. P. Pandey and C. S. Kim, *Chem. Eng. Technol.*, 2011, **34**, 29–41.

31 A. Y. Khodakov, W. Chu and P. Fongarland, *Chem. Rev.*, 2007, **107**, 1692–1744.

32 J. H. Clark, R. Luque and A. S. Matharu, *Annu. Rev. Chem. Biomol. Eng.*, 2012, **3**, 183–207.

33 F. G. Calvo-Flores and J. A. Dobado, *ChemSusChem*, 2010, **3**, 1227–1235.

34 J. Zhu, X. Pan and R. S. Zalesny, Jr., *Appl. Microbiol. Biotechnol.*, 2010, **87**, 847–857.

35 J. Gierer, *Wood Sci. Technol.*, 1980, **14**, 241–266.

36 J. B. Lindsey and B. Tollens, *Liebigs Ann. Chem.*, 1892, **267**, 341–366.

37 J. Y. Zhu, X. J. Pan, G. S. Wang and R. Gleisner, *Bioresour. Technol.*, 2009, **100**, 2411–2418.

38 CycleWood solutions, http://cyclewood.com/technology/, (accessed October 2015).

39 C. Fargues, Á. Mathias and A. Rodrigues, *Ind. Eng. Chem. Res.*, 1996, **35**, 28–36.

40 A. Lindner and G. Wegener, *J. Wood Chem. Technol.*, 1988, **8**, 323–340.

41 X. Pan, C. Arato, N. Gilkes, D. Gregg, W. Mabee, K. Pye, Z. Xiao, X. Zhang and J. Saddler, *Biotechnol. Bioeng.*, 2005, **90**, 473–481.

42 T. Ikeda, K. Holtman, J. F. Kadla, H.-m. Chang and H. Jameel, *J. Agric. Food Chem.*, 2002, **50**, 129–135.

43 J. S. Luterbacher, J. M. Rand, D. M. Alonso, J. Han, J. T. Youngquist, C. T. Maravelias, B. F. Pfleger and J. A. Dumesic, *Science*, 2014, **343**, 277–280.

44 J. Sauer and H. Adkins, *J. Am. Chem. Soc.*, 1937, **59**, 1–3.

45 J. V. Vaughen and W. A. Lazier, *J. Am. Chem. Soc.*, 1931, **53**, 3719–3728.

46 F. Krafft, *Ber. Dtsch. Chem. Ges.*, 1877, **10**, 2034–2036.

47 E. E. Harris, J. D'Ianni and H. Adkins, *J. Am. Chem. Soc.*, 1938, **60**, 1467–1470.

48 C. P. Brewer, L. M. Cooke and H. Hibbert, *J. Am. Chem. Soc.*, 1948, **70**, 57–59.

49 L. W. Covert and H. Adkins, *J. Am. Chem. Soc.*, 1932, **54**, 4116–4117.

50 J. M. Pepper and H. Hibbert, *J. Am. Chem. Soc.*, 1948, **70**, 67–71.

51 For representative publications demonstrating NMR analysis of lignin, see: (*a*) G. Gellerstedt and D. Robert, *Acta Chem. Scand.*, 1987, **B41**, 541–546; (*b*) C.-L. Chen and D. Robert, *Methods Enzymol.*, 1988, **161**, 137–174; (*c*) N. Fukagawa, G. Meshitsuka and A. Ishizu, *J. Wood Chem. Technol.*, 1991, **11**, 373–396; (*d*) R. M. Ede and I. Kilpeläinen, *Res. Chem. Intermed.*, 1995, **21**, 313–328; (*e*) I. Kilpeläinen, J. Sipilä, G. Brunow and K. Lundquist, *J. Agric. Food Chem.*, 1994, **42**, 2790–2794; (*f*) E. Ammalahti, G. Brunow, M. Bardet, D. Robert and I. Kilpeläinen, *J. Agric. Food Chem.*, 1998, **46**, 5113–5117; (*g*) D. V. Evtuguin, C. P. Neto, A. M. S. Silva, P. M. Domingues, F. M. L. Amado, D. Robert and O. Faix, *J. Agric. Food Chem.*, 2001, **49**, 4252–4261.

52 NMR Database of Lignin and Cell Wall Model Compounds, http://www.ars.usda.gov/SP2UserFiles/Place/36553000/software/NMR/NMR_DataBase_Intro_&_Index.pdf. (accessed October 2015).

53 R. Jana, T. P. Pathak and M. S. Sigman, *Chem. Rev.*, 2011, **111**, 1417–1492.

54 G. A. Molander and B. Canturk, *Angew. Chem., Int. Ed.*, 2009, **48**, 9240–9261.

55 A. Roglans, A. Pla-Quintana and M. Moreno-Mañas, *Chem. Rev.*, 2006, **106**, 4622–4643.

56 A. C. Hillier, G. A. Grasa, M. S. Viciu, H. M. Lee, C. Yang and S. P. Nolan, *J. Organomet. Chem.*, 2002, **653**, 69–82.

57 G. Evano, N. Blanchard and M. Toumi, *Chem. Rev.*, 2008, **108**, 3054–3131.

58 G. Cahiez and A. Moyeux, *Chem. Rev.*, 2010, **110**, 1435–1462.

59 T. Sperger, I. A. Sanhueza, I. Kalvet and F. Schoenebeck, *Chem. Rev.*, 2015, **115**, 9532–9586.

60 J. Cornella, C. Zarate and R. Martin, *Chem. Soc. Rev.*, 2014, **43**, 8081–8097.

61 M. Tobisu and N. Chatani, *Acc. Chem. Res.*, 2015, **48**, 1717–1726.

62 E. Geist, A. Kirschning and T. Schmidt, *Nat. Prod. Rep.*, 2014, **31**, 441–448.

63 E. Wenkert, E. L. Michelotti and C. S. Swindell, *J. Am. Chem. Soc.*, 1979, **101**, 2246–2247.

64 J. W. Dankwardt, *Angew. Chem., Int. Ed.*, 2004, **43**, 2428–2432.

65 D.-G. Yu, B.-J. Li and Z.-J. Shi, *Acc. Chem. Res.*, 2010, **43**, 1486–1495.

66 B.-J. Li, D.-G. Yu, C.-L. Sun and Z.-J. Shi, *Chem. – Eur. J.*, 2011, **17**, 1728–1759.

67 B. M. Rosen, K. W. Quasdorf, D. A. Wilson, N. Zhang, A.-M. Resmerita, N. K. Garg and V. Percec, *Chem. Rev.*, 2011, **111**, 1346–1416.

68 P. Álvarez-Bercedo and R. Martin, *J. Am. Chem. Soc.*, 2010, **132**, 17352–17353.

69 A. G. Sergeev and J. F. Hartwig, *Science*, 2011, **332**, 439–443.

70 Sigma-Aldrich. http://www.sigmaaldrich.com/catalog/search?term=MFCD07369796&interface=MDL%20No.&N=0&mode=mode%20matchall&lang=en&region=US&focus=product (accessed October 2015).

This journal is © The Royal Society of Chemistry 2016

Org. Biomol. Chem., 2016, **14**, 1853–1914 | 1911

71 A. G. Sergeev, J. D. Webb and J. F. Hartwig, *J. Am. Chem. Soc.*, 2012, **134**, 20226–20229.

72 P. Kelley, S. Lin, G. Edouard, M. W. Day and T. Agapie, *J. Am. Chem. Soc.*, 2012, **134**, 5480–5483.

73 J. Cornella, E. Gómez-Bengoa and R. Martin, *J. Am. Chem. Soc.*, 2013, **135**, 1997–2009.

74 For examples of β-hydride elimination from Pd and Pt complexes, see: (*a*) F. Ozawa, T. Ito and A. Yamamoto, *J. Am. Chem. Soc.*, 1980, **102**, 6457–6463; (*b*) S. Komiya, T. Morimoto, A. Yamamoto and T. Yamamoto, *Organometallics*, 1982, **1**, 1528–1536; (*c*) H. Bryndza, J. C. Calabresse, M. Marsi, C. Roe, W. Tam and J. Bercaw, *J. Am. Chem. Soc.*, 1986, **108**, 4805–4813.

75 J. He, C. Zhao and J. A. Lercher, *J. Am. Chem. Soc.*, 2012, **134**, 20768–20775.

76 J. Zakzeski, P. C. A. Bruijnincx, A. L. Jongerius and B. M. Weckhuysen, *Chem. Rev.*, 2010, **110**, 3552–3599.

77 G. S. Macala, T. D. Matson, C. L. Johnson, R. S. Lewis, A. V. Iretskii and P. C. Ford, *ChemSusChem*, 2009, **2**, 215–217.

78 C. Zhao, Y. Kou, A. A. Lemonidou, X. Li and J. A. Lercher, *Chem. Commun.*, 2010, **46**, 412–414.

79 V. Molinari, C. Giordano, M. Antonietti and D. Esposito, *J. Am. Chem. Soc.*, 2014, **136**, 1758–1761.

80 N. Yan, C. Zhao, P. J. Dyson, C. Wang, L. Liu and Y. Kou, *ChemSusChem*, 2008, **1**, 626–629.

81 D. M. Alonso, S. G. Wettstein and J. A. Dumesic, *Chem. Soc. Rev.*, 2012, **41**, 8075–8098.

82 X. Wang and R. Rinaldi, *Energy Environ. Sci.*, 2012, **5**, 8244–8260.

83 S. Sawadjoon, A. Lundstedt and J. S. M. Samec, *ACS Catal.*, 2013, **3**, 635–642.

84 M. V. Galkin, S. Sawadjoon, V. Rohde, M. Dawange and J. S. M. Samec, *ChemCatChem*, 2014, **6**, 179–184.

85 M. V. Galkin and J. S. M. Samec, *ChemSusChem*, 2014, **7**, 2154–2158.

86 X. Zhou, J. Mitra and T. B. Rauchfuss, *ChemSusChem*, 2014, **7**, 1623–1626.

87 P. Rousu, P. Rousu and J. Anttila, *Resour., Conserv. Recycl.*, 2002, **35**, 85–103.

88 A. N. Desnoyer, B. Fartel, K. C. MacLeod, B. O. Patrick and K. M. Smith, *Organometallics*, 2012, **31**, 7625–7628.

89 Y. Ren, M. Yan, J. Wang, Z. C. Zhang and K. Yao, *Angew. Chem., Int. Ed.*, 2013, **52**, 12674–12678.

90 J. A. Widegren and R. G. Finke, *J. Mol. Catal. A: Chem.*, 2003, **198**, 317–341.

91 S. Kusumoto and K. Nozaki, *Nat. Commun.*, 2015, **6**, 6296.

92 C. K. Prier, D. A. Rankic and D. W. C. MacMillan, *Chem. Rev.*, 2013, **113**, 5322–5363.

93 J. J. Douglas, J. D. Nguyen, K. P. Cole and C. R. J. Stephenson, *Aldrichimica Acta*, 2014, **47**, 15–25.

94 D. M. Schultz and T. P. Yoon, *Science*, 2014, **343**, 1239176.

95 J. M. R. Narayanam and C. R. J. Stephenson, *Chem. Soc. Rev.*, 2011, **40**, 102–113.

96 K. Kalyanasundaram, *Coord. Chem. Rev.*, 1982, **46**, 159–244.

97 A. Juris, V. Balzani, F. Barigelletti, S. Campagna, P. Belser and A. von Zelewsky, *Coord. Chem. Rev.*, 1988, **84**, 85–277.

98 E. Hasegawa, S. Takizawa, T. Seida, A. Yamaguchi, N. Yamaguchi, N. Chiba, T. Takahashi, H. Ikeda and K. Akiyama, *Tetrahedron*, 2006, **62**, 6581–6588.

99 M.-H. Larraufie, R. Pellet, L. Fensterbank, J.-P. Goddard, E. Lacôte, M. Malacria and C. Ollivier, *Angew. Chem., Int. Ed.*, 2011, **50**, 4463–4466.

100 M. A. Mercadante, C. B. Kelly, J. M. Bobbitt, L. J. Tilley and N. E. Leadbeater, *Nat. Protoc.*, 2013, **8**, 666–676.

101 J. D. Nguyen, B. S. Matsuura and C. R. J. Stephenson, *J. Am. Chem. Soc.*, 2014, **136**, 1218–1221.

102 S. Kim, S. C. Chmely, M. R. Nimlos, Y. J. Bomble, T. D. Foust, R. S. Paton and G. T. Beckham, *J. Phys. Chem. Lett.*, 2011, **2**, 2846–2852.

103 G. A. Molander and G. Hahn, *J. Org. Chem.*, 1986, **51**, 1135–1138.

104 E. Hasegawa and D. P. Curran, *J. Org. Chem.*, 1993, **58**, 5008–5010.

105 P. R. Chopade, E. Prasad and R. A. Flowers, II, *J. Am. Chem. Soc.*, 2004, **126**, 44–45.

106 G. A. Molander and G. Hahn, *J. Org. Chem.*, 1986, **51**, 2596–2599.

107 J. M. R. Narayanam, J. W. Tucker and C. R. J. Stephenson, *J. Am. Chem. Soc.*, 2009, **131**, 8756–8757.

108 J. W. Tucker, J. D. Nguyen, J. M. R. Narayanam, S. W. Krabbe and C. R. J. Stephenson, *Chem. Commun.*, 2010, **46**, 4985–4987.

109 J. D. Nguyen, E. M. D'Amato, J. M. R. Narayanam and C. R. J. Stephenson, *Nat. Chem.*, 2012, **4**, 854–859.

110 J. W. Tucker, Y. Zhang, T. F. Jamison and C. R. J. Stephenson, *Angew. Chem., Int. Ed.*, 2012, **51**, 4144–4147.

111 F. R. Bou-Hamdan and P. H. Seeberger, *Chem. Sci.*, 2012, **3**, 1612–1616.

112 M. Tien and T. K. Kirk, *Proc. Natl. Acad. Sci. U. S. A.*, 1984, **81**, 2280–2284.

113 M. Kuwahara, J. K. Glenn, M. A. Morgan and M. H. Gold, *FEBS Lett.*, 1984, **169**, 247–250.

114 H. E. Schoemaker, P. J. Harvey, R. M. Bowen and J. M. Palmer, *FEBS Lett.*, 1985, **183**, 7–12.

115 M. Tien and T. K. Kirk, *Science*, 1983, **221**, 661–663.

116 S. H. Lim, K. Nahm, C. S. Ra, D. W. Cho, U. C. Yoon, J. A. Latham, D. Dunaway-Mariano and P. S. Mariano, *J. Org. Chem.*, 2013, **78**, 9431–9443.

117 B. Meunier, *Chem. Rev.*, 1992, **92**, 1411–1456.

118 M. Shimada, T. Habe, T. Umezawa, T. Higuchi and T. Okamoto, *Biochem. Biophys. Res. Commun.*, 1984, **122**, 1247–1252.

119 T. Habe, M. Shimada, T. Okamoto, B. Panijpan and T. Higuchi, *J. Chem. Soc., Chem. Commun.*, 1985, 1323–1324.

120 M. Shimada, T. Habe, T. Higuchi, T. Okamoto and B. Panijpan, *Holzforschung*, 1987, **41**, 277–285.

121 E. A. Mayeda, *J. Am. Chem. Soc.*, 1975, **97**, 4012–4015.

1912 | *Org. Biomol. Chem.*, 2016, **14**, 1853–1914

This journal is © The Royal Society of Chemistry 2016

122 P. J. Kersten, M. Tien, B. Kalyanaraman and T. K. Kirk, *J. Biol. Chem.*, 1985, **260**, 2609–2612.

123 A. Paszczynski, R. L. Crawford and R. A. Blanchette, *Appl. Environ. Microbiol.*, 1988, **54**, 62–68.

124 G. Labat and B. Meunier, *J. Org. Chem.*, 1989, **54**, 5008–5011.

125 C. Crestini, R. Saladino, P. Tagliatesta and T. Boschi, *Bioorg. Med. Chem.*, 1999, **7**, 1897–1905.

126 F. Cui, T. Wijesekera, D. Dolphin, R. Farrell and P. Skerker, *J. Biotechnol.*, 1993, **30**, 15–26.

127 F. Cui and D. Dolphin, *Bioorg. Med. Chem.*, 1994, **2**, 735–742.

128 F. Cui and D. Dolphin, *Can. J. Chem.*, 1995, **73**, 2153–2157.

129 P. Zucca, G. Mocci, A. Rescigno and E. Sanjust, *J. Mol. Catal. A: Chem.*, 2007, **278**, 220–227.

130 P. Zucca, F. Sollai, A. Garau, A. Rescigno and E. Sanjust, *J. Mol. Catal. A: Chem.*, 2009, **306**, 89–96.

131 C. Crestini, A. Pastorini and P. Tagliatesta, *J. Mol. Catal. A: Chem.*, 2004, **208**, 195–202.

132 C. Crestini, A. Pastorini and P. Tagliatesta, *Eur. J. Inorg. Chem.*, 2004, 4477–4483.

133 C. Zhu, W. Ding, T. Shen, C. Tang, C. Sun, S. Xu, Y. Chen, J. Wu and H. Ying, *ChemSusChem*, 2015, **8**, 1768–1778.

134 W. Zhu and W. T. Ford, *J. Mol. Catal.*, 1993, **78**, 367–378.

135 F. Cui and D. Dolphin, *Bioorg. Med. Chem.*, 1995, **3**, 471–477.

136 R. D. Jones, D. A. Summerville and F. Basolo, *Chem. Rev.*, 1979, **79**, 139–179.

137 J. Piera and J.-E. Bäckvall, *Angew. Chem., Int. Ed.*, 2008, **47**, 3506–3523.

138 For reviews on metal Schiff-base complexes, see for example: (*a*) P. G. Cozzi, *Chem. Soc. Rev.*, 2004, **33**, 410–421; (*b*) K. C. Gupta and A. K. Sutar, *Coord. Chem. Rev.*, 2008, **252**, 1420–1450; (*c*) S. Matsunaga and M. Shibasaki, *Chem. Commun.*, 2014, **50**, 1044–1057.

139 For reactivity studies of Co-Schiff base complexes with O_2, see for example: (*a*) C. Floriani and F. Calderazzo, *J. Chem. Soc. A*, 1969, 946–953; (*b*) D. Chen and A. E. Martell, *Inorg. Chem.*, 1987, **26**, 1026–1030; (*c*) D. Chen, A. E. Martell and Y. Sun, *Inorg. Chem.*, 1989, **28**, 2647–2652.

140 F. Basolo, B. M. Hoffman and J. A. Ibers, *Acc. Chem. Res.*, 1975, **8**, 384–392.

141 R. S. Drago, B. B. Corden and C. W. Barnes, *J. Am. Chem. Soc.*, 1986, **108**, 2453–2454.

142 J. J. Bozell, B. R. Hames and D. R. Dimmel, *J. Org. Chem.*, 1995, **60**, 2398–2404.

143 C. Canevali, M. Orlandi, L. Pardi, B. Rindone, R. Scotti, J. Sipilä and F. Morazzoni, *J. Chem. Soc., Dalton Trans.*, 2002, 3007–3014.

144 V. Sippola, O. Krause and T. Vuorinen, *J. Wood Chem. Technol.*, 2004, **24**, 323–340.

145 K. Kervinen, H. Korpi, M. Leskelä and T. Repo, *J. Mol. Catal. A: Chem.*, 2003, **203**, 9–19.

146 K. Kervinen, M. Allmendinger, M. Leskelä, T. Repo and B. Rieger, *Phys. Chem. Chem. Phys.*, 2003, **5**, 4450–4454.

147 K. Kervinen, H. Korpi, J. G. Mesu, F. Soulimani, T. Repo, B. Rieger, M. Leskelä and B. M. Weckhuysen, *Eur. J. Inorg. Chem.*, 2005, 2591–2599.

148 S. K. Badamali, R. Luque, J. H. Clark and S. W. Breeden, *Catal. Commun.*, 2009, **10**, 1010–1013.

149 S. K. Badamali, R. Luque, J. H. Clark and S. W. Breeden, *Catal. Commun.*, 2011, **12**, 993–995.

150 D. Cedeno and J. J. Bozell, *Tetrahedron Lett.*, 2012, **53**, 2380–2383.

151 B. Biannic and J. J. Bozell, *Org. Lett.*, 2013, **15**, 2730–2733.

152 B. Biannic, J. J. Bozell and T. Elder, *Green Chem.*, 2014, **16**, 3635–3642.

153 A. M. Khenkin and R. Neumann, *J. Am. Chem. Soc.*, 2008, **130**, 14474–14476.

154 E. Takezawa, S. Sakaguchi and Y. Ishii, *Org. Lett.*, 1999, **1**, 713–715.

155 T. R. Felthouse, *J. Am. Chem. Soc.*, 1987, **109**, 7566–7568.

156 S. Barroso, G. Blay, I. Fernández, J. R. Pedro, R. Ruiz-García, E. Pardo, F. Lloret and M. C. Muñoz, *J. Mol. Catal. A: Chem.*, 2006, **243**, 214–220.

157 S. Riaño, D. Fernández and L. Fadini, *Catal. Commun.*, 2008, **9**, 1282–1285.

158 J. A. L. da Silva, J. J. R. Fraústo da Silva and A. J. L. Pombeiro, *Coord. Chem. Rev.*, 2011, **255**, 2232–2248.

159 T. Hirao, *Coord. Chem. Rev.*, 2003, **237**, 271–279.

160 S. Gazi, W. K. H. Ng, R. Ganguly, A. M. P. Moeljadi, H. Hirao and H. S. Soo, *Chem. Sci.*, 2015, **6**, 7130–7142.

161 S. K. Hanson, R. T. Baker, J. C. Gordon, B. L. Scott and D. L. Thorn, *Inorg. Chem.*, 2010, **49**, 5611–5618.

162 S. K. Hanson, R. T. Baker, J. C. Gordon, B. L. Scott, A. D. Sutton and D. L. Thorn, *J. Am. Chem. Soc.*, 2009, **131**, 428–429.

163 S. K. Hanson, R. Wu and L. A. Silks, *Org. Lett.*, 2011, **13**, 1908–1911.

164 For mechanistic investigations, see: (*a*) B. N. Wigington, M. L. Drummond, T. R. Cundari, D. L. Thorn, S. K. Hanson and S. L. Scott, *Chem. – Eur. J.*, 2012, **18**, 14981–14988; (*b*) S. K. Hanson, R. T. Baker, J. C. Gordon, B. L. Scott, L. A. Silks and D. L. Thorn, *J. Am. Chem. Soc.*, 2010, **132**, 17804–17816.

165 G. Zhang, B. L. Scott, R. Wu, L. A. Silks and S. K. Hanson, *Inorg. Chem.*, 2012, **51**, 7354–7361.

166 S. Son and F. D. Toste, *Angew. Chem., Int. Ed.*, 2010, **49**, 3791–3794.

167 S. K. Hanson, R. Wu and L. A. Silks, *Angew. Chem., Int. Ed.*, 2012, **51**, 3410–3413.

168 B. Sedai, C. Díaz-Urrutia, R. T. Baker, R. Wu, L. A. Silks and S. K. Hanson, *ACS Catal.*, 2013, **3**, 3111–3122.

169 V. L. Pardini, C. Z. Smith, J. H. P. Utley, R. R. Vargas and H. Viertler, *J. Org. Chem.*, 1991, **56**, 7305–7313.

170 V. L. Pardini, R. R. Vargas, H. Viertler and J. H. P. Utley, *Tetrahedron*, 1992, **48**, 1221–1228.

171 S. Wertz and A. Studer, *Green Chem.*, 2013, **15**, 3116–3134.

172 J. M. Bobbitt, C. Brückner and N. Merbouh, *Org. React.*, 2009, **74**, 103–424.

This journal is © The Royal Society of Chemistry 2016

Org. Biomol. Chem., 2016, **14**, 1853–1914 | **1913**

173 T. Vogler and A. Studer, *Synthesis*, 2008, 1979–1993.
174 R. A. Sheldon and I. W. C. E. Arends, *Adv. Synth. Catal.*, 2004, **346**, 1051–1071.
175 Q. Cao, L. M. Dornan, L. Rogan, N. L. Hughes and M. J. Muldoon, *Chem. Commun.*, 2014, **50**, 4524–4543.
176 L. Tebben and A. Studer, *Angew. Chem., Int. Ed.*, 2011, **50**, 5034–5068.
177 B. Sedai, C. Díaz-Urrutia, R. T. Baker, R. Wu, L. A. Silks and S. K. Hanson, *ACS Catal.*, 2011, **1**, 794–804.
178 P. Gamez, I. W. C. E. Arends, J. Reedijk and R. A. Sheldon, *Chem. Commun.*, 2003, 2414–2415.
179 P. Gamez, I. W. C. E. Arends, R. A. Sheldon and J. Reedijk, *Adv. Synth. Catal.*, 2004, **346**, 805–811.
180 A. Rahimi, A. Azarpira, H. Kim, J. Ralph and S. S. Stahl, *J. Am. Chem. Soc.*, 2013, **135**, 6415–6418.
181 B. Sedai and R. T. Baker, *Adv. Synth. Catal.*, 2014, **356**, 3563–3574.
182 B. L. Ryland and S. S. Stahl, *Angew. Chem., Int. Ed.*, 2014, **53**, 8824–8838.
183 C. Parmeggiani and F. Cardona, *Green Chem.*, 2012, **14**, 547–564.
184 S. D. McCann and S. S. Stahl, *Acc. Chem. Res.*, 2015, **48**, 1756–1766.
185 B. L. Ryland, S. D. McCann, T. C. Brunold and S. S. Stahl, *J. Am. Chem. Soc.*, 2014, **136**, 12166–12173.
186 M. F. Semmelhack, C. R. Schmid, D. A. Cortes and C. S. Chou, *J. Am. Chem. Soc.*, 1984, **106**, 3374–3376.
187 E. T. T. Kumpulainen and A. M. P. Koskinen, *Chem. – Eur. J.*, 2009, **15**, 10901–10911.
188 T. A. Hamlin, C. B. Kelly, J. M. Ovian, R. J. Wiles, L. J. Tilley and N. E. Leadbeater, *J. Org. Chem.*, 2015, **80**, 8150–8167.
189 A. Dijksman, I. W. C. E. Arends and R. A. Sheldon, *Org. Biomol. Chem.*, 2003, **1**, 3232–3237.
190 J. M. Hoover, B. L. Ryland and S. S. Stahl, *J. Am. Chem. Soc.*, 2013, **135**, 2357–2367.
191 J. M. Hoover, B. L. Ryland and S. S. Stahl, *ACS Catal.*, 2013, **3**, 2599–2605.
192 J. Zhang, Y. Liu, S. Chiba and T.-P. Loh, *Chem. Commun.*, 2013, **49**, 11439–11441.
193 A. Rahimi, A. Ulbrich, J. J. Coon and S. S. Stahl, *Nature*, 2014, **515**, 249–252.
194 C. S. Lancefield, O. S. Ojo, F. Tran and N. J. Westwood, *Angew. Chem., Int. Ed.*, 2015, **54**, 258–262.
195 J. M. Nichols, L. M. Bishop, R. G. Bergman and J. A. Ellman, *J. Am. Chem. Soc.*, 2010, **132**, 12554–12555.
196 N. A. Owston, A. J. Parker and J. M. J. Williams, *Chem. Commun.*, 2008, 624–625.
197 R. L. Chowdhury and J.-E. Bäckvall, *J. Chem. Soc., Chem. Commun.*, 1991, 1063–1064.

198 F. Kakiuchi, M. Usui, S. Ueno, N. Chatani and S. Murai, *J. Am. Chem. Soc.*, 2004, **126**, 2706–2707.
199 Y. Zhao and V. Snieckus, *J. Am. Chem. Soc.*, 2014, **136**, 11224–11227.
200 S. C. Chmely, S. Kim, P. N. Ciesielski, G. Jimenez-Oses, R. S. Paton and G. T. Beckham, *ACS Catal.*, 2013, **3**, 963–974.
201 A. Wu, B. O. Patrick, E. Chung and B. R. James, *Dalton Trans.*, 2012, **41**, 11093–11106.
202 A. Wu, B. O. Patrick and B. R. James, *Inorg. Chem. Commun.*, 2012, **24**, 11–15.
203 A. Wu, J. M. Lauzon and B. R. James, *Catal. Lett.*, 2015, **145**, 511–518.
204 L. Benhamou, V. César, N. Lugan and G. Lavigne, *Organometallics*, 2007, **26**, 4673–4676.
205 C. Qu, T. Kishimoto, M. Kishino, M. Hamada and N. Nakajima, *J. Agric. Food Chem.*, 2011, **59**, 5382–5389.
206 T. Sonoda, T. Ona, H. Yokoi, Y. Ishida, H. Ohtani and S. Tsuge, *Anal. Chem.*, 2001, **73**, 5429–5435.
207 W. Huo, W. Li, M. Zhang, W. Fan, H.-m. Chang and H. Jameel, *Catal. Lett.*, 2014, **144**, 1159–1163.
208 C. S. Cho, B. T. Kim, T.-J. Kim and S. C. Shim, *Tetrahedron Lett.*, 2002, **43**, 7987–7989.
209 R. Martínez, D. J. Ramón and M. Yus, *Tetrahedron*, 2006, **62**, 8988–9001.
210 T. Kuwahara, T. Fukuyama and I. Ryu, *Org. Lett.*, 2012, **14**, 4703–4705.
211 For selected reviews on hydrogen borrowing strategies, see: (*a*) C. Gunanathan and D. Milstein, *Science*, 2013, **341**, 1229712; (*b*) G. E. Dobereiner and R. H. Crabtree, *Chem. Rev.*, 2010, **110**, 681–703; (*c*) G. Guillena, D. J. Ramón and M. Yus, *Chem. Rev.*, 2010, **110**, 1611–1641; (*d*) M. H. S. A. Hamid, P. A. Slatford and J. M. J. Williams, *Adv. Synth. Catal.*, 2007, **349**, 1555–1575.
212 D. Weickmann and B. Plietker, *ChemCatChem*, 2013, **5**, 2170–2173.
213 T. vom Stein, T. Weigand, C. Merkens, J. Klankermayer and W. Leitner, *ChemCatChem*, 2013, **5**, 439–441.
214 T. vom Stein, T. den Hartog, J. Buendia, S. Stoychev, J. Mottweiler, C. Bolm, J. Klankermayer and W. Leitner, *Angew. Chem., Int. Ed.*, 2015, **54**, 5859–5863.
215 J. M. W. Chan, S. Bauer, H. Sorek, S. Sreekumar, K. Wang and F. D. Toste, *ACS Catal.*, 2013, **3**, 1369–1377.
216 R. G. Harms, I. I. E. Markovits, M. Drees, W. A. Herrmann, M. Cokoja and F. E. Kühn, *ChemSusChem*, 2014, **7**, 429–434.
217 M. V. Galkin, C. Dahlstrand and J. S. M. Samec, *ChemSusChem*, 2015, **8**, 2187–2192.
218 I. Horiuti and M. Polanyi, *Trans. Faraday Soc.*, 1934, **30**, 1164–1172.
219 F. Zaera, *Phys. Chem. Chem. Phys.*, 2013, **15**, 11988–12003.

1914 | *Org. Biomol. Chem.*, 2016, **14**, 1853–1914

This journal is © The Royal Society of Chemistry 2016